AD-A148 011 A SCHEME FOR SHORT-TERM PREDICTION OF HYDROMETEORS USING ADVECTION AND PH. (U) PENNSYLVANIA STATE UNIV UNIVERSITY PARK DEPT OF METEOROLOGY G S FORBES ET AL. 1/2

UNCLASSIFIED JUL 84 AFGL-TR-84-0199 F19628-82-K-0023 F/G 4/2 NL

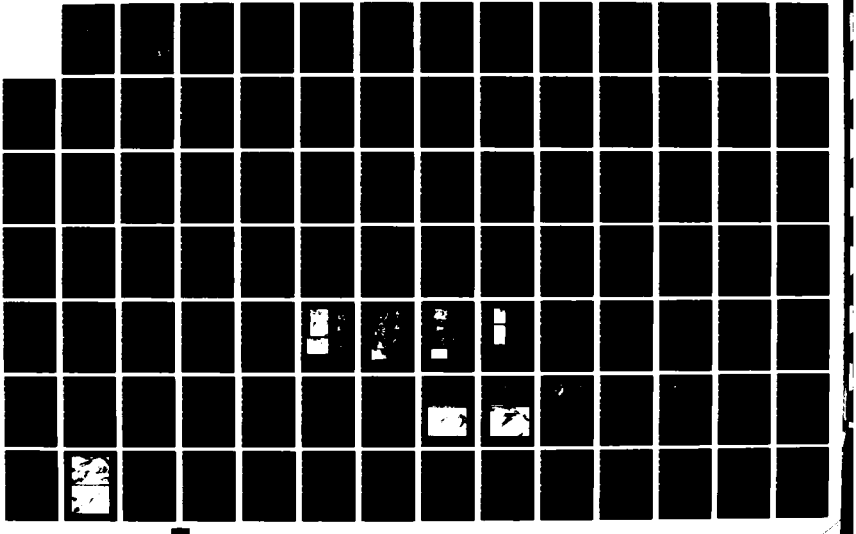

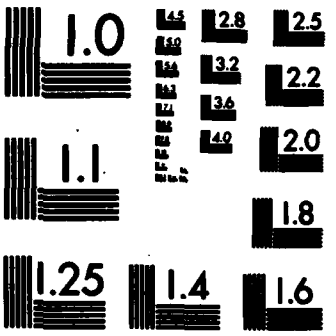

MICROCOPY RESOLUTION TEST CHART
NATIONAL BUREAU OF STANDARDS-1963-A

AFGL-TR-84-0199

(12)

A SCHEME FOR SHORT-TERM PREDICTION OF HYDROMETEORS USING ADVECTION AND PHYSICAL FORCING

G.S. Forbes
J.J. Cahir
W.D. Lottes
E. Araujo
P.O.G. Heppner
R.L. Scheinhartz

The Pennsylvania State University
Department of Meteorology
University Park, Pennsylvania 16802

Final Report
February 1982 - July 1984

July 1984

AIR FORCE GEOPHYSICS LABORATORY
AIR FORCE SYSTEMS COMMAND
UNITED STATES AIR FORCE
HANSCOM AFB, MASSACHUSETTS 01731

CR

This report has been reviewed by the ESD Public Affairs Office (PA) and is releasable to the National Technical Information Service (NTIS).

This technical report has been reviewed and is approved for publication.

H. STUART MUENCH
Contract Monitor

H. ALBERT BROWN, Acting Chief
Atmospheric Prediction Branch

FOR THE COMMANDER

KENNETH R. HARDY, Acting Director
Atmospheric Sciences Division

Qualified requestors may obtain additional copies from the Defense Technical Information Center. All others should apply to the National Technical Information Service.

If your address has changed, or if you wish to be removed from the mailing list, or if the addressee is no longer employed by your organization, please notify AFGL/DAA, Hanscom AFB, MA 01731. This will assist us in maintaining a current mailing list.

Do not return copies of this report unless contractual obligations or notices on a specific document requires that it be returned.

Unclassified

SECURITY CLASSIFICATION OF THIS PAGE (When Data Entered)

REPORT DOCUMENTATION PAGE	READ INSTRUCTIONS BEFORE COMPLETING FORM
1. REPORT NUMBER: AFGL-TR-84-0199	2. GOVT ACCESSION NO. / 3. RECIPIENT'S CATALOG NUMBER
4. TITLE (and Subtitle): A Scheme for Short-Term Prediction of Hydrometeors Using Advection and Physical Forcing	5. TYPE OF REPORT & PERIOD COVERED: Final Rept. 1982-1984
	6. PERFORMING ORG. REPORT NUMBER
7. AUTHOR(s): G. S. Forbes, J.J. Cahir, W.D. Lottes, E. Araujo, P.O.G. Heppner, R.L. Scheinhartz	8. CONTRACT OR GRANT NUMBER(s): F19628-82-K-0023
9. PERFORMING ORGANIZATION NAME AND ADDRESS: The Pennsylvania State University, University Park, PA 16802	10. PROGRAM ELEMENT, PROJECT, TASK AREA & WORK UNIT NUMBERS: 62101F, 667010BB
11. CONTROLLING OFFICE NAME AND ADDRESS: Air Force Geophysics Laboratory, Hanscom AFB, Massachusetts 01731, Monitor/H.Stuart Muench/LYP	12. REPORT DATE: July 1984
	13. NUMBER OF PAGES: 116
14. MONITORING AGENCY NAME & ADDRESS(if different from Controlling Office)	15. SECURITY CLASS. (of this report): Unclassified
	15a. DECLASSIFICATION/DOWNGRADING SCHEDULE

16. DISTRIBUTION STATEMENT (of this Report)

Approved for public release; distribution unlimited.

17. DISTRIBUTION STATEMENT (of the abstract entered in Block 20, if different from Report)

18. SUPPLEMENTARY NOTES

19. KEY WORDS (Continue on reverse side if necessary and identify by block number)

Weather forecasting
Statistical Weather Prediction
Convection Forecasting
Cloudiness forecasting
Wintertime cloud vortices
LFM Relative Humidity

20. ABSTRACT (Continue on reverse side if necessary and identify by block number)

We have developed a number of schemes which show skills varying from modest to impressive, depending upon the weather regime. These schemes are interactive, and their successful implementation requires a man-machine mix.

The approaches taken in this research project have primarily→cont.

DD FORM 1 JAN 73 1473

Unclassified

SECURITY CLASSIFICATION OF THIS PAGE (When Data Entered)

Unclassified
SECURITY CLASSIFICATION OF THIS PAGE(When Data Entered)

20. Abstract (Continued)

cont → focused upon the developmental or evolving, i.e. non-steady-state aspects of the problem of short-term forecasting of cloudiness and precipitation. Most of our schemes have incorporated a translational contribution either explicitly or implicitly, however.

The approaches taken in this research project have addressed the problem of cloudiness and precipitation forecasting on meso-alpha and larger scales. The approaches, by virtue of treating the developmental aspects of the short-term forecasting problem, have inherently bypassed the problem of persistence or persistence climatology being such a hard "forecast" to beat.

The nature of our approach has forced us to provide pieces of the overall solution to the problem of short-term forecasting. We have treated the difficult developmental contributions, and these developments occur by different processes in different weather situations. Accordingly, we have developed schemes for a number of different weather regimes and some guidelines for applying these schemes. The situations treated include:

large-scale humidity change,
mean relative humidity as an indicator of precipitation probability,
statistical prediction of cloudiness change in summer daytime and winter nighttime,
location of afternoon showers in summer,
summer precipitation intensity,
radiation fog,
continuation of daytime convection into summer nighttime,
nocturnal thunderstorms,
wintertime lake vortices, and
wintertime polar vortices.

Unclassified
SECURITY CLASSIFICATION OF THIS PAGE(When Data Entered)

Table of Contents

List of Figures

Page

List of Tables

Page

1. PROGRAM SUMMARY

As a science, meteorology is in the unique position of having a direct voice to the public on a daily basis, and of putting forth its credibility for judgement with equal frequency. Thus, it is distressing to hear the radio announcer read a forecast of sunny and warm when it is raining outside. The impression of incompetence is immediate and lasting, irregardless of how accurate the remainder of the forecast may have been. Therefore, it would appear that Browning (1982) has succinctly stated a key challenge and opportunity for the meteorological community--to improve the quality of forecasts of local weather for the period up to 12 hours ahead.

The objective of this research project has been to develop a scheme for short-term forecasting of hydrometeors; i.e., clouds and precipitation. Perhaps to a laboratory physicist the development of clouds and precipitation is conceptually and experimentally simple; readily accomplished through controlled cooling of moist air. For the practicing meteorologist, however, the forecasting of clouds and precipitation is made quite difficult because of the number of ways the atmosphere can achieve the required cooling and by the ability of atmospheric processes to alter the prevailing vapor content of the air. From a broad perspective, then, the challenge of this research (and of weather forecasting, in general) is to render a diversity of atmospheric processes into a format analogous to a controlled experiment. Just as a chemist knows that a certain combination of ingredients will react to produce a particular new substance, the forecaster needs to know the combination of conditions that results in clouds, or rain, or clearing.

In attempting to render the generalized problem of weather forecasting more tractable, historically there have been breakthroughs achieved through a number of techniques. Certainly one breakthrough was the recognition that

much weather is produced by organized systems that translate, and forecast gains were made through use of the concepts of steering and wave propagation. A logical subsequent breakthrough was the recognition that weather systems were not steady, but evolved in response to (a) localized forcings or instabilities which were often geographic, topographic, or diurnal in nature and affected portions of the system, or (b) inherent instabilities of the environment on a scale larger than the system and affecting the entire system, or (c) feedbacks induced between various elements of the evolving weather system affecting either portions of the system or the system as a whole. Finally, just as the chemist has formulae for reactions, numerical models solve formulae of the atmosphere to predict the end product of its combination of ingredients.

These historical breakthroughs have had the most impact on our ability to forecast meteorological quantities which are characteristic of synoptic scales and of a considerable depth of the atmosphere, such as sea-level pressures, heights of the pressure surfaces, and (to a lesser extent) layer relative humidities. Much progress remains to be achieved in our ability to forecast cloudiness and precipitation, especially over short time periods and mesoscale areas.

Indeed, the present state of short-range prediction of cloudiness/humidity is alarmingly crude when compared to the progress achieved in forecasting the mass (pressure) field. Particular problems include the smallness of the horizontal scale of moisture features relative to wind and pressure fields (Lilly and Perkey, 1976); the unsuitability of most remote sensing approaches for cloudy regions, where moisture is usually high and always interesting; and possibly some neglect by theoreticians, who tend to think of moisture as an inert contaminant which adds unnecessary terms to the equations.

However, recent developments give reason to be optimistic that the moisture field will be increasingly recognized, observed, and analyzed. These include the planned deployment of NEXRAD Doppler radars, the development of high-frequency profiler sounding capabilities at VHF/UHF frequencies, and the emergence of interesting new or revitalized theoretical/diagnostic ideas for interpreting mesoscale phenomena, such as symmetric instability, the influence of the vertical distribution of shear, the vertical distribution of heating, and the decisive role played by large-scale flows interacting with the terrain.

As an interim approach, pending the promising developments of the next decade or so, the participants in this project have put together a practical method for short-range moisture (cloudiness) prediction based on the present state of the observations and science. Included in this approach are some new tools and ideas, refinements of old ones, information that should be helpful in interpreting the products of current technology (the numerical models), and a heavy dose of skepticism about what forecasters can and should do regarding this problem.

This last point should be amplified. The best first approximation as a short range prediction (3-9 h) of visibility and/or ceiling is very often the persistence, or better still, the persistence climatology[1] forecast. Almost no forecasts will beat persistence climatology at 0-3 h, and it is hard to beat at 3-9 h. Thus, we attempt to focus only on those situations where substantial changes are in some sense likely. We would expect the forecaster to leave well-enough alone unless our ideas and procedures persuaded him or her that a particular situation was one that called for a departure from the normal trend.

---

[1]This climatology indicates the most likely future conditions, based upon the initial condition, thereby allowing for diurnal trends.

Accordingly, this report focuses on statistical techniques that can be applied to forecast satellite brightness, or infrared flux change, given that change is possible. There is a method for dealing with intense deep persisting convection along frontal zones, and for identifying and estimating the persistence of small vortices. Finally, there is a very complete diagnosis of short-range humidity forecasts of a numerical model, to help the forecaster recognize the value and the dangers of extracting humidity forecasts of this type and applying them. Overall, there is a strategy implicit in this approach which could be encapsulated: "If it isn't broken, don't fix it, but keep your senses sharp so that you can tell when it might break, and your tools handy for when it does."

1.1 Philosophy of the Approaches Taken

A variety of methods are being investigated as possible ways to improve the 0-12 hour forecast, as demonstrated by the papers at the first Nowcasting Symposium (European Space Agency, 1981). Browning (1982) has indicated that "nowcasting" is the practice of making 0-2 hour forecasts, and comprises providing a detailed description of the current weather, along with forecasts obtained by extrapolation. Very-short-range forecasting, for periods out to 12 hours ahead, involves both linear extrapolation methods and dynamical or other methods which seek to account for development and decay of the weather system.

We have been making some initial examinations of two approaches which fall under the "other" category of methods for very-short-range forecasting. One approach involves the use of a trajectory scheme in situations when the air is undergoing gradual large-scale slantwise ascent (i.e., within a baroclinic zone). Starting from the observed and forecast locations of the weather system, the scheme uses backward trajectories to determine the

upstream locations where the air (which subsequently enters the weather system) was once situated within a surface-based planetary boundary layer. By examining the observed weather conditions at the upstream locations, it is possible to determine whether the propagating weather system will be drawing upon air of differing characteristics as time progresses, and to infer the effect of the differing characteristics upon the weather system evolution. For example, a thunderstorm will likely decrease in intensity as it propagates into a region where the air is noticeably drier. A detailed account of the trajectory scheme is given by Forbes et al. (1984) and we have applied this approach specifically to the problem of forecasting nocturnal convection (Section 5.3).

A second approach which we have investigated for potential use in short-term forecasting is a statistical approach, using observations as well as forecast data from operational numerical models. Aside from satellite imagery, the scheme does not at present use any special data; merely data from routine observing stations spaced about 100-150 km apart at the surface and about 400 km apart aloft. Thus, we are focusing on meso-alpha-scale weather systems and assuming that their evolution is influenced by the large-scale environment.

In the above schemes using the second approach we have used both observed and forecast data. Continual improvement is being attained in numerical model forecasts of parameters such as surface pressure, heights of pressure surfaces, layer thicknesses, layer mean winds, and layer mean humidities. Numerical model forecasts of these types of parameters are being used operationally for predicting other meteorological parameters such as ceiling, visibility, probability of precipitation, surface temperature, etc. (Glahn and Lowry, 1972). These forecasts, referred to as MOS (model output statistics)

forecasts, also continue to improve. In the MOS approach, regression equations are developed between predictand parameter values and values of assorted predictors consisting of forecasted and observed quantities. A large sample is obtained by compositing data over a period of a few years.

One limitation of the MOS approach is that the compositing procedure produces regression equations that chiefly represent normal weather situations. The unusual situations, in which certain physical processes become abnormally important, are not handled well. Unfortunately, it is often these same situations, again because of their abnormal and infrequent nature, that also cause the subjective (human) forecasts to be in error.

The results reported here indicate that there is another way to produce statistical forecasts, which we call "regime model output statistics" or "REMOS". In this (our second) approach, the developmental sample is objectively stratified into various weather regimes, and different regression equations are developed for each regime. Provided that objective procedures can be specified to reliably identify the regime, and that sufficiently large developmental samples can be obtained, the number of regimes is seemingly unlimited.

The advantage of the REMOS approach is that different parameters (representing different physical processes) can have different weights in various regimes. One parameter may be extremely important in one regime and virtually irrelevant in another. Most MOS regression equations, developed using data composited from a variety of regimes, naturally assign a "middle-of-the-road" weight to the parameter. This compromises the potential usefulness of the parameter in certain weather regimes. It should be pointed out, however, that some MOS prediction equations, such as those for thunderstorm and severe thunderstorm probability (Charba, 1979a,b) and precipitation type

(Bocchieri and Maglaras, 1983) have been developed through essentially a REMOS approach.

The development of the REMOS technique is a three-phase process. It is first necessary to objectively define the various weather regimes. Second, a large number of situations must be identified and composited for each regime. Third, this composite data set must be used to select predictor variables and to develop multiple linear regression equations. At this juncture we have identified several weather regimes for investigation. Our data sets are not extremely large, however, so we do not intend to suggest that we have developed the best possible regression equations for these regimes.

In many cases a mesoscale weather regime can be identified in satellite or radar imagery. This suggests that the REMOS approach will be most powerful if designed to allow for interactive operational use. The subsequent behavior of existing squall lines and other thunderstorm systems might logically be investigated in this way; we have used such an approach to predict how long afternoon showers will persist into the evening (section 5.1). Polar vortices and lake vortices are other phenomena treated in this way (Chaper 6). We have also applied this type of approach to the forecasting of short-term changes in cloudiness based upon initial-hour satellite imagery (sections 3.1 and 4.1).

The greatest challenge, however, may be in predicting the formation of mesoscale systems. Whereas such mesoscale systems might be readily identified after they form, in order to use the REMOS approach it is necessary to identify large-scale conditions conducive to the occurrence of such phenomena. As elucidated by Pielke (1982), some of these systems may form in response to synoptic-scale proceses or instabilities developing within travelling synoptic-scale weather systems, while others may be induced by terrain-controlled processes. To treat this forecasting situation, we have assumed that the

recent upper-air and surface observations contain more information than forecasts developed from older data. This variation of the REMOS approach, then, differs from MOS in that only observed data are used. Afternoon and nighttime convection (and to a lesser extent, fog) have been treated in this manner (sections 3.2, 3.3, 4.2, 5.2).

1.2 Outline of a Scheme

In order to try to match the skill of certain predictor variables to particular forecasting situations or weather regimes, a REMOS approach has been adopted in this research, as discussed above. Through this approach, a number of individual forecast modules have been generated. This section encloses these modules within a master framework or decision tree which, if adapted operationally, would help the forecaster to identify and select modules available for use.

The master framework is portrayed in Figures 1.2.1, 1.2.2 and 1.2.3, which deal with continental spring/summer regimes, continental fall/winter regimes, and maritime regimes, respectively. To examine the individual modules, cross-references are given to sections of this report where they are summarized. Most of these modules were developed completely through AFGL funding, though a few were developed earlier and simply adapted for inclusion in this master framework. A list of the tasks supported by AFGL funding is presented as Appendix 1. Appendix 2 lists project personnel. Appendix 3 lists project publications.

1.3 Conclusions

We have developed a number of schemes which show skills varying from modest to impressive, depending upon the weather regime. These schemes are interactive, and their successful implementation requires a man-machine mix.

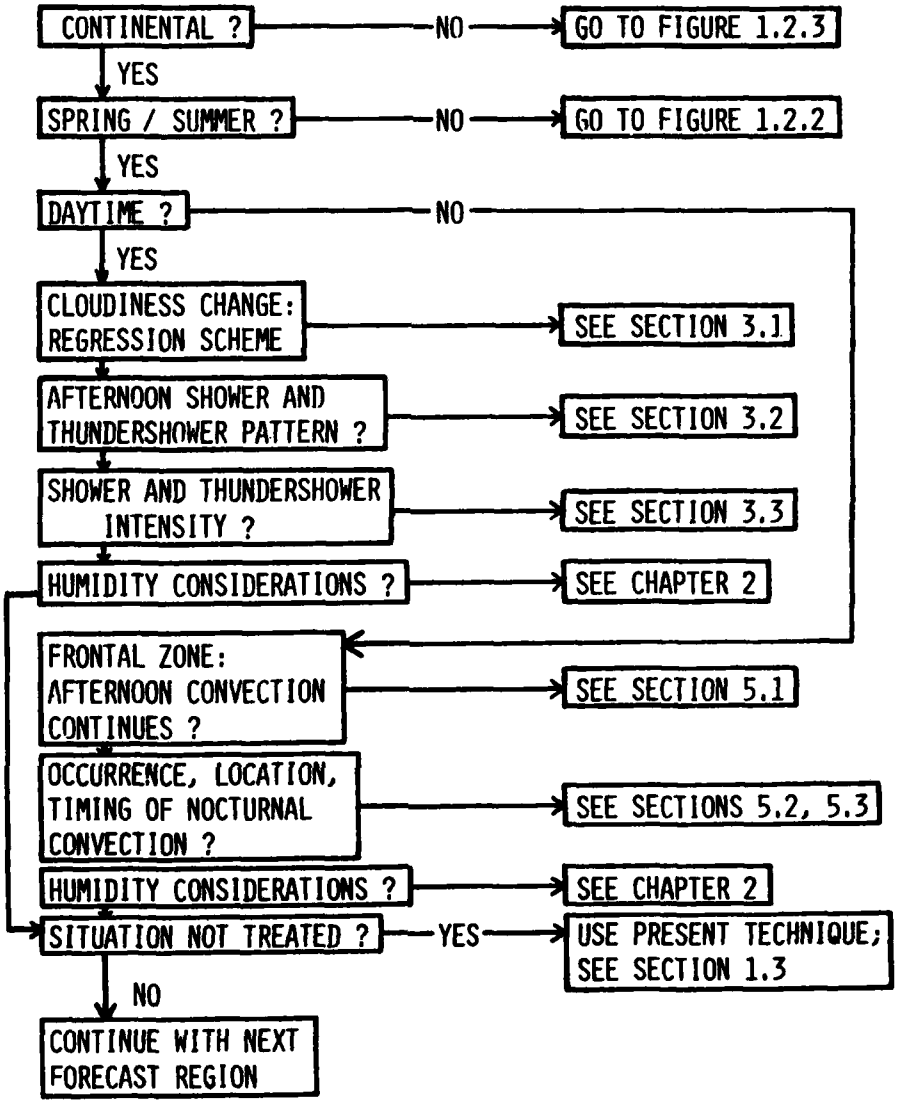

Figure 1.2.1. Framework for implementing continental spring and summer prediction schemes described in the text.

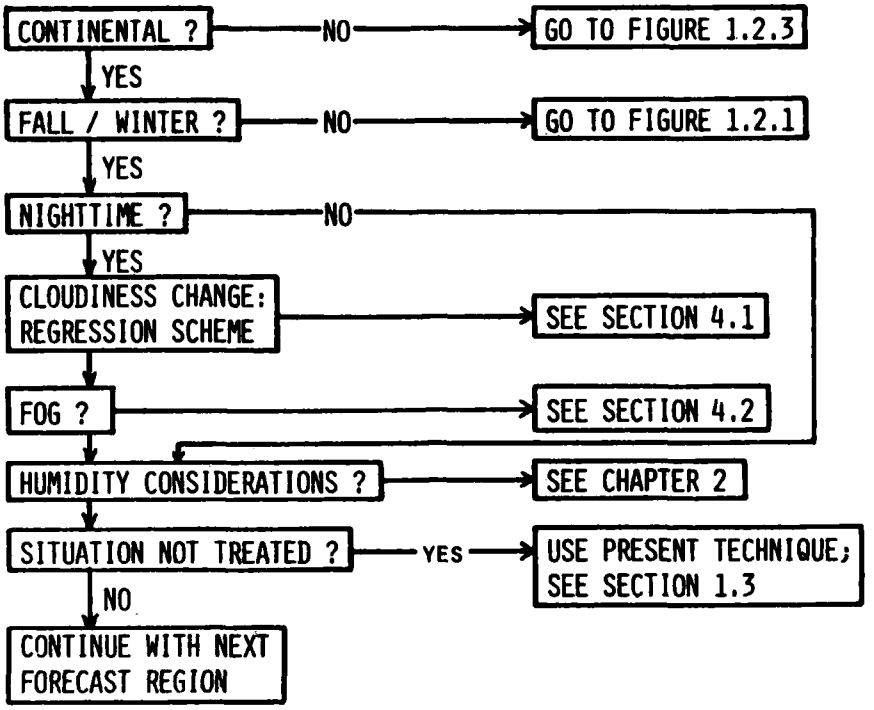

Figure 1.2.2. Framework for implementing continental fall and winter prediction schemes described in the text.

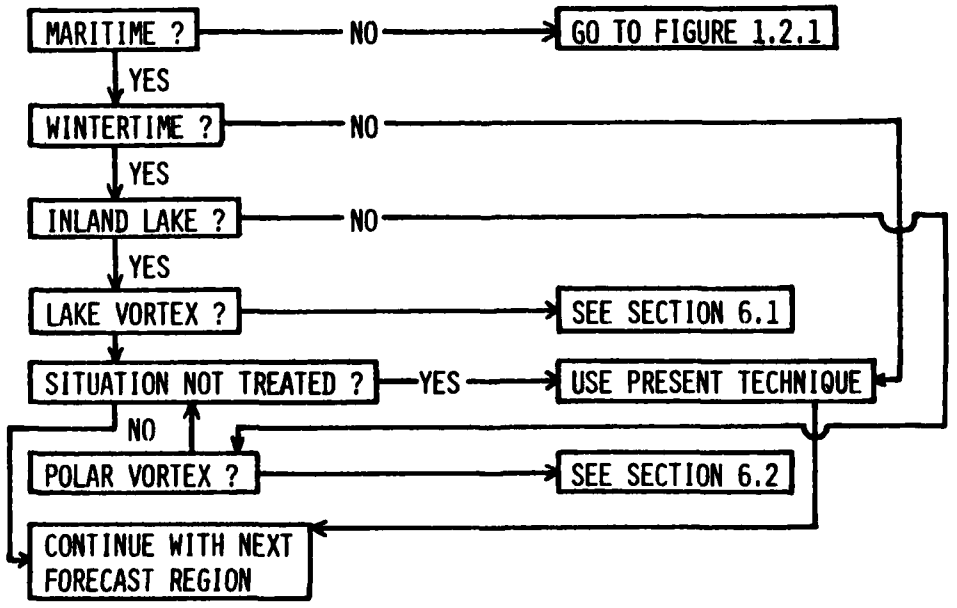

Figure 1.2.3. Framework for implementing maritime prediction schemes described in the text.

We have developed these schemes on the Penn State minicomputer system (Cahir et al., 1976; 1981), although they could also work on the AFGL interactive system (Chisolm and Jackson, 1984).

The approaches taken in this research project have primarily focused upon the developmental or evolving, i.e., non-steady-state, aspects of the problem of short-term cloudiness and precipitation forecasting. Others, for example Muench (1981, 1984), Austin and Bellon (1982), and Browning and Collier (1982), have dealt extensively with short-term forecasting through extrapolation of existing weather features. Most of our schemes have incorporated this translational contribution, however, either explicitly or implicitly. For example, the regression equations for short-term count change prediction implicitly include the effects of translation because certain LFM forecast quantities, such as 6-hour relative humidity change, account for system movement. The ACTIVEX Scheme for nocturnal thunderstorm forecasting incorporates system movement in two ways: (1) by using trajectories which, in combination with the diurnally-changing latent instability, may allow convective regions to move; (2) by requiring the forecaster to interactively enter a phase speed which accounts for movement of the low-level jet or front which would cause the zone of anabatic flow to translate. The FLUX scheme and the polar vortex study give rules for the translation of these systems in relation to observed winds. Additionally, Forbes (1983) observed that meso-alpha-scale cyclones translate with the winds at the level of non-divergence and averaged spatially over the extent of the system, and Muench (1984) has independently achieved modest success by using 80% of the spatially-averaged 500 mb flow. Finally, Araujo (1984) has experimented with the incorporation of a satellite infrared count-change forecast obtained via extrapolation as one predictor in a multiple linear regression study of short-term cloudiness change.

The approaches taken in this research project have addressed only the problem of cloudiness and precipitation forecasting on meso-alpha and larger scales. Conventional meteorological data is available operationally on these scales, and appears to be useful in addressing the developmental aspects of the short-term forecasting problem. Smaller-scale observations are available operationally in the form of satellite and radar data, which the previously-mentioned extrapolation schemes use to make very-small-scale predictions. Such forecasts, however, are seriously degraded by developmental contributions which are often linked to the localized terrain (Muench, 1981; Hill et al., 1981). This suggests that a complete short-term forecasting system must include some form of data base that will enable the forecaster to anticipate these localized contributions to non-steady translation. Two studies which might be considered as models of such a scheme have been performed by Hill (1981) and Weaver and Kelly (1982). The former deals with orographic enhancement of rainfall as a function of wind direction, while the latter gives a climatology of the diurnal patterns of satellite-detected convection in a mountainous region.

Most of our studies, by virtue of treating the developmental aspects of the short-term forecasting problem, have inherently bypassed the problem of persistence or persistence climatology. We have designed our schemes to predict changes from some initial state, rather than the pattern at some final time. This approach has been moderately successful, and it is likely that greater successes have been thwarted by the fact that persistence <u>is</u> rather common over a meso-alpha-scale region in a 6-hour period. Thus, the burden for our schemes has been to give a strong signal in the non-persistence situations.

Finally, the nature of our approach has forced us to provide pieces of the overall solution to the problem of short-term forecasting. We have treated the difficult developmental contributions, and these developments occur by different proceses in different weather situations. Accordingly, we have developed schemes for a number of different weather regimes and some guidelines for applying these schemes. It has not been possible, of course, to provide a scheme for every situation. That would require far more time, and it may never be possible for such a scheme to be 100% comprehensive. In the event that a situation is encountered which we have not treated, the forecaster will need to use some other technique at his or her disposal. This may include his or her personal experience "data base", an extrapolation technique, or a statistical technique such as GEM (Miller, 1981).

2. LARGE-SCALE HUMIDITY FIELD CONSIDERATIONS

2.1 LFM Humidity Analyses and Forecasts

Predictions of relative humidity are a key element of most forecast decisions regarding cloudiness and its evolution. Dorian (1983) has investigated the accuracy of the LFM-II analyses and forecasts of mean and layer humidities and learned that there are different biases in the various layers, which change value with time. These have been summarized by Forbes et al. (1983), and a detailed analysis has been prepared by Dorian et al. (1984). Only a few forecasting guidelines are reproduced here.

Forecasting guidelines:

- There are a number of ways in which numerical models can develop biases, especially in regard to humidity. However, changes to the operational models are made at irregular intervals, such that the biases may also change. We do not know if the guidelines below are still quantitatively accurate in 1984, but recommend that forecasters think about these types of errors. We recommend using a minicomputer scheme to generate a recent (such as one-month) history of the model performance, continually updated, for operational forecasting purposes.
- The changing biases of the 1981-82 version of the LFM-II, on an annual basis, are shown in Fig. 2.1.1. (1) There is a moist bias in the initial analyses of relative humidity in each level. (2) The lowest two layers and the vertical mean humidity dry with time, such that the lowest two layers have a dry bias by 24h. (3) The top layer becomes moister with time.
- The net drying with time in the lowest two layers occurs because the model does not produce enough moistening when the initially-low humidities are increasing. This trend is worst in summer and fall.

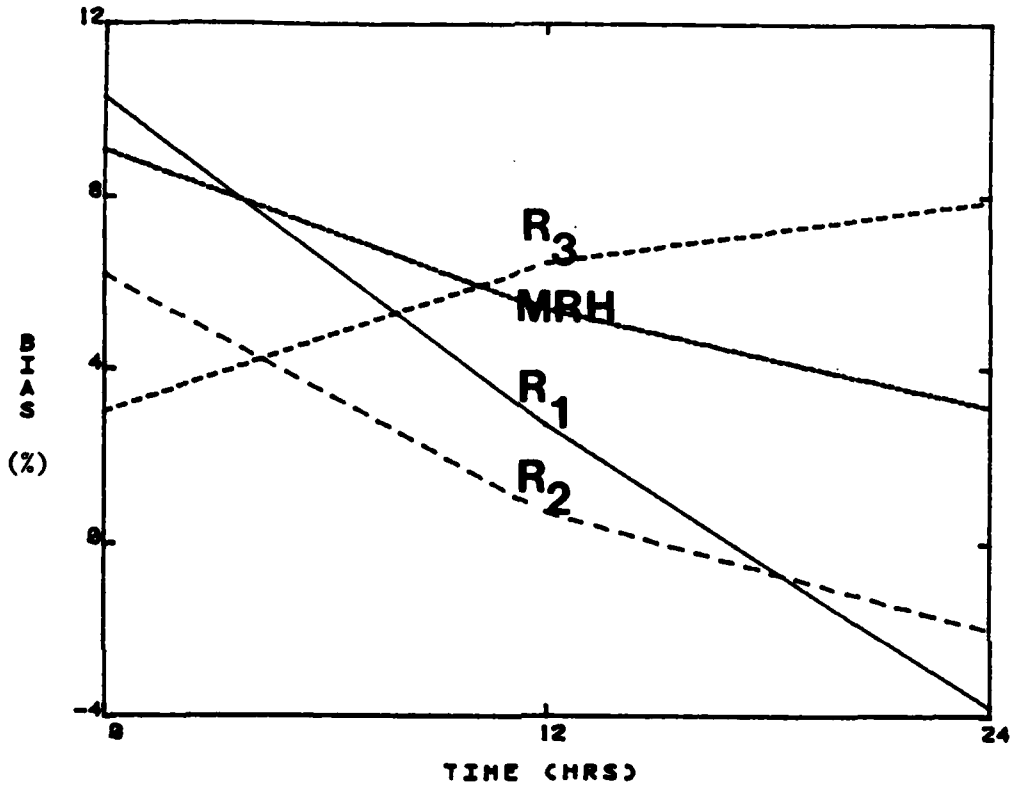

Figure 2.1.1. Temporal evolution of the annual LFM-II (1981-82) bias, in layers. From Dorian (1983).

- The net moistening with time in the top layer occurs because the model does not produce enough drying when the initially-high humidities are decreasing. This trend is worst in spring.
- The seasonal biases are listed in Table 2.1.1.
- There is a difference, especially in the lowest layer, between the biases of the two (0000 and 1200 GMT) forecast cycles, as shown in Table 2.1.2, arising as a combination of initial analysis error and failure of the LFM to produce a realistic diurnal cycle. Notice that the biases in the 12h forecasts are large and of different signs in the two cycles.
- There are geographically-linked error patterns, most pronounced in winter and spring, as shown in Figures 2.1.2 and 2.1.3.
- There are systematic errors associated with various synoptic regimes, as discussed by Dorian (1983). (1) The LFM tends to underforecast the moistening of the mean relative humidity when the flow is off the Gulf of Mexico; this can be 20% in 24h. (2) The LFM underforecasts moistening ahead of cold fronts, such that the mean humidities are often 20% greater in the LFM maximum. (3) The LFM underforecasts drying behind cold fronts, such that the mean humidities are often 30% drier in the LFM minimum. (4) In New England winter anticyclones the LFM mean humidities are often 10-20% too high near the anticyclone center and 10-20% too low in the area of onshore flow. (5) Humidity gradients are usually sharper than forecast by the LFM.

Table 2.1.1

Mean Errors of LFM Layer Humidities
(From Dorian, 1983)

	00 hr Mean	12 hr Mean	24 hr Mean
FALL			
R_1	11.0	1.3	-3.8
R_2	4.7	-0.3	-2.6
R_3	2.1	6.0	8.9
MRH	9.0	5.5	4.2
WINTER			
R_1	10.1	3.3	-2.6
R_2	7.5	3.7	1.7
R_3	7.4	7.3	10.2
MRH	9.6	6.1	4.6
SPRING			
R_1	9.6	5.3	-2.6
R_2	5.9	-0.4	-1.8
R_3	3.5	7.2	10.7
MRH	8.7	4.7	3.9
SUMMER			
R_1	10.6	0.8	-6.0
R_2	6.7	-0.4	-5.2
R_3	-1.0	5.4	1.9
MRH	9.0	5.2	-0.3
ANNUAL			
R_1	10.3	2.7	-3.8
R_2	6.2	0.7	-2.0
R_3	3.0	6.5	7.9
MRH	9.1	5.4	3.1

Table 2.1.2

Comparison of Layer 1 Humidities (percent) from 0000 and 1200 GMT Forecast Cycles (From Dorian et al., 1984)

	0000 GMT Cycle LFM/RAOB/CORR	1200 GMT Cycle LFM/RAOB/CORR
0 h	Valid 0000 GMT 68/59/0.86	Valid 1200 GMT 83/71/0.80
12 h	Valid 1200 GMT 64/73/0.70	Valid 0000 GMT 72/58/0.63
24 h	Valid 0000 GMT 56/59/0.65	Valid 1200 GMT 68/72/0.44

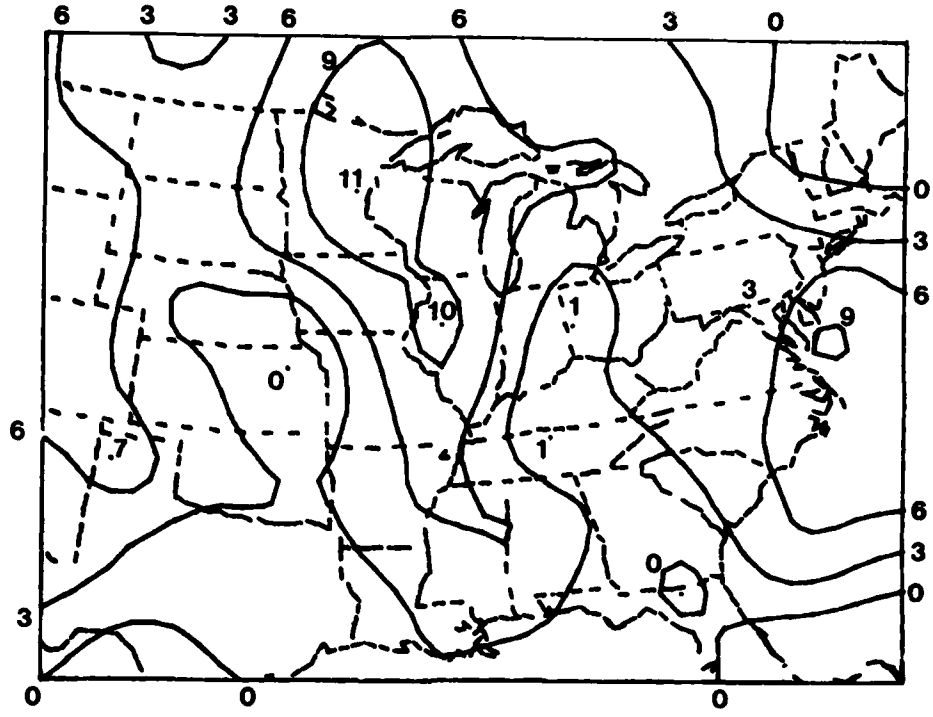

Figure 2.1.2. Annual mean error of the 24 h LFM-II mean relative humidity forecast (forecast minus observed). The domain mean is 3%, and differences of more than 6% are significant at the 95% confidence level.

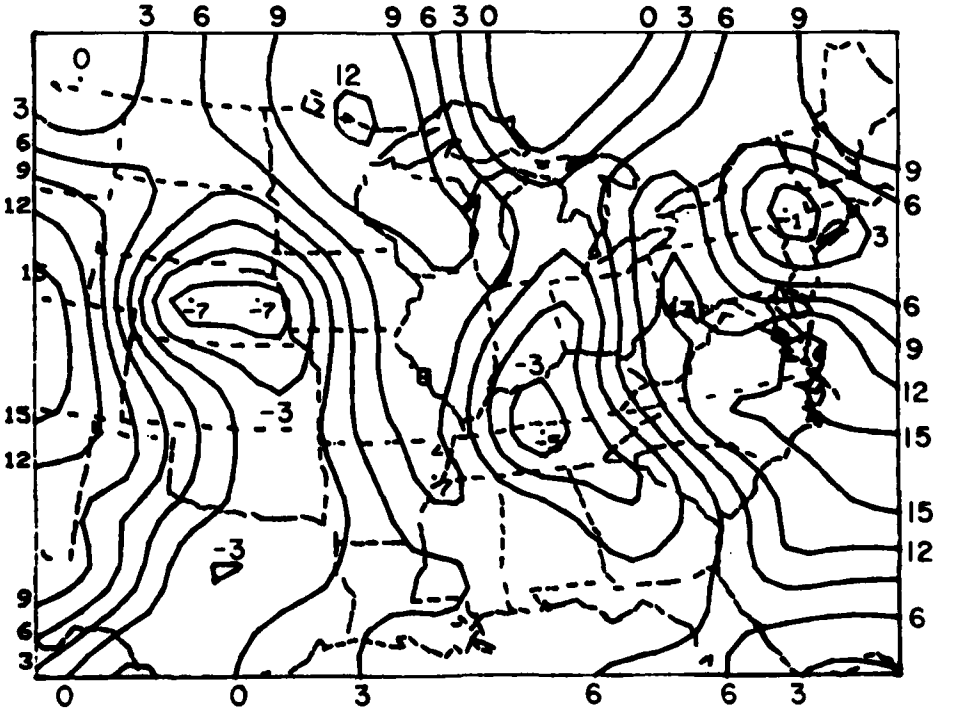

Figure 2.1.3. Mean error of the LFM-II 24 h forecast of mean relative humidity in spring. The domain mean is 3%, and differences of more than 14% are significant at the 95% confidence level.

2.2 Relative Humidity Estimates from Hourly Surface Observations

A simulated 1000-500 mb mean relative humidity is generated by an algorithm developed at Penn State, similar to that of Fye (1978), which uses hourly observations of cloud cover, current weather, and surface relative humidity. This matches the observed mean relative humidity, in the mean, to within 2% at 0000 and 1200 GMT in all seasons except summer.

Forecasting guidelines:

- Simulated humidities have about a 6% dry bias in summer at 0000 and 1200 GMT.
- Simulated humidities do not have variances as large as the atmosphere.
- Simulated humidities fail to capture the diurnal cycle. This appears to occur because observers underestimate the cloud cover during the nighttime.

2.3 Mean Relative Humidity as an Indicator of Probability of Precipitation

Based on a 10-case dependent sample from the winter and spring of 1978-1979 and a 7-case independent sample from the winter of 1978-1979, Cahir (1980) reported that the 1000-500 mb mean relative humidity and the 850-700 mb average moisture divergence provided useful indications of the instantaneous probability of precipitation. As the moisture divergence did not pose a strong constraint, it is suggested that LFM forecasts of mean relative humidity, after bias correction, can provide a useful forecast of regions of instantaneous precipitation.

Forecasting guidelines:

- Regions showing mean relative humidity of at least 55% and having values of 850-700 mb average moisture divergence $\leq 3 \times 10^{-5}$ g kg^{-1} s^{-1} have a 63% instantaneous probability of precipitation (with a threat score of 0.55).
- The probability of instantaneous precipitation is a function of the mean relative humidity in regions where the average 850-700 mb moisture divergence $\leq 3 \times 10^{-5}$ g kg^{-1} s^{-1}; as shown in Table 2.3.1.

Table 2.3.1

Instantaneous Probability of Precipitation as a Function of 1000-500 mb Mean Relative Humidity
(From Cahir, 1980)

$\overline{\text{REL}}$	POP
$\geq$ 90%	86%
$\geq$ 80%	81%
$\geq$ 70%	75%
$\geq$ 55%	60%
$\geq$ 50%	57%

3. SCHEMES FOR CONTINENTAL SPRING AND SUMMER DAYTIME REGIMES

The schemes presented here take into consideration the fact that weather, especially in the convective season, is influenced both by travelling weather systems and by more localized processes related to diurnal and differential heating. The first scheme primarily allows for the large-scale changes associated with travelling weather systems. The cloudiness change is averaged over a mesoscale area, large enough that spectacular thunderstorm development could occur within the regions and yet not radically alter the average cloudiness in the region. The second and third schemes treat these convective developments more explicitly.

3.1 Statistical Prediction of Cloudiness Change

Since clouds can be produced by a number of physical processes, forecasting of cloudiness is a challenge. It would seem that a REMOS approach is worth investigation, however, in that the relative importance of the various physical processes may be quite different in various weather regimes. We have approached the problem of short-term forecasting of cloudiness through use of satellite imagery, observed data, and forecast data from the LFM model. Rather than trying to predict the exact location of individual clouds and clear areas, we have sought to predict the character of the cloudiness over a mesoscale area with radius of about 50 km, comparable to the half-distance between commercial airports in the eastern United States. Furthermore, we have sought to predict the 6-hour change of average cloudiness, since we wish to be able to indicate when conditions will depart from persistence.

As a measure of cloudiness and cloudiness change, we have used count values (essentially gray shades) and temporal changes in count values of visible and infrared imagery from the GOES East satellite. The count values, ranging from 0 to 255, increase as the visible brightness increases. In order to obtain area-averaged count changes, we averaged count values from a number

of adjacent pixels using a scheme developed by Chapman (1983). This scheme also (1) normalizes the brightness to account for variations in solar zenith angle, (2) removes spikes in the data (state borders), and (3) standardizes the image brightness to account for any signal strength variations in the phone line by which the data are received.

Table 3.1.1 shows some results of experiments by Scheinhartz (1984) regarding development of regression equations relating 6-hour brightness change between morning and afternoon to conditions observed during the morning and to forecasts from the LFM. The regression equations were developed for the region of the United States east of the Mississippi River using 30 days between 31 March and 9 August 1983. Shown in the table are the ranks of the predictor parameters and their individual contributions to reduction of

Table 3.1.1.

RANK OF PREDICTORS AND INDIVIDUAL CONTRIBUTIONS TO EXPLAINED VARIANCE FOR VARIOUS PREDICTIONS OF VISIBLE BRIGHTNESS CHANGE BETWEEN 1500 AND 2100 GMT DURING SPRING AND SUMMER 1983

Predictor	Entire Domain	Partly Cloudy	Clear	Cloudy	warm Thickness	Cold Thickness	Large Brightness Change
1500 GMT Brightness	1 (0.126)	3 (0.032)	4 (0.022)	4 (0.013)	1 (0.209)	1 (0.166)	1 (0.456)
1200 GMT 1000-700 mb Thickness	2 (0.114)	2 (0.100)	1 (0.160)	2 (0.090)	4 (0.034)	4 (0.027)	3 (0.072)
LFM Forecast 12-24 h Mean RH Change	3 (0.090)	1 (0.229)	3 (0.043)	1 (0.105)	2 (0.051)	2 (0.104)	3 (0.136)
1200 GMT K Index	4 (0.022)	5 (0.015)	2 (0.051)		3 (0.033)		
1200 GMT Surface Windspeed	5 (0.014)	4 (0.015)		3 (0.023)		3 (0.068)	(0.017)
1200-1500 GMT Surface P Change		6 (0.012)					
1200-1500 GMT Surface T Change			5 (0.019)				
1500 GMT Surface P					5 (0.028)	5 (0.012)	
1500 GMT Surface Moisture Div				5 (0.012)			
Number of Grid Points	16588	4168	8764	3657	9759	6829	4282
Cumulative Reduction of Variance	0.366	0.403	0.295	0.243	0.355	0.377	0.681
Cumulative Correlation	0.605	0.635	0.543	0.493	0.596	0.614	0.825

Not useful as predictors: surface dew point depression, surface and 700 mb geostrophic vorticity

variance for the entire domain and for 6 subsets of the domain. Also shown are the cumulative reduction of variance and multiple correlation coefficient.

The regression equation for the entire domain is

$$\Delta BRT = 567.197 - 0.463\ BRT - 0.178\ THK + 1.525\Delta MRH + 0.423\ KIX + 0.983\ WSP \quad , \qquad (3.1.1)$$

where the variables are listed in Table 3.1.1. By comparing (3.1.1) and Table 3.1.1 it can be seen that the initial brightness is the leading predictor, and indicates that morning clouds give way to afternoon sunshine and vice versa. Physically, this relationship may be partially attributed to the movement of organized cloud systems, and partially attributed to the differential heating mechanism discussed by Weiss and Purdom (1974). The impact of the term becomes one of treating persistence climatology. Other physical relationships are suggested by (3.1.1) and Table 3.1.1: (1) cold thicknesses favor afternoon cloudiness due to destabilization via insolation; (2) large-scale relative humidity increase or decrease correlates well to cloudiness change; (3) K index values indicate the potential for afternoon convection; (4) large surface wind speeds favor afternoon cloudiness due to mixing.

Table 3.1.1 indicates that it is possible to use initial brightness as a stratifying variable. When data points were classified as being in either clear, cloudy, or partly cloudy regimes at 1500 GMT, initial brightness became less important within a regime and meteorological predictor variables took on increased importance. The ability to predict changes in initially partly cloudy regimes (regions containing either scattered clouds or an edge of a large cloud deck) was enhanced.

A stratification by 1000-700 mb thickness value shows the relative importance of static stability (K index) in warm regimes and mixing (large surface windspeeds) in cold regimes. It is likely that a more sophisticated, perhaps interactively-classified regime system can yield better results.

The final column, selected for pedagogical rather than pragmatic purposes, shows that large brightness changes (increases and decreases; 38 < Δ count < -18) are most easily related to predictor variables. While not operationally useful, the latter experiment suggests that there is a limit to the skill attainable via any stratification scheme. The experiment also indicates that small positive and negative brightness changes are not easily distinguished. Thus, it might be worthwhile to use a modified predictand variable in which all small brightness changes are set to zero, while the values for large changes are retained.

Additional details of the statistical prediction scheme are presented in Appendix 4 and will be reported in the M.S. Thesis of R. Scheinhartz. In general, the cloudiness change patterns are predicted rather well, but the magnitude of the changes are underforecast.

Forecasting guidelines:

- The area-averaged brightness (count value) change between 1500 and 2100 GMT is given by Equation 3.1.1.
- Partly cloudy regions at 1500 GMT (80 $\leq$ count value $\leq$ 120) are treated slightly better with

$$\Delta BRT = 594.674 + 1.994\Delta MRH - 0.184THK - 0.555BRT + 1.310WSP + 0.367KIX - 4.133\Delta P \quad , \tag{3.1.2}$$

where the variables are as defined in Table 3.1.1.

- Regions of cold thickness at 1200 GMT (THK < 2965 m) can be treated by using

$$\Delta BRT = -319.465 - 0.318BRT + 1.415\Delta MRH + 2.498WSP - 0.105THK + 0.641PRS \quad , \tag{3.1.3}$$

where the variables are as defined in Table 3.1.1.

3.2 Location of Afternoon Showers

Forbes et al. (1982) developed an interactive minicomputer scheme for short-term forecasting of the location of afternoon convection, based upon surface and upper-air data available operationally by 1515 GMT. The scheme incorporates three physical concepts regarding the initiation and focusing of "garden-variety" showers and thundershowers. (1) Garden-variety convection is favored in regions of latent instability where mid-level air is not so dry that the convection is eroded via entrainemnt. The K-index (George, 1960) is commonly used as a measure of the likelihood of this type of convection. (2) Surface moisture convergence serves to fuel the convection and is often a precursor to convective development (e.g. Hudson, 1971). (3) Thunderstorms preferably form along mesoscale front-like boundaries which are often associated with differential heating. Thus, convection tends to form at the edges of morning cloud patches (Weiss and Purdom, 1974).

The Forbes et al. (1982) scheme gives a yes or no forecast of afternoon convection in a 2° latitude x 2° longitude region, which has area equal to a circle of about 62 km radius. Forecasts verified at 2135 GMT were correct about 70% of the time with a threat score of about 0.46.

Forecast guidelines:

- Forecast afternoon convection where 3 criteria are met simultaneously at a location:
  1. K-index is greater than 15 at 1200 GMT;
  2. there is surface moisture convergence (negative moisture divergence) at 1500 GMT;
  3. the location is on the strong-heating side of a region of differential heating between 1000 and 1500 GMT (i.e. the Laplacian of the 5h temperature change is negative).

- Thunderstorms are most likely where the surface moisture divergence and Laplacian of the 5h temperature change are quite negative.
- Severe thunderstorms can occur if there is large-scale lifting even if the K-index < 15.

3.3 Precipitation Intensity

Person (1983) examined precipitation amounts for about 30 days in June and July 1982. The highest probabilities of precipitation ($\geq$ .03 cm) and heavy precipitation ($\geq$ 1.27 cm) between 1800 GMT and 0000 GMT were found to occur near the region where there was surface moisture convergence along a front or mesoscale boundary at 1500 GMT. An index, TRW, was devised to quantify this joint event,

$$TRW = (\nabla\cdot(q\vec{V}))|\nabla|\nabla\theta_w||\quad , \tag{3.3.1}$$

where q is the surface mixing ratio, V is the surface wind velocity, and θ_w is the surface wet bulb potential temperature. The term in parentheses is the surface moisture divergence (negative for moisture convergence) and the absolute value term locates the edge of the gradient zones. It is similar to the Laplacian, but shows positive values at both the warm and cold sides of the frontal zone. To confine the consideration to the warm side of fronts, values of (3.3.1) are considered only at locations where the Laplacian of θ_w is negative. This scheme has been used by Cahir and Lottes (1982) for front location. The formulation (3.3.1) is superior to one using the Laplacian directly, because the Laplacian is more sensitive to the curvature of the front and gives inconsistent intensities for equal-intensity fronts of different curvature.

Forecasting guidelines:

- Precipitation between 1800 and 0000 GMT is most likely near the location of the largest negative values of TRW at 1500 GMT (see dot in Fig 3.3.1).
- Precipitation of at least 1.27 cm between 1800 and 0000 GMT is most likely in the dotted regions of Fig. 3.3.1. These are located along and ahead of the front (located left to right in the center of the figure) and downshear with respect to the thermal wind associated with the front. The dotted regions have probabilities in excess of the sample climatological probability of 1.8%.

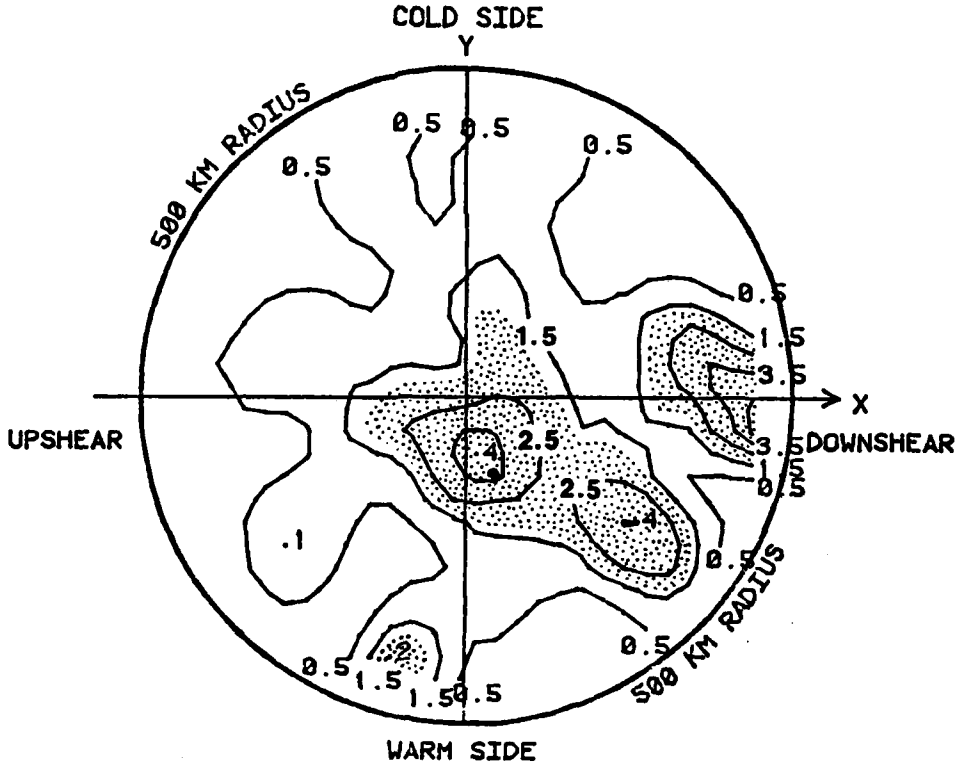

Figure 3.3.1. Composite analysis of the probability of 1.27 cm or more of precipitation between 1800 and 0000 GMT, relative to the TRW maximum at the center of the circle. The stippled region has probability in excess of the sample climatology. The left-right line through the center is parallel to the surface front, as defined by isopleths of wet-bulb potential temperature. The dot somewhat below the right of center is the location of largest precipitation probability of any intensity. From Person (1983).

4. SCHEMES FOR CONTINENTAL FALL AND WINTER NIGHTTIME REGIMES

During fall and winter the cloudiness-change patterns are fairly well determined by the influence of large-scale weather systems. At night, however, fog is a frequent problem, especially in the fall. Accordingly, we describe below two schemes for treating these aspects of the forecasting problem. It appears that the use and prediction of changes in infrared count values, however, is more difficult than with visible count values.

4.1 Statistical Prediction of Cloudiness Change

Satellite imagery was collected on 18 nights between 7 December 1982 and 2 April 1983 (all but two cases were in winter). A pair of images was collected, at 0000 and 0600 GMT on each date. Data were collected, averaged, and processed in a manner identical to that used with visible imagery (see section 3.1.1) via programs developed by Chapman (1983). In this case the imagery was infrared, so that count values relate to radiative temperature. "Un-enhanced" imagery was used, NESDIS Curve ZA (Clark, 1983), in order to have the count value-temperature relationship be unique and as linear as possible. Count value increases indicate cooling, which generally is associated with increasing cloud coverage or height. Count value decreases indicate warming, which generally accompanies the lowering of cloud tops or clearing.

Becuase of the diurnal temperature cycle, infrared imagery exhibits changes of count value in regions of clear sky. That is, the earth's surface cools during the night. Steps were taken to attempt to remove this non-meteorological signal; the sample-average of all nocturnal count value increases (cooling) was subtracted from the field of count change for each case.

Twelve predictor fields were selected or devised from LFM forecasts and observed 0000 GMT data. These are listed in Table 4.1.1. Most of these are self-explanatory, but three joint predictor variables were developed which m erit a bit of discussion. One of these is termed "boundary-layer forcing" (BLF) and combines the observed surface relative geostrophic vorticity and the observed surface dewpoint depression at 0000 GMT. This predictor value is increasingly negative under conditions of large negative vorticity (frictionally-induced divergence) and large dewpoint depression. The predictor value is positive under conditions of positive vorticity (frictionally-induced convergence). Regions where the dewpoint depression is zero are mathematically assigned predictor value zero under positive vorticity (convergent) conditions, as clouds are already likely and the potential for cloudiness increase is greatly reduced.

Another joint predictor variable is the weighted vertical velocity (WVV), which combines the observed 1000-500 mb mean relative humidity at 0000 GMT and a quasi-geostrophic vertical velocity (omega) calculated from 0000 GMT observations (Carlson, 1982). The predictor value is the value of the quasi-geostrophic omega times a weighting factor which is maximum (0.25) at mean relative humidity of 60% and has value of zero at humidities $40 \geq MRH \geq 80$. This predictor was designed to concentrate on regions of intermediate moisture, where vertical velocity is likely to have a sudden impact, as opposed to very dry or very moist regions where a longer period may be needed to produce a cloudiness change.

A third joint predictor is the transition vertical velocity (TVV), which uses observed 1000-500 mb mean relative humidity at 0000 GMT and the LFM forecasts of vertical velocity for 0000 and 0600 GMT. The transition vertical velocity is a maximum when the sign of the vertical velocity changes between

0000 and 0600 GMT and the 0000 GMT mean relative humidity is moderate (70%). The predictor has a value of zero if the vertical velocity does not change sign, and at humidities $40 \geq MRH \geq 100$. If the vertical velocity changes sign, the predictor has the value of the 0600 GMT vertical velocity weighted by a factor which varies with the 0000 GMT mean relative humidity. The weighting factor is 1 at 70% and varies linearly to 0 at 40% and 100%. This predictor is designed to maximize skill at cloud edges.

Despite the inclusion of these complicated predictor variables, the predictions of nighttime count change were less accurate than those using visible imagery. This appears to relate to the comparative uniformity of the averaged infrared data. Prediction equations were developed for the entire domain, for high (count $\geq$ 90), middle, and low (count $\leq$ 60) count values (i.e., cloud tops), and for the pedagogical sample of large count changes. The cumulative reduction of variance for each equation, and the relative contribution of the various terms, is presented in Table 4.1.1.

It can be seen from Table 4.1.1 that, aside from the initial count value, the predictors generally showed little skill in predicting infrared count change. The coefficient of the count value term was negative in each instance, indicating that there was a tendency for initially cloudy regions to become less cloudy, and vice versa. The initial count value was virtually meaningless in relation to low clouds, as might be expected, but no other predictor did well, either--the total explained variance was 10%. For high clouds there was more room for optimism, as about half of the explained variance of 30% was contributed by predictors other than initial count value.

Table 4.1.1

Rank of Predictors and Percent Contribution to Cumulative Explained Variance for Various Predictions of Infrared Count Change Between 0000 and 0600 GMT During Winter 1982-1983

Predictor	Entire Domain	Low Clouds	Middle Clouds	High Clouds	Large Count Change
0000 GMT Count Value	1 90.8%	6 5.5%	1 83.3%	1 46.7%	1 94.9%
LFM Forecast 12-18 h P Change	2 2.9%	7 4.7%	3 5.2%	7 4.2%	2 2.5%
LFM Forecast 12-18 h Mean RH Change	3 2.8%	1 32.8%	2 7.0%		
0000 GMT Boundary Layer Forcing	4 2.2%	5 8.9%	4 3.8%		3 1.6%
LFM Forecast 12-18 h Lifted Index Change	5 1.4%	4 9.3%	5 0.7%	5 6.2%	5 0.4%
LFM Forecast 12-18 h 1000-500 mb Thickness Change				2 17.0%	4 0.6%
0000 GMT 850 mb U Component		3 16.0%		6 6.2%	
0000 GMT 500 mb Wind Speed		2 22.9%			
0000 GMT 850 V Component				3 12.8%	
0000 GMT 200 mb V Component				4 7.1%	
Explained Variance (R^2)	0.25	0.10	0.17	0.30	0.66
Number of Grid Points	13275	3890	8317	1038	1650

Not useful as predictors: weighted vertical velocity, transition vertical velocity.

Table 4.1.2.

Rank of Predictors and Percent Contribution to Cumulative Explained Variance for Various Predictions of Infrared Count Change Between 0000 and 0600 GMT During Winter 1982-1983 When Count Change Due to Steering is Included as a Predictor

Predictor	Entire Domain	% of Explained Variance
Count Change Due to Advection of 0000 GMT Count Pattern	1	84
0000 GMT Count Value	2	9
LFM Forecast 12-18 h Mean RH Change	3	
LFM Forecast 12-18h 1000-500 mb Thickness Change	4	
LFM Forecast 12-18 h Lifted Index Change	5	7
0000 GMT 200 mv V Component	6	
0000 GMT Boundary Layer Forcing	7	
Explained Variance (R^2)	0.48	
Number of Grid Points	13275	

Forecasting Guidelines:

- The area-averaged count value change between 0000-0600 GMT, after allowing for non-meteorological diurnal changes, is

$$\Delta COUNT = 25.88 - 0.405\ COUNT - 0.323\Delta P + 0.111\Delta MRH - 0.492\Delta BLF + 0.289\Delta LI \quad , \qquad (4.1.1)$$

where the variables are defined in Table 4.1.1.

- Regions of initial high cloudiness (initial count $\geq$ 90) are treated slightly better with

$$\Delta COUNT = 94.11 - 1.123COUNT + 1.689\Delta THK - 0.192V_{850} - 0.110V_{200} + 0.917\Delta LI - 0.188U_{850} - 0.731\Delta P \quad , \qquad (4.1.2)$$

where the variables are defined in Table 4.1.1.

- The equations are better for predicting clearing regions and changes in regions of high clouds than for predicting increasing clouds or low and middle clouds.
- The equations are better for predicting cloudiness change patterns than for predicting the magnitude of the count change.

The overall dominance of the initial count value suggests that the cloud patterns were largely translating rather than developing or dissipating. Araujo has experimented further with a new predictor which consists of a "steered" initial count field, allowed to move downwind with the mid-tropospheric trough and ridge pattern. This predictor field has been included with those of Table 4.1.1, and new equations have been developed. Thus, this scheme conceptually explicitly treated movement plus developmental aspects of cloudiness change. The results (Table 4.1.2) indicate that (1) the steering term alone explains considerably more of the variance than that of equations (4.1.1) and (4.1.2) and (2) the other predictors no longer contribute much

once the steered brightness term is used. This is apparently due to the dominance of the IR count-change pattern by high clouds, which evolve rather slowly. A similar experiment will be done with the visible count changes of section 3.1.

Forecasting guidelines:

- Use the forecasted translation velocity of the 500 mb vorticity maximum or minimum nearest the main cloud pattern to advect the initial count value field 6 hrs ahead. The count changes implied by this movement are due to the steady-state steering.
- The area-averaged count value change between 0000-0600 GMT, after allowing for non-meteorological diurnal changes, is

$$\begin{aligned}\Delta\text{COUNT} = {} & 9.05 + 0.529\ \text{COUNT ADV} - 0.166\ \text{COUNT} \\ & + 0.100\ \Delta\text{MRH} + 0.197\ \Delta\text{THK} + 0.275\ \Delta\text{LI} \\ & + 0.016\ V_{200} - 0.242\ \text{BLF} \quad ,\end{aligned} \tag{4.1.3}$$

where the variables are as defined in Table 4.1.2.

4.2 Radiation Fog

Cahir et al. (1978) adapted the scheme of Zverev (1972) for forecasting the dewpoint depression at sunrise based primarily upon the expected nighttime cloudiness and wind speed. The scheme does not explicitly predict fog, but does give some guidance for such a forecast. We initially considered expanding the scheme to account for two factors favorable for fog formation: previous rain and clearing of cloudy skies around time of sunset. However, we chose to deploy our resources on other topics.

Forecasting guidelines:

- Consider the nighttime cloudiness, perhaps using techniques described in sections of this report, and wind speed.
- Use the nomogram below (Figure 4.2.1.) to estimate the nocturnal cooling under clear skies and correct for cloud cover (factor m),

$$T_{min} = T_{19} - m\Delta T_{clear} \quad , \qquad (4.2.1)$$

where T_{min} is the minimum temperature, T_{19} is the air temperature at 1900 local time, and m and ΔT are determined from Figure 4.2.1.

- Consider the probable dewpoint shortly before sunrise, and obtain a forecasted dewpoint depression, $\Delta T_d = T_{min} - T_d$.
- Fog probability can be assessed subjectively from the smallness of the forecasted sunrise dewpoint depression, which will be low when there are clear skies, calm winds, an initially low dewpoint depression, and wet ground.

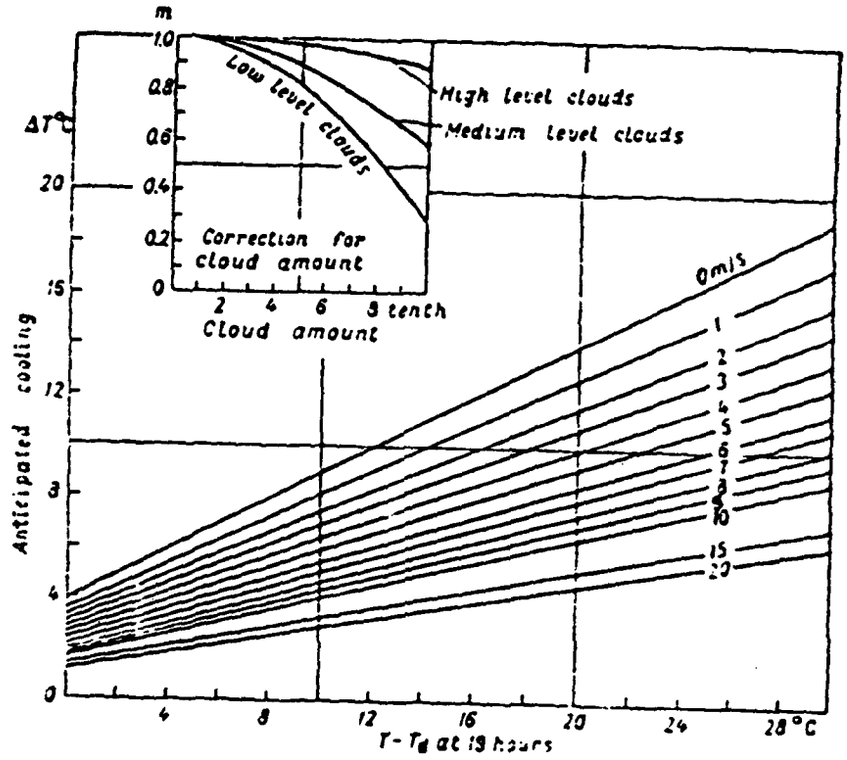

Figure 4.2.1. Graph for forecasting the night minimum temperature from observations at 1800–2000 local time. From Zverev (1972).

5. SCHEMES FOR SPRING AND SUMMER NIGHTTIME CONTINENTAL REGIMES

5.1 Continuation of Daytime Convection

The TRW technique (Person, 1983; see section 3.3 of this report) was examined in relation to the duration of afternoon convection on 30 days of June and July 1982. The relationship was far from foolproof, but long-lasting convection was typically associated with moisture convergence along a well-defined frontal boundary. Specifically, large negative values of TRW at 2100 GMT were indicative of convection persisting beyond midnight. TRW is defined by

$$TRW = (\nabla \cdot q\vec{V})|\nabla|\nabla\theta_w|| \quad , \tag{5.1.1}$$

where q is the surface mixing ratio, $\vec{V}$ is the surface wind velocity, and θ_w is the surface wet bulb potential temperature. The term in parentheses is the surface moisture divergence and the absolute value term is similar to the Laplacian (apart from sign) in that it locates the edges of gradient zones. Cahir and Lottes (1982) have used the gradient term in an objective scheme to locate fronts or front-like boundaries. Thus, TRW is large and negative where moisture convergence (negative divergence) is located along a well-defined front. Only the warm-side edge of the gradient zone should be considered.

Forecasting guidelines:

- Afternoon convection dies out 79% of the time by 0300 GMT when the 2100 GMT value of TRW > -15.
- Afternoon convection continues beyond 0300 GMT 81% of the time when the 2100 GMT value of TRW is $\leq$ -15.
- Convection to be considered must lie within a radius of 300 km from the TRW "maximum", and the technique applies to the VIP level 3 echo; afternoon convection tends to be along the front or in the warm sector

and shift to the cold sector (elevated convection in overrunning flow) during the night.

- Convection sometimes persists, even if the 2100 GMT value of TRW is low, in situations when the 0000 or 0300 GMT values GMT values of TRW become ≤ -15.
- There is a weak tendency for very small values of TRW to be associated with the shortest durations and for very large values to be associated with the longest durations (see Figure 5.1.1).

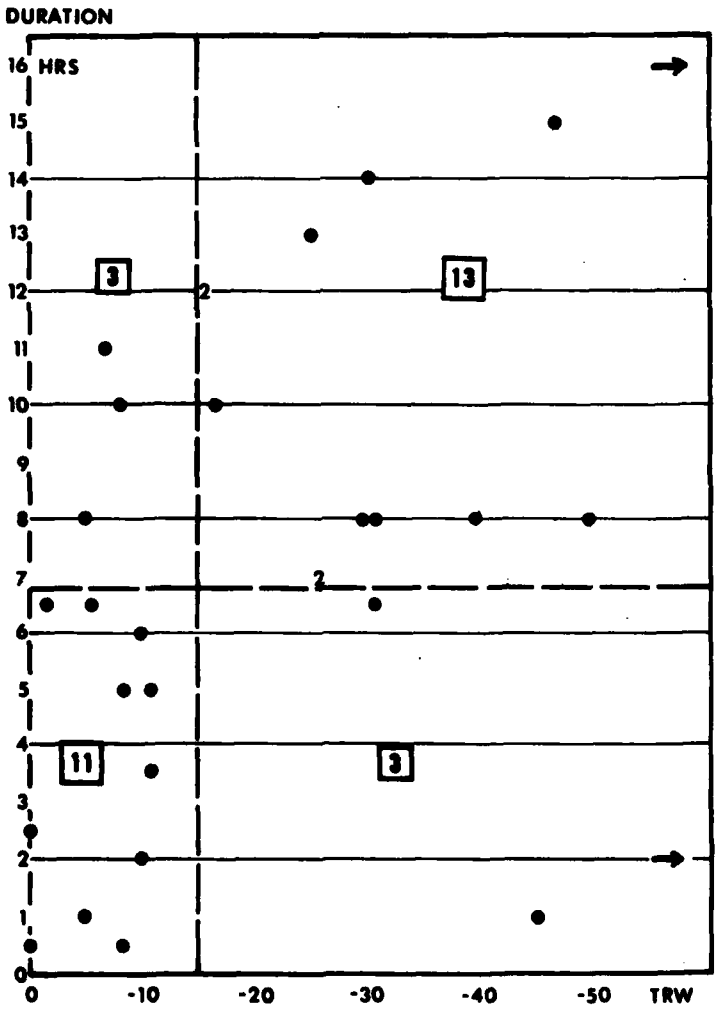

Figure 5.1.1. Duration of afternoon convection beyond 2100 GMT based upon the 2100 GMT value of TRW.

5.2 Nocturnal Thunderstorms

Over a period of years a number of researchers at Penn State (Otten et al., 1984) have examined cases of nighttime thunderstorms. More than 30 cases have been examined. These studies indicate that nocturnal convection is commonly associated with an anabatic flow of air of large wet-bulb potential temperature which overruns a sloping frontal surface. The frontal surface is generally of synoptic-scale origin, though meso-alpha-scale outflow boundaries may also suffice. The front or boundary is associated with horizontal gradients of wet-bulb potential temperature and potential temperature. Adjacent to the front in the warm sector is a tongue or pocket of air of maximum latent instability, manifested by large values of θ_w. The values are typically largest in mid- or late afternoon when the warm-sector boundary layer has been heated to its maximum temperature by insolation.

In the situation described by Otten et al. (1984), the nocturnal convection is elevated. That is, the planetary boundary layer (PBL) beneath the elevated frontal surface at the site of the convection is latently stable, being colder and drier at the onset of convection than the anabatic flow above. Thus, the diurnal evolution of convection is not related to the conditions in the stable boundary layer at the convection site, but <u>is</u> related to the evolution of the boundary layer in the <u>adjacent</u> warm sector (i.e. upwind of the site).

Otten et al. (1984) have shown that the occurrence and location of nocturnal thunderstorms can be forecasted accurately in these situations by considering the regions where the flow near the top of the warm sector PBL at 2100-0000 GMT is directed toward, and is ascending over, the frontal surface. This has been referred to as the "FLUX technique", wherein convection is expected when there is large positive advection of surface θ_w by the 850-700 mb

mean wind. In order to allow for translation, the convection was forecasted downwind of the advection maximum, using the 700 mb wind, by a distance equal to $\overline{V}\cdot\Delta t$, where Δt is the number of hours after 0000 GMT. Merritt and Fritsch (1984) have studied the motion of nocturnal convective systems in more detail.

Forecasting guidelines (Otten et al., 1984):

- Examine regions of the warm sector adjacent to frontal zones (especially warm or stationary fronts) for latent instability, determined by inspection of stability index values and soundings.
- Concentrate on regions where the 850-700 mb mean wind crosses the isopleths of surface wet-bulb potential temperature at 0000 GMT. The wind should be directed from the warm sector toward the cold sector.
- Frontal zones which are poorly defined (without a difference of wet-bulb potential temperature of at least 8°C between the warm and cold air masses adjoining the frontal zone or without a gradient of at least 6°C per 500 km) cannot be considered probable regions of formation of nighttime thunderstorm complexes.
- The value of "FLUX",

$$\text{FLUX} = -\vec{V}_{850}\cdot\nabla\theta_{w\ sfc} \quad , \tag{5.2.1}$$

should exceed $12\text{x}10^{-5}$ K s^{-1} and the maxima should be located in the the center or slightly toward the warm side of the frontal zone. FLUX maxima located too far toward the cold side of the frontal zone indicate that the anabatic flow may not be originating within the latently-unstable warm sector.

- If more than one FLUX maximum occurs, each is expected to be associated with a nocturnal thunderstorm system.

- Thunderstorms are expected to occur within 110 km of the projected FLUX maximum position, which translates downwind with the 700 mb wind. A test of the technique gave 79% correct and a threat score of 0.50.
- Accuracy can be improved slightly by anticipating any changes in the 700 mb wind that will occur overnight (i.e., with adjusted steering). A test of the adjusted steering technique gave 86% correct and a threat score of 0.67.

5.3 A Trajectory Scheme for Forecasting the Onset of Nocturnal Convection

Forbes et al. (1984a) have described a simple interactive trajectory scheme for predicting the occurrence or non-occurrence of nocturnal convection and the location and time of onset of any predicted convection. This scheme is called ACTIVEX, Anafront Activation Experiment. Figure 5.3.1 summarizes the four steps involved in this scheme, lists the interaction required, and gives names of computer programs and key subroutines which comprise the scheme on the Penn State minicomputer system.

The underlying concepts of the ACTIVEX scheme are: (1) nocturnal convection occurs primarily above anabatic frontal zones; (2) convection develops when latently-unstable air from the warm sector is lifted over the frontal surface sufficiently to release its potential instability; (3) the ascent requires a finite "transit time" between the warm sector and the convective location which is typically 6–9 h; (4) the nocturnal convection is a transit-delayed response to the afternoon heating and mixing in the warm sector which generates a maximum of latent instability (θ_w) at the top of the PBL at about 2100 GMT. Thus, the ACTIVEX scheme uses the FLUX technique of section 5.2 in conjunction with warm-sector surface wet bulb potential temperatures at various times of day to predict the buoyancy which may arise along the isentropic trajectories.

Use of the ACTIVEX Scheme:

- The region of interest is near the FLUX maximum (see section 5.2) and up to about 200 km along the front on both sides of the FLUX maximum. This region is defined for the purposes of keeping the number of trajectory computations within the capacity of a minicomputer.
- The anabatic zone of interest will move if (1) the front moves and/or (2) the 850–700 mb flow pattern shifts. The forecaster must consider the

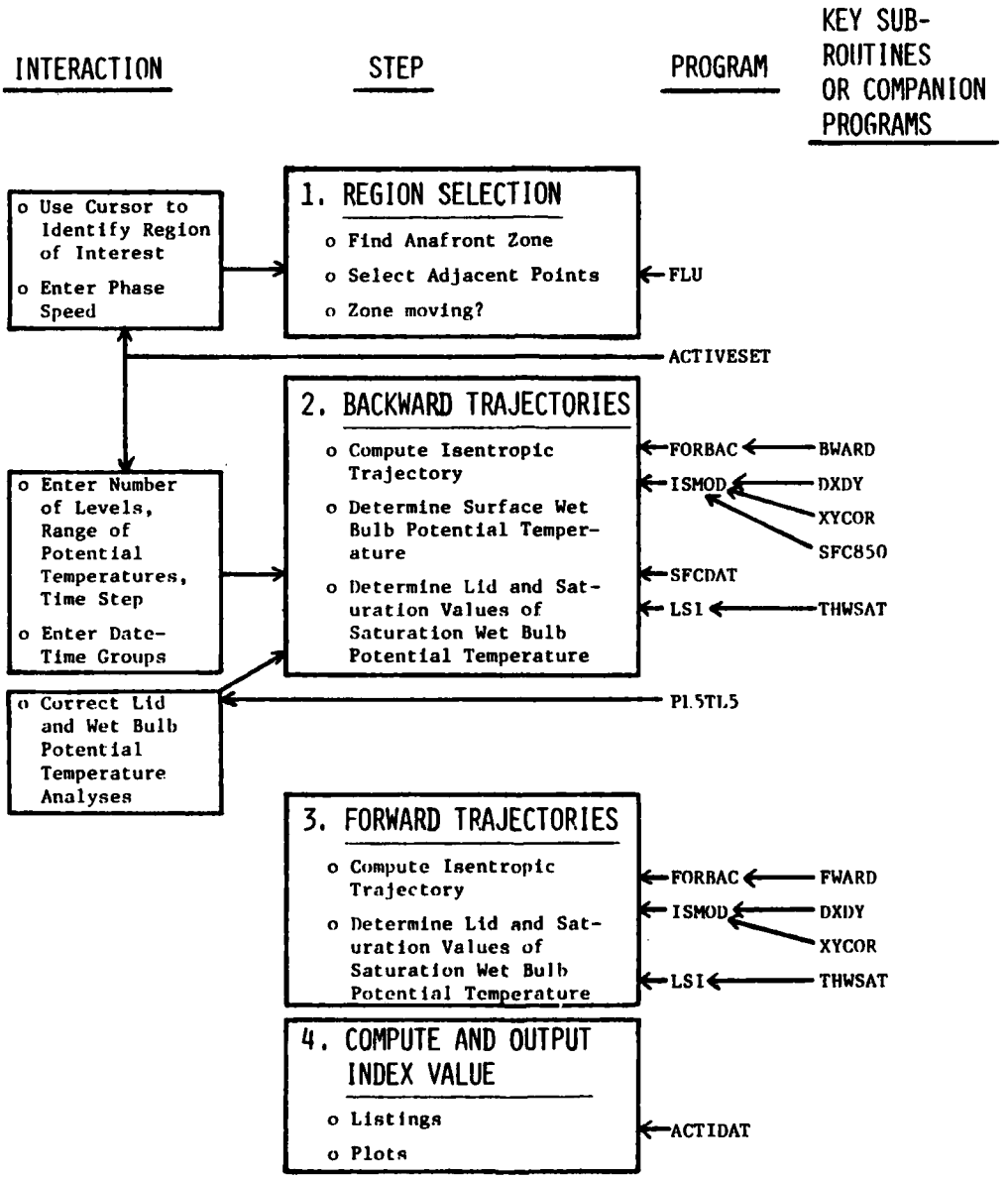

Figure 5.3.1. Concepts and components of the ACTIVEX scheme.

translation of low-level jets (usually with the speed of the mid-tropospheric system), any shifting wind direction, and front movement in order to forecast the movement of the FLUX maximum and specify this "phase speed".

- Usually there is a range of potential temperatures in the warm sector, spatially and temporally. These must be specified in order to compute isentropic trajectories.
- The forecaster can choose the number of isentropic surfaces used (usually enough to have surfaces 2 K apart), the time step of the trajectory calculations (usually 2 h), and the hours of surface observations examined for the latent instability calculations.
- The forecaster must inspect (and correct, if necessary) the objective analysis values of surface θ_w, lid pressure level, and lid θ_{sw}.
- An "index of supercriticality" takes on positive values when the rising parcel (plume) has (1) reached saturation and (2) attained positive buoyancy.

The ACTIVEX scheme has been tested on seven cases, which have also been studied in detail with more conventional forecasting approaches. The ACTIVEX trajectories have been checked against those done by hand using both 0000 and 1200 GMT data, and against LFM trajectory forecasts. Detailed results are presented by Heppner (1984), and are only briefly summarized here. Appendix 5 (which is also a paper by Forbes and Heppner, 1984) further substantiates the hypothesis regarding the cause of the nocturnal nature.

Interpretation of ACTIVEX results:

- The phase speed of the FLUX maximum is usually reasonably approximated by the speed of the front, except when a well-defined low-level jet is present. In that case, the intersection of the (moving) low-level jet and the (moving) front gives the best phase speed.

- The nocturnal convection often occurs in a mid-tropospheric confluence zone, with a weak wave in the northern branch. The low-level wind speed and the anabatic component tend to increase as this wave approaches the convective region.
- Because of the above gradient flow increase, and because of the development of a nocturnal jet, the 0000 GMT winds usually underestimate the true nighttime winds. Incorporation of these effects would improve the trajectories, which generally head in the correct direction but move too slowly. A 20% empirical increase would help.
- The increased wind speeds would improve the forecasts, as the potential instability would be released a bit sooner. The present forecasts are a bit late in starting the convection.
- The use of surface wet bulb potential temperature causes the latent instability of the anabatic flow to be overestimated. Despite turbulent mixing in an adiabatic layer, the mixing ratio typically decreases with height (e.g. Schaefer, 1975; Mahrt, 1975), such that there is also a decrease in θ_w with height in the warm-sector PBL. This needs to be accounted for in the scheme, either in a manner similar to those of Pearson et al. (1967); Mogil and Bonner (1971); Steyaert and Darkow (1973), and Darkow and Tansey (1982), or simply by allowing for the θ_w at the top of the PBL to be 1-2°C cooler than at the surface. This has the effect of requiring an index of supercriticality of + 1 to + 2 (instead of zero) for convective onset.

6. SCHEMES FOR MARITIME REGIMES

With orographic influences absent and diurnal influences suppressed, in some ways the cloud systems over maritime regions are more easy to understand and forecast than those over land. Nevertheless, there are mesoscale bands commonly present in large cloud systems, and mesoscale cloud systems often develop and evolve rapidly when cold air lies over warmer water. Two mesoscale cloud systems which undergo a short-term evolution have been researched, wintertime mesoscale lake vortices (Forbes and Merritt, 1984) and polar vortices (Forbes and Lottes, 1982, 1984). Forecasting guidelines are summarized below.

6.1 Wintertime Mesoscale Lake Vortices

Well-defined mesoscale vortices occasionally (about once per month) form over Lake Michigan, Lake Superior, and Lake Huron in wintertime when the lakes are unfrozen and the air temperature is colder than the water temperature. They range in character from swirls of cloud streets, to a swirl of cloud bands, to a miniature comma cloud. The vortices are typically accompanied by a cyclonic wind circulation of about 5 ms^{-1} and a pressure perturbation of about 1 mb, with showers of snow (steadier snow in the miniature commas) and gusty winds beneath the cloud bands. Travelling cloud bands of the vortices generally deposit less than 2 cm of snow, but may produce locally heavier snows when the bands are quasi-stationary. The vortices appear to form over the lake shortly before sunrise, remain over the lake during the morning, and move inland during later afternoon. For additional details, consult Forbes and Merritt (1984).

Forecasting guidelines:

- Favored by a weak synoptic-scale pressure gradient when the high-pressure system is over or just west of the lake.

- Favored by a mesoscale trough of low pressure over the lake and its associated "land-breeze" convergence, arising in response to the warm lake.
- Often form as disturbances on a band of clouds over the center of the lake, which should be monitored.
- Not associated with typical large-scale cyclogenetic mechanisms; in fact, weak negative vorticity advection and weak cold advection are typically present.

6.2 Polar Vortices

Polar lows and other cold-air vortices are mesoscale phenomena whose existence can be deduced from satellite imagery, and are therefore ideal for treatment with a REMOS approach. Forbes and Lottes (1982, 1984) have examined a sample of 133 cold-air vortices which occurred over the North Atlantic and adjacent seas during the winter of 1981-82. Some of the vortices, detected at their inception via satellite imagery, went on to become intense polar lows, whereas others remained trivial disturbances. These papers indicated that during the first 18 hours of their lifetimes there were a number of differences in the cloud patterns and large-scale environments between vortices which eventually developed and those which remained trivial.

It is expected (but not tested) that these guidelines also apply in the North Pacific and the Mediterranean, where cold-air vortices are also common. The phenomena seem rare in the Gulf of Mexico and western Atlantic.

Forecasting guidelines:

- Satellite imagery can be used to estimate the deficit pressure associated with a cold-air vortex, using Table 6.2.1. Illustrations of the various cloud pattern categories are shown in Figure 6.2.1.

Table 6.2.1

Deficit Pressure of Polar Vortices as a Function of Cloud Pattern

(From Forbes and Lottes, 1982)

CATEGORY	DESCRIPTION	MEAN ΔP
1	COMMA, DEEP SPIRAL	10.1 ± 6.1mb
2	"MERRY-GO-ROUND" OR RING OF VORTICES	8.7 ± 3.2
3	CRESCENT	3.5 ± 2.4
4	OVAL, SOLID MASS	5.7 ± 1.2
5	MULTIPLE DEEP BANDS	4.0 ± 2.3
6	MULTIPLE SHALLOW BANDS	3.5 ± 2.2
7	SINGLE DEEP BAND	4.0 ± 1.4
8	SINGLE SHALLOW BAND	0.0
9	SWIRL IN CUMULUS STREETS	2.9 ± 2.1
STRONG COMMA	DIAMETER > 3.5 DEG LAT OR > 0.5 REVOLUTION)	12.7 ± 6.6
MINOR COMMA	(DIAMETER $\leq$ 3.5 DEG LAT AND $\leq$ 0.5 REVOLUTION)	7.0 ± 3.5

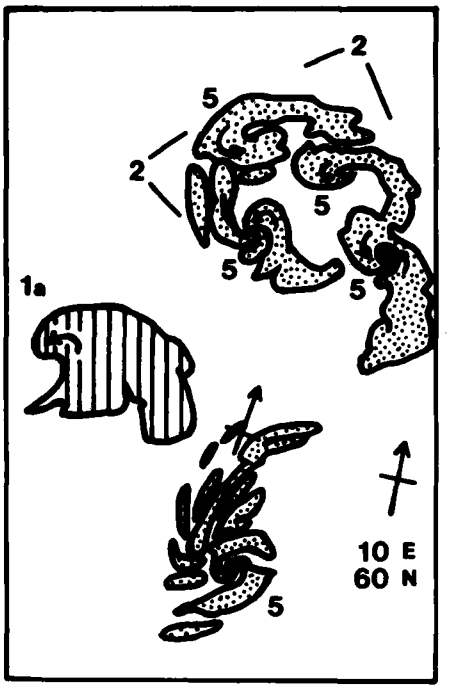

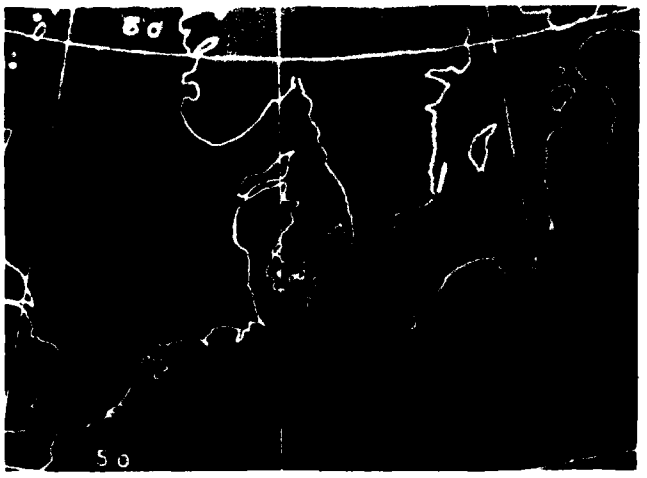

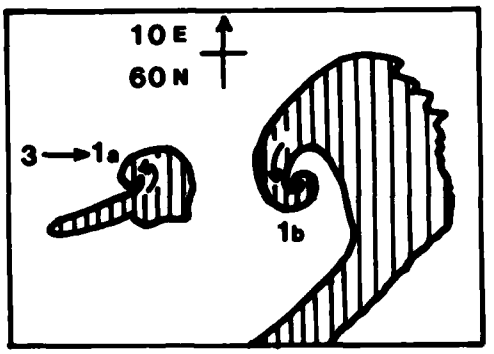

Figure 6.2.1. Illustrations of the categories of cloud configurations of polar vortices; see text for details. Crosses are reference latitude/longitude intersections; arrowheads signify North. From Forbes and Lottes (1984).

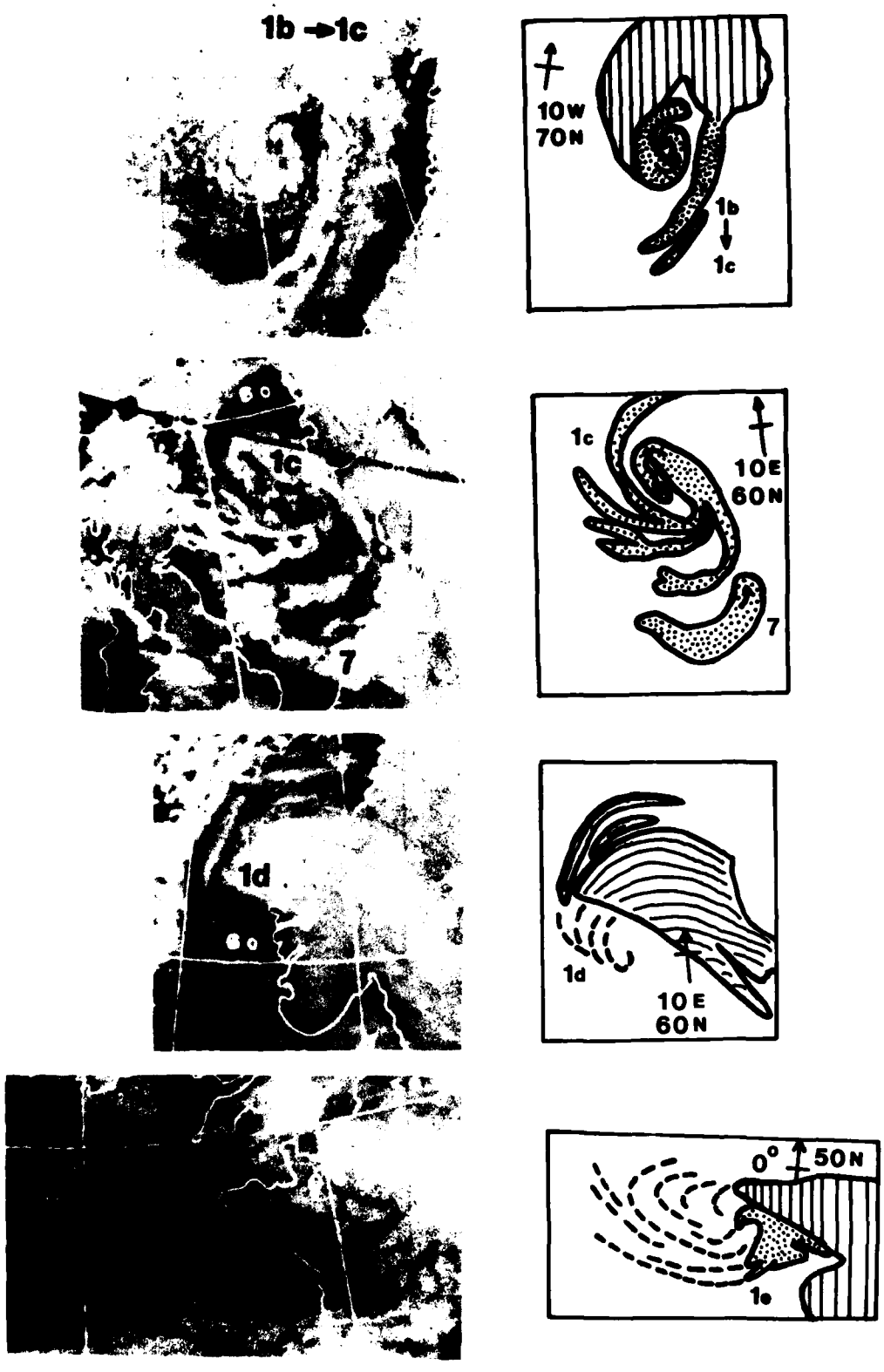

Figure 6.2.1. Cont'd.

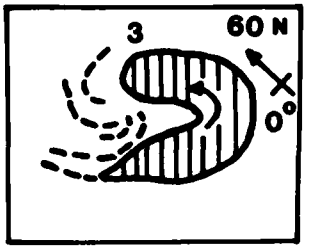

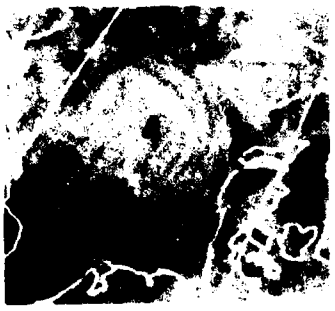

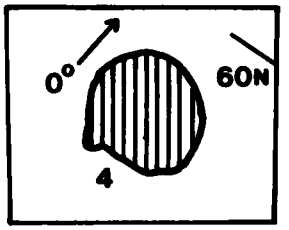

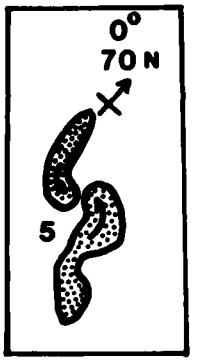

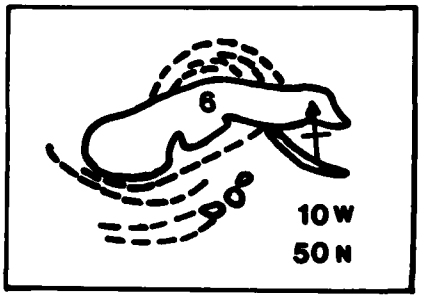

Figure 6.2.1. Cont'd.

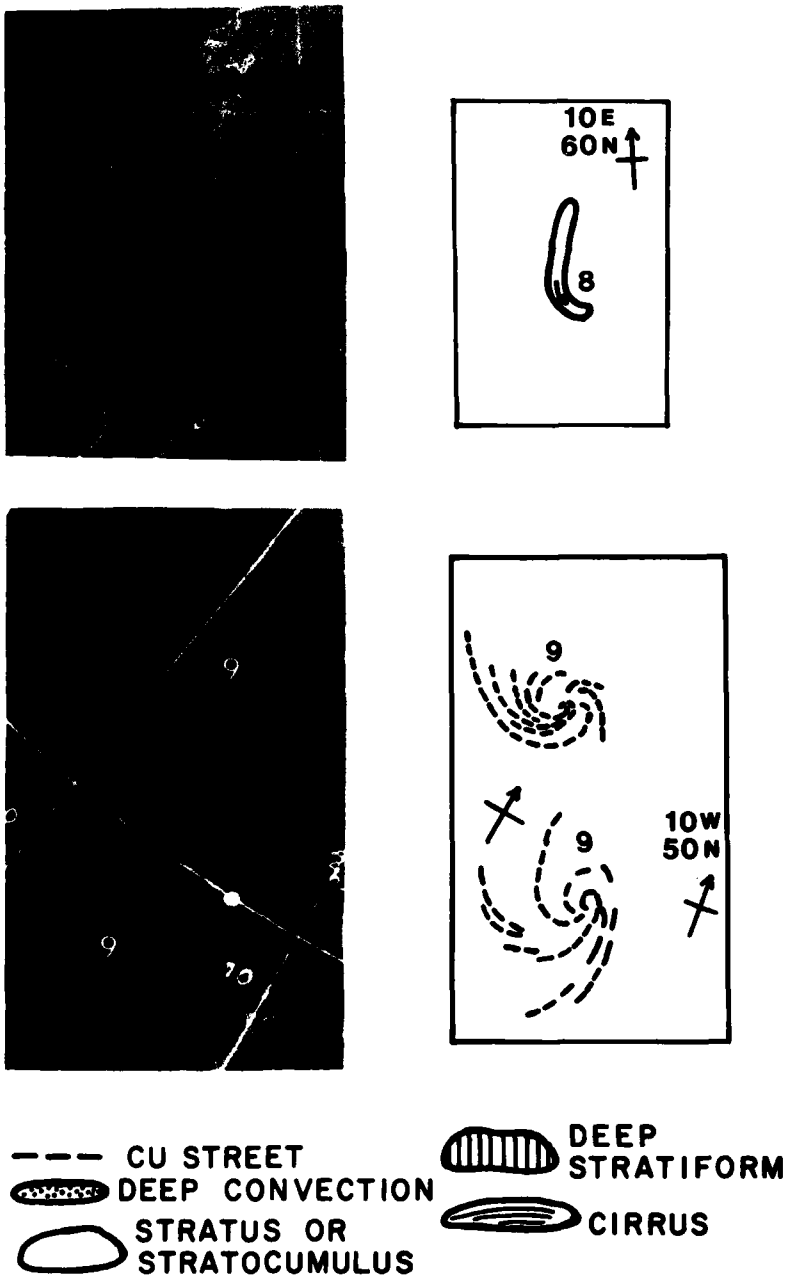

Figure 6.2.1. Cont'd.

- The cloud category gives a first estimate of whether the vortex will remain insignificant, become a steady (moderate) disturbance, or develop into a significant storm. Table 6.2.2 shows the probabilities of expected development based upon instantaneous category examination.
- If previous satellite imagery is consulted and it can be ascertained that the vortex has not yet been in category 1 or 2 shape, then Table 6.2.3 gives a more reliable probability of the future development.
- Vortices which are developing, or those having already developed, frequently have a vertical wind shear that is reversed from normal. That is, the mid-tropospheric wind and thermal wind are nearly opposite in direction. See Table 6.2.4.
- Developing polar vortices tend to occur under conditions of weak positive advections of absolute and thermal vorticity, whereas non-developing vortices tend to have negative values of those advections.

Statistical Prediction

Forbes et al. (1984b) further examined the Forbes and Lottes (1982) data base and developed a statistical prediction equation to determine which newly-detected vortices bear continued monitoring as potential polar lows. They defined the vortex category (CAT) in terms of the ultimate vortex development: 0 indicates an insignificant disturbance, 0.5 indicates a modest disturbance of about 5 mb pressure deficit, and 1.0 denotes a developing polar low which attains a pressure deficit of more than 8 mb. The prediction equation is

$$\begin{aligned} CAT = {} & -3.36 + 0.610\ CLDCONFG + 0.151\ DIA - 0.006\ UG + 0.038\ UT \\ & - 0.006\ AVGWSP + 0.009\ LAT + 0.010\ AVGTMP \quad . \end{aligned} \tag{6.2.1}$$

Table 6.2.2

Relationship Between Cloud Category and Vortex Nature

CATEGORY	SIGNIFICANT (Developing or Dissipating Comma)	STEADY	INSIGNIFICANT
1	79%	21%	0%
2	100%	0%	0%
3	47%	24%	29%
4	40%	10%	50%
5	19%	26%	55%
6	0%	33%	67%
7	0%	50%	50%
8	0%	0%	100%
9	13%	13%	74%
STRONG COMMA	91%	9%	0%
MINOR COMMA	65%	35%	0%

Table 6.2.3

Probability of Vortex Nature Based Upon Cloud Cateogry, If Category 1 or 2 Has Not Yet Been Reached

CATEGORY	DEVELOPING	STEADY	INSIGNIFICANT
3	50%	19%	31%
4	40%	10%	50%
5	10%	28%	62%
6	0%	25%	75%
7	0%	33%	67%
8	0%	0%	100%
9	0%	15%	85%

In 6.2.1, CLDCONFG is the probability of a polar low developing, given the initial cloud configuration (see Table 6.2.5); DIA is the diameter of the vortex circulation in degrees of latitude; UG is the u component of the 1000 mb geostrophic wind in m s^{-1}; UT is the u component of the 1000 mb thermal wind in m s^{-1} $(km)^{-1}$; AVGWSP is the 1000-500 mb average wind speed in m s^{-1}; LAT is the latitude; AVGTMP is the mean temperature in the 1000-500 mb layer in °K. The predictors are listed in decreasing order of importance, the multiple correlation coefficient is 0.703, and the root-mean-square error in CAT is 0.27. Thus, it is possible to predict developing vs. non-developing polar vortices.

Table 6.2.4.

Vertical Wind Shear and Vortex Nature

NATURE	NORMAL SHEAR	REVERSED SHEAR
Developing	21%	79%
Steady	67%	33%
Insignificant	68%	32%
Dissipating Comma	33%	67%

Table 6.2.5.

Relationship Between Cloud Configuration and CLDCONFG Parameter

Cloud Configuration	CLDCONFG
Comma Shape	0.79
"Merry-go-round" or Ring of Vortices	1.00
Crescent Shape	0.50
Solid Oval or Circular Mass	0.40
Multiple Deep Bands	0.10
Shallow Bands, Single Band	0.00

Appendix 1.

Major Project Tasks

Quantitative Satellite Data Processing Capability Development

- Scheme for co-locating minicomputer objective analyses of conventional data on satellite imagery.
- Scheme to obtain area-averaged satellite count values to match grid points of objective analyses.
- Adjustments of satellite imagery (removal of overlaid state borders, adjustment for non-meteorological fluctuations of image brightness, etc.)
- Scheme for overlaying minicomputer objective analyses on satellite image.

Archiving of Satellite Imagery for Research Tasks

Regression Equations for Spring/Summer Daytime Visible Count Value Change

- Predictor selection (case studies)
- Generation of predictor and predictand fields
- Software for input and output from statistical package (BDMP)
- Generation and analysis of regression equations

LFM Humidity Studies

- Biases and RMS errors of analyses and forecasts to 24 h
- Biases and RMS errors of humidity-change forecasts
- Geographically-linked systematic error patterns
- Systematic error patterns by weather regime
- Accuracy of humidity estimates based upon cloud observations

Nocturnal Convection Studies

Studies of duration of continued afternoon convection

Case studies of newly-developing nocturnal convection

Development of trajectory scheme for prediction of the location and timing of nocturnal convection

Wintertime Mesoscale Lake Vortex Studies

Polar Vortex Studies

Prediction based upon satellite imagery

Prediction based upon environmental conditions

Development of multiple regression prediction equation

Review of Past Minicomputer Studies

Afternoon convection scheme

Heavy precipitation scheme

Radiation fog scheme

Development of Master Framework for Short-Term Prediction Scheme

(In addition, we made some preliminary investigations regarding the use of VAS water vapor channel data and LFM trajectories as elements of a forecast scheme, as well as a scheme for automated classification of the fractional cloud cover within our averaging regions. It was not feasible to adopt these ideas for the present research, however.)

Appendix 2.

List of Project Participants

Gregory S. Forbes, Principal Investigator

John J. Cahir, Co-Principal Investigator

Walter D. Lottes, Research Assistant

Kathy Chapman, Graduate Student

Paul A. Dorian, Graduate Student

Ernesto Araujo, Graduate Student

Paul O. G. Heppner, Graduate Student

Robert L. Scheinhartz, Graduate Student

Occasional assistance was also provided by: Dr. Tom Trimarchi, Arthur Person, Gary Salamon, Andrew Miller, Doug Litchfield, and a number of students.

The authors are grateful for the typing assistance of Delores Corman, Nancy Warner, and Joann Singer. The administrative assistance of Kathy Matason and Don Fornwalt is greatly appreciated. The authors benefited from discussions with the AFGL monitors, H. Stuart Muench and Don Chisolm.

Appendix 3.

List of Papers and Reports Prepared
(Listed chronologically)

Forbes, G.S. and W.D. Lottes, 1982: Characteristics and evolution of mesoscale cloud vortices occurring in polar airstreams. Preprints, Conf. on Cloud Physics, Chicago, Am. Meteor. Soc., p. 310-313.

Forbes, G.S., J.J. Cahir, P. Dorian, W.D. Lottes and K. Chapman, 1983: Development of a technique for short-term prediction of hydrometeors using advection and physical forcing. Scientific Rept. No. 1, Air Force Geophysics Laboratory Contract F19628-82-K-0023 and AFGL Tech. Rpt. 83-0082, 72 pp.

Chapman, K., 1983: Interactive use of combined minicomputer and satellite technology capabilities in assessing short-term changes in cloud patterns. M.S. Thesis, The Pennsylvania State University, 66 pp.

Dorian, P., 1983: Interactive use of minicomputer capabilities in assessing short-term humidity forecasts by the LFM-II model. M.S. Thesis, The Pennsylvania State University, 84 pp.

Forbes, G.S. and J.H. Merritt, 1984: Mesoscale vortices over the Great Lakes in wintertime. Mon. Wea. Rev., 112, 377-381.

Forbes, G.S., P.O.G. Heppner, J.J. Cahir and W.D. Lottes, 1984: Prediction of delayed-onset nocturnal convection based on air trajectories. Preprints, 10th Conf. on Wea. Forecasting and Analysis, Clearwater Beach, FL, Am. Meteor. Soc., 474-479.

Forbes, G.S., R.L. Scheinhartz, E. Araujo, W.D. Lottes and J.J. Cahir, 1984: Short-term forecasting using a REMOS approach. Proc., 2nd Int'l. Symp. on Nowcasting, Norrkoping, Sweden, 379-384.

Forbes, G.S. and W.D. Lottes, 1984: Classification of mesoscale vortices in polar airstreams and the influence of the large-scale environment on their evolutions. Accepted for publication in Tellus.

Dorian, P.A., G.S. Forbes and J.J. Cahir, 1984: Evaluation of humidity forecasts of an operational model. Submitted to Mon. Wea. Rev..

Otten, H.A.F.M., J.J. Cahir, G.S. Forbes, P.A. Hubanks and W.D. Lottes, 1984: A technique for short-term forecasting of the development of nocturnal convective complexes. Submitted to Mon. Wea. Rev..

Forbes, G.S. and P.O.G. Heppner, 1984: New evidence on the cause of nocturnal thunderstorms. Submitted to J. Atmos. Sci.

Forbes, G.S., 1984: Statistical forecasting of the short-term changes of mesoscale systems--polar lows as a demonstration of concept. To be submitted to Tellus.

Araujo, E., 1984: Forecasting short-term cloudiness change as inferred from cold-season nighttime infrared satellite imagery. M.S. Thesis, The Pennsylvania State University, in progress.

Heppner, P.O.G., 1984: Application of an air trajectory model to test a theory concerning nocturnal thunderstorm development. M.S. Thesis, The Pennsylvania State University, in progress.

Scheinhartz, R.L., 1985: Forecasting short-term cloudiness change as inferred from warm-season daytime visible statellite imagery. M.S. Thesis, The Pennsylvania State University, in progress.

Appendix 4

STATISTICAL PREDICTION OF CLOUDINESS CHANGE

Details of the techniques used in preparing the predictand fields (satellite data) and the predictor fields (LFM forecast data and observed data) have been presented by Forbes et al. (1983) and by Chapman (1983). Summaries of the results of studies of short-term changes in summer daytime visible and winter nighttime infrared count values, using these techniques, have been presented in sections 3.1 and 4.1, respectively. The purpose of this appendix is to discuss a few interesting results of the studies, and to present examples. Complete documentations of these studies are being prepared by Scheinhartz (1985) and Araujo (1984).

A4.1 Spring and Summer Daytime

Regression equations and contributions to the reduction of variance by the various predictors have been presented in section 3.1. Table A4.1 presents the individual correlation coefficients between the various predictors and the six-hour change of visible count values, for the 30-case sample. For reference, the ranks (in terms of contribution to reduction of variance) in the equations of section 3.1 are also shown.

It can be seen from Table A4.1 that some of the predictors with fairly large correlation coefficients, as large as 0.634 for the large-brightness-change stratification, were not used in the final regression scheme. This is because these predictors were highly correlated with some other previously-selected predictor, usually initial brightness count value. Thus, they did not provide any substantial amount of additional information.

An interesting result of these studies is that surface moisture divergence had virtually no correlation to brightness change for any stratification. This was unexpected, as surface moisture convergence has been shown

Table A4.1

Rank of Predictors and Individual Correlations to Visible Brightness Change

Between 1500 and 2100 GMT During Spring/Summer 1983

Predictor	Entire Domain	Partly Cloudy	Clear	Cloudy	Warm Thickness	Cold Thickness	Large Brightness Change
1500 GMT Brightness	1 -0.355	3 -0.130	4 -0.149	4 -0.130	1 -0.407	1 -0.457	1 -0.675
1200 GMT 1000-700 mb Thickness	2 -0.269	2 -0.385	1 -0.401	2 -0.286	4 0.008	4 -0.153	3 -0.361
LFM Forecast 12-24h Mean RH Change	3 0.331	1 0.479	3 0.227	1 0.323	2 0.253	2 0.354	2 0.518
1200 GMT K Index	4 -0.297	5 -0.336	2 -0.158	x -0.243	3 -0.063	x -0.342	x -0.508
1200 GMT Surface Wind Speed	5 0.139	4 0.264	x 0.139	3 0.254	x -0.069	3 0.197	4 0.198
1200-1500 GMT Surface P Change	x -0.136	6 -0.279	x -0.137	x -0.100	x -0.200	x -0.061	x -0.224
1200-1500 GMT Surface T Change	x 0.275	x 0.214	5 -0.084	x 0.088	x 0.331	x 0.318	x 0.592
1500 GMT Surface P	x 0.134	x 0.006	x 0.111	x -0.100	5 -0.004	5 0.269	x 0.261
1500 GMT Surface Moisture Div.	x 0.001	x -0.095	x -0.112	5 -0.018	x -0.012	x 0.028	x 0.048
1500 GMT Surface Dewpoint Depression	x 0.346	x 0.276	x 0.082	x 0.281	x 0.293	x 0.373	x 0.634
1200 GMT, 500 mb Absolute Geostrophic Vort.	x 0.020	x -0.030	x 0.060	x 0.100	x -0.080	x 0.038	x 0.021

to be useful in short-term forecasting of showers and thundershowers (Forbes et al., 1982), and had a modest correlation to brightness change in a smaller sample (Forbes et al., 1983). This suggests that the regression equations are highly dependent upon both sample size and nature. Forbes et al. (1983) have previously shown that the correlation coefficients vary substantially between cases of different weather regimes (stratiform versus convective). Further illustration of this is presented in the following examples.

Statistically, the regression equations presented in section 3.1 appear to possess modest skill. Aside from the pedagogical stratification of large brightness change, the cumulative reduction of variance is about 0.4. A case-by-case inspection of the fields predicted via equation (3.1.1), however, suggests that the predicted fields are rather useful. The fields lose apparent skill by having less amplitude than the observed field of brightness count-change, but generally capture the pattern of change rather well. We may consider an inflation factor to bring this out more clearly.

The case of 25 May 1983 is an excellent example of the skill of the regression equation at predicting the brightness-change pattern. Figure A4.1 shows the initial (1430 GMT) averaged brightness and satellite imagery. There is a well-defined band of frontal clouds across MI, IN, and IL which is chiefly due to large-scale (as opposed to convective) forcing. Over the western Atlantic, a band of stratus clouds extends toward Delaware, and some convective clouds extend toward South Carolina. By 2030 GMT, Figure A4.2, the frontal band has moved eastward into Ontario, Ohio, Kentucky, and Tennessee. The Delaware stratus band has dissipated somewhat, but convective clouds have grown in western North Carolina and along the GA/SC border.

Figure A4.3 shows the observed 6-hour brightness change and the brightness change predicted through use of eq. (3.1.1). It can be seen that the band of brightness decreases across MI, IN, and IL is shown in the predicted

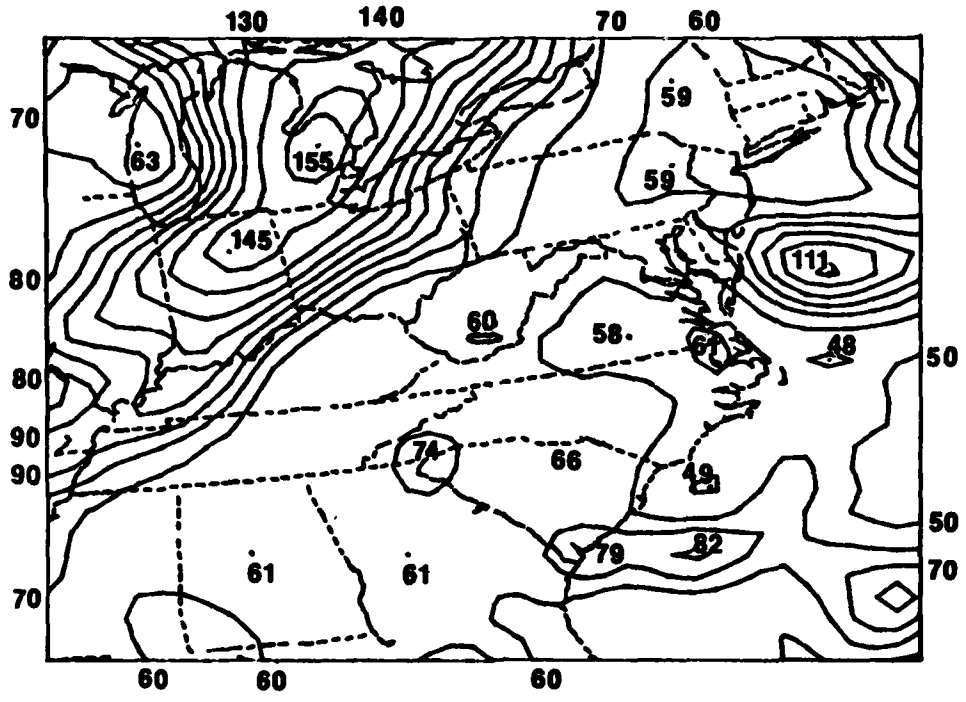

a

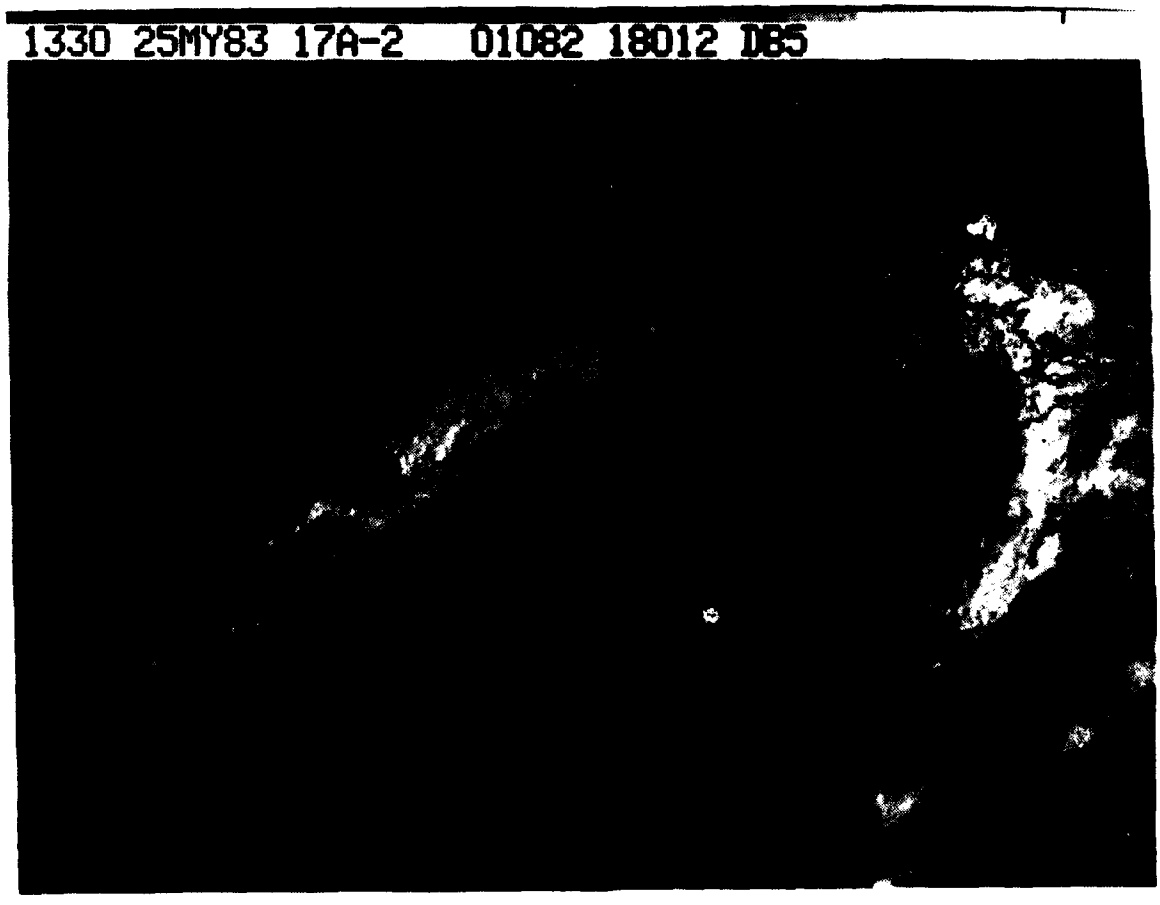

b

Figure A4.1. Averaged brightness (count values) at 1430 and satellite imagery at 1330 GMT on 25 May 1983.

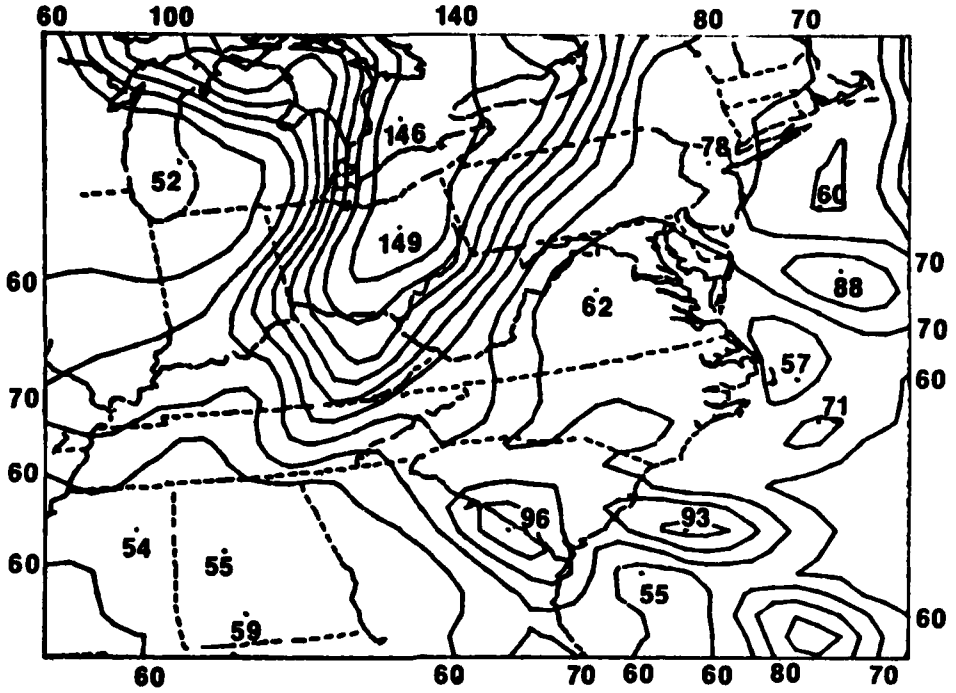

a

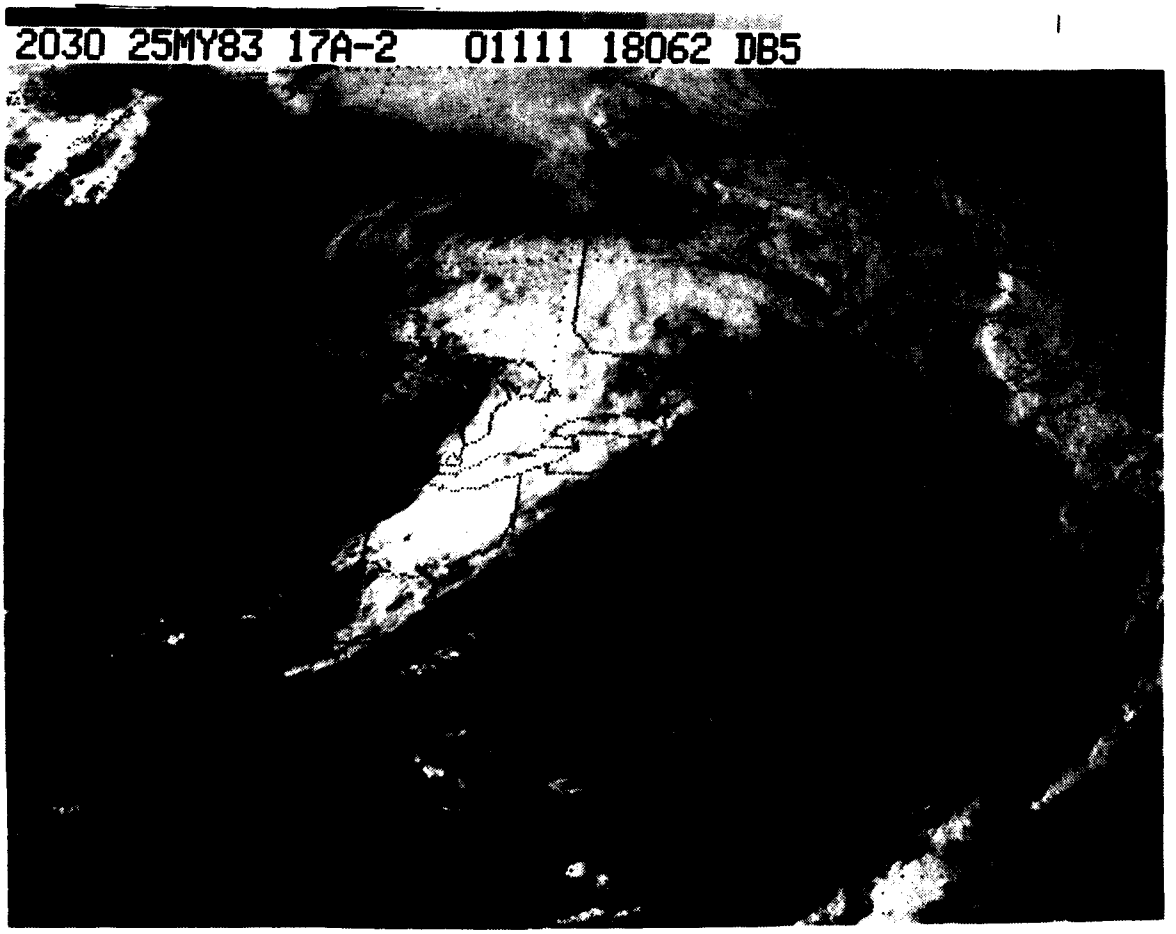

b

Figure A4.2. Averaged brightness (count values) and satellite imagery at 2030 GMT on 25 May 1983.

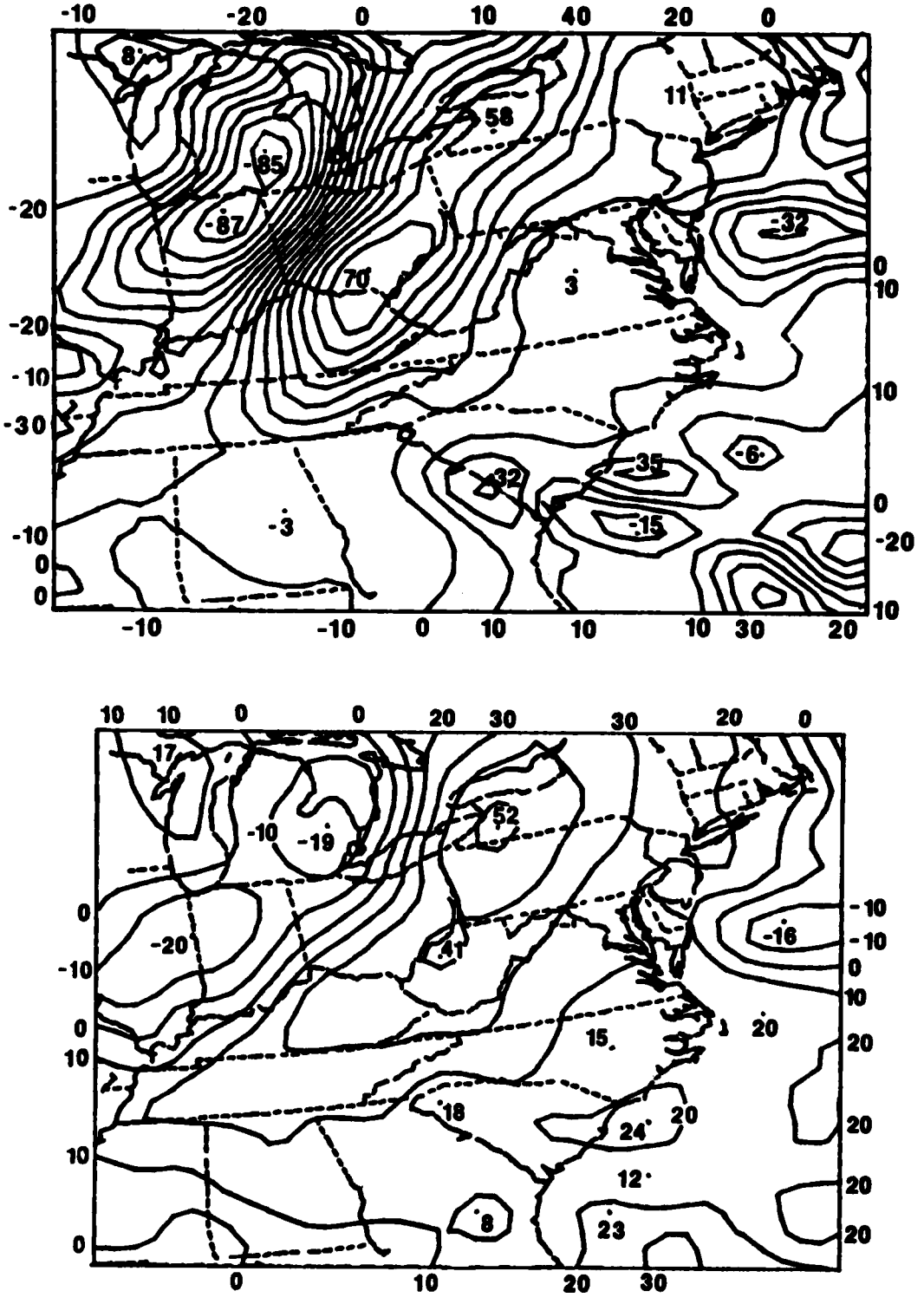

Figure A4.3. Observed (a) and predicted (b) 6-hour brightness (count value) change between 1430 and 2030 GMT on 25 May 1983.

field, but predicted changes are less than 20 counts whereas decreases of up to 87 counts were observed. Similarly, the band of brightness increases from western NY to eastern TN is present in the predicted pattern, but with subdued amplitude. The patterns off DE and over SC exhibit the same traits. The predicted pattern even has a lobe of maximum brightness increases in west central NC, where modest convective clouds developed.

Figure A4.1a and A4.4-A4.7 show the 5 predictor fields used to generate the predicted brightness change (Fig A4.3b). It can be seen that the initial brightness, the leading predictor in the 20-case sample (Fig. A4.3a), correlates quite well with the observed brightness change (Fig. A4.3a) in the initially cloudy regions, but much less so elsewhere.

The coefficient of the initial brightness term in eq. (3.11) is -0.463, so this term contributed brightness decreases of up to -70 in MI and IN. Since the predicted decreases were only up to -20, the other 4 terms made a substantial contribution to reducing the amount of brightness decrease. The other 4 terms also contributed totally to the areas where brightness increased, as there were no initial negative brightnesses.

The second predictor in the 30-case sample is 1000-700 mb thickness, shown in Fig. A4.4. The coefficient is -0.178, such that this term would have contributed to a relative brightness increase in a band from southeastern MI to souther IL and to a relative minimum from eastern NY to central TN. Overall, however, the thickness and brightness change patterns are not well correlated, as revealed in Table A4.2, such that the thickness term is degrading the results in this case.

The third predictor in the 30-case sample is the LFM forecast of 12-hour humidity change, Figure A4.5. The best correlation here is in the area of

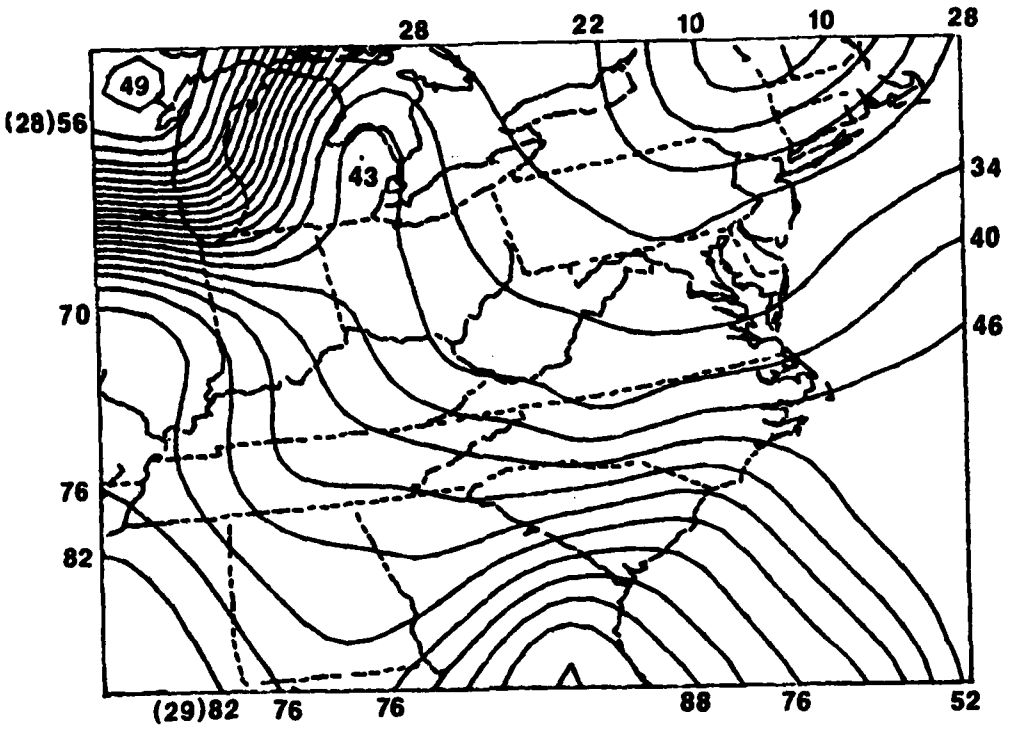

Figure A4.4. 1000-700 mb thickness (meters, with 2800 or 2900 subtracted) at 1200 GMT on 25 May 1983.

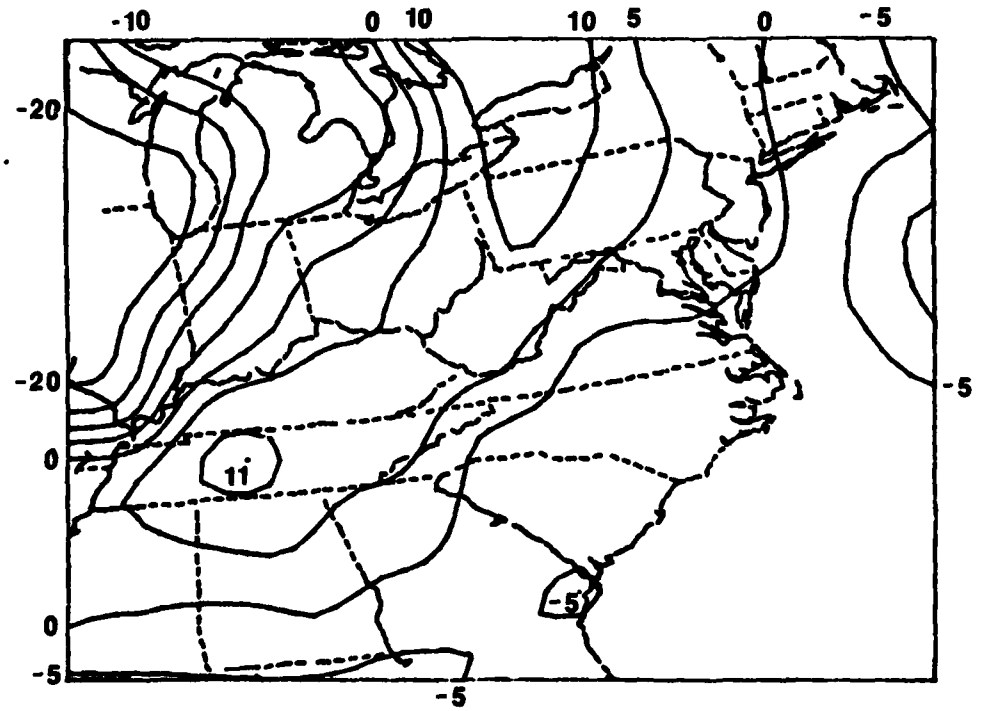

Figure A4.5. LFM forecast of 12-hour change of mean relative humidity, ending at 0000 GMT on 26 May 1983.

Table A4.2

Individual Correlations of Predictors to 1430-2030 GMT

Visible Brightness Change on 25 May 1983,and for 30-Case Sample

Predictor	1- Case Correlation	30-Case Correlation	30-Case Rank
1500 GMT Brightness	-0.593	-0.355	1
1200 GMT 1000-700 mb Thickness	-0.093	-0.269	2
LFM Forecast 12-24 h Mean RH Change	0.597	0.331	3
1200 GMT K Index	-0.236	-0.297	4
1200 GMT Surface Windspeed	-0.152	0.139	5
1200-1500 GMT Surface P Change	-0.524	-0.136	x
1200-1500 GMT Surface T Change	0.526	0.275	x
1500 GMT Surface P	0.252	0.134	x
1500 GMT Surface Moisture Div	0.104	0.001	x
1500 GMT Surface Dewpoint Depression	0.523	0.346	x
1200 GMT, 500 mb Absolute Geostrophic Vorticity	0.118	0.020	x

synoptic-scale brightness increases from western NY to central TN, with much poorer correlation elsewhere. The coefficient of this term in eq. (3.1.1) is 1.525, so that this term contributed to an increase of brightness of up to 20% in the band of brightness increases.

The fourth predictor in the 30-case sample is the K-Index, Figure A4.6. The coefficient in eq. (3.1.1) is 0.423, so that this term is contributing to brightness increases from MI to IL. There is some correlation in other regions, except in the synoptic-scale band of brightness increases.

The fifth predictor in the 30-case sample is surface wind speed, Figure A4,7. In this case the correlation is opposite from that in the 30-case sample (Table A4.2), so the contributions of this term are fortuitous.

It should be noted that in this case three predictors with large (>0.5) correlation coefficients were not used: surface dewpoint depression, surface temperature change, and surface pressure change. In each instance the correlation in this case was much higher than in the 30-case sample. An inspection of these fields indicates that the amplitude of the main synoptic drying and moistening bands would have been somewhat better had the regression equation included these terms.

Figure A4.8 shows the initial and final visible satellite imagery for another case, that of 17 June 1983. Figure A4.9 shows the observed and statistically-predicted brightness count changes for this case. The case again was considerably influenced by synoptic-scale forcing, but also had a substantial convective component, as convective developments occurred in MS, in a line from western PA southward along the Appalachians, in central KY and TN, and along the Ohio River near Cincinnati. It can be seen that these developments were not predicted well, though the overall patterns of increasing and decreasing cloudiness were reasonably accurate.

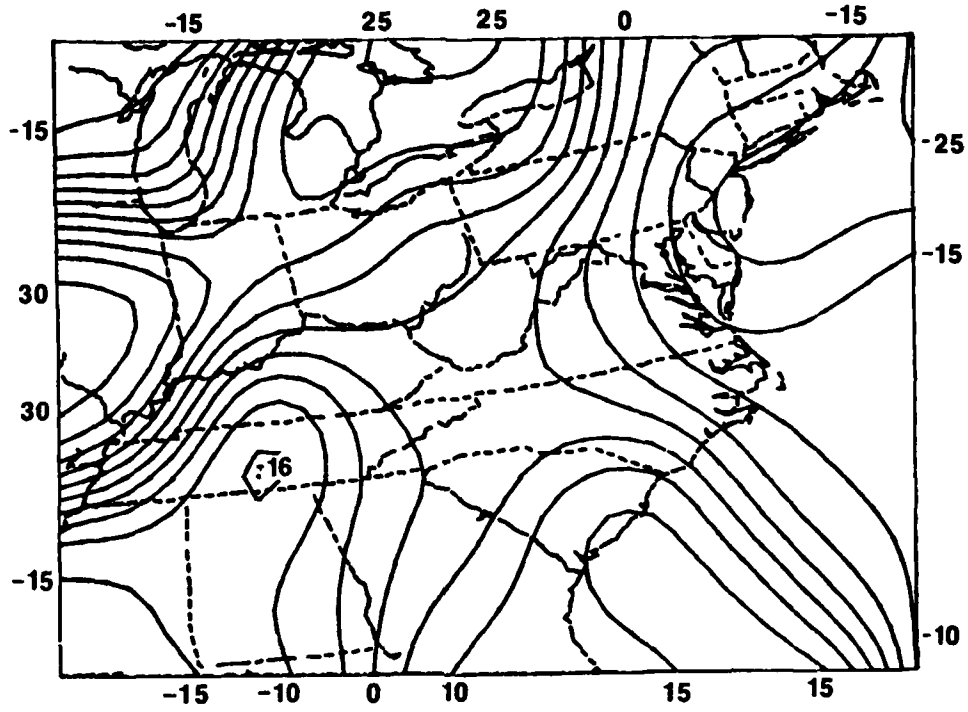

Figure A4.6. K-Index at 1200 GMT on 25 May 1983.

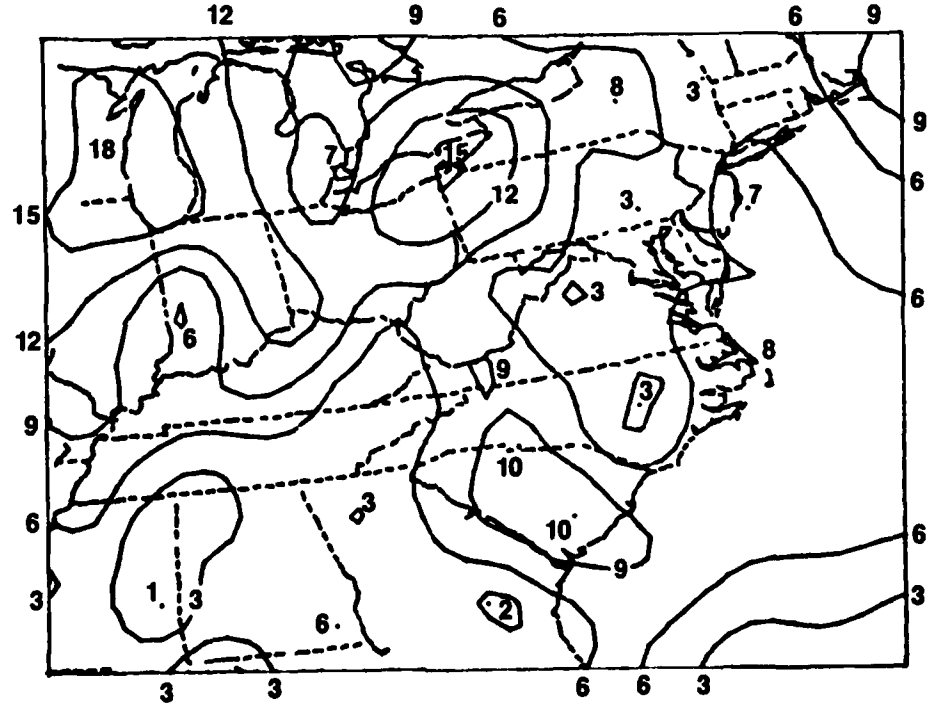

Figure A4.7 Surface wind speed (knots) at 1500 GMT on 25 May 1983.

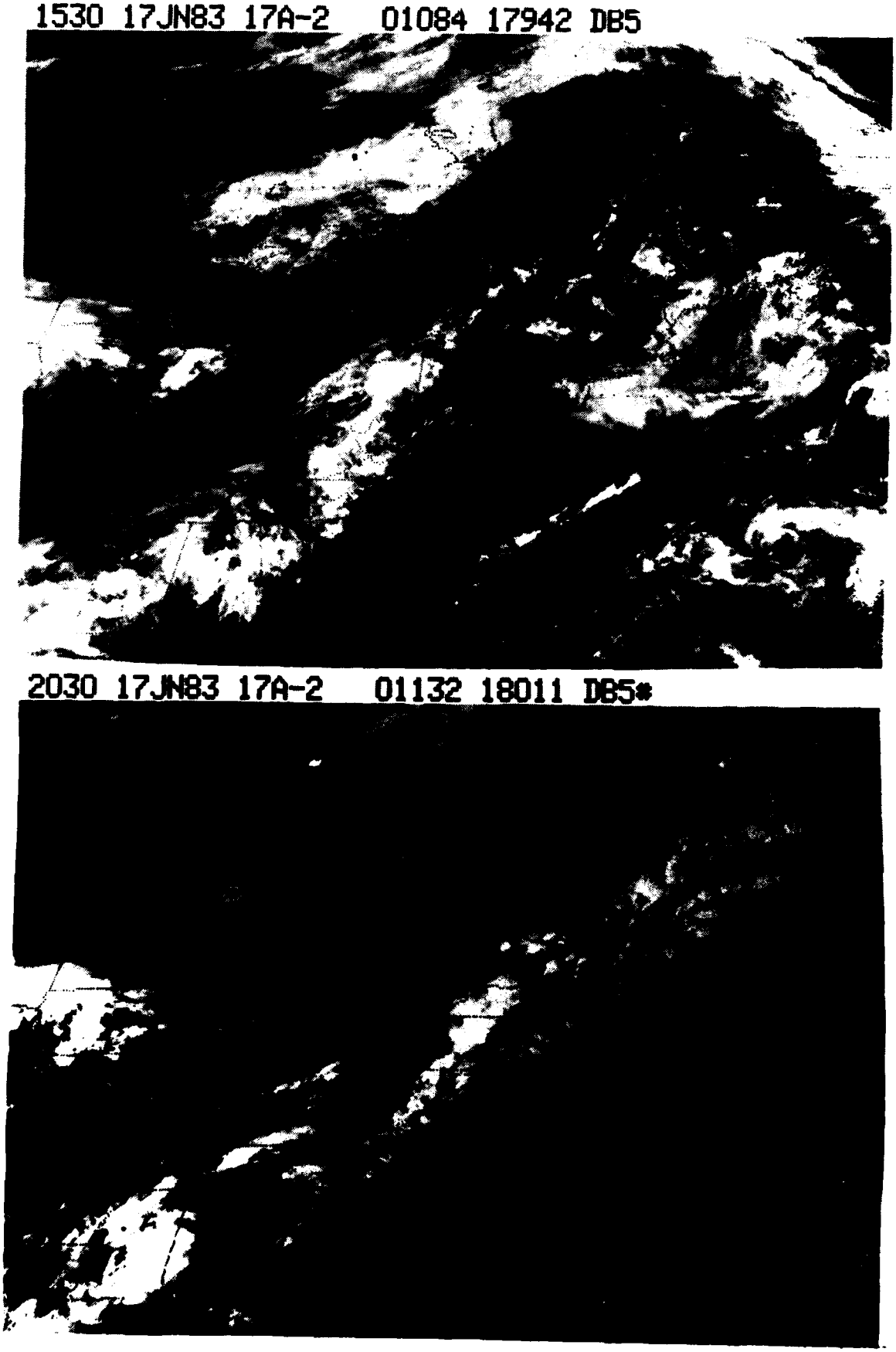

Figure A4.8. Visible satellite imagery at 1530 and 2030 GMT on 17 June 1983.

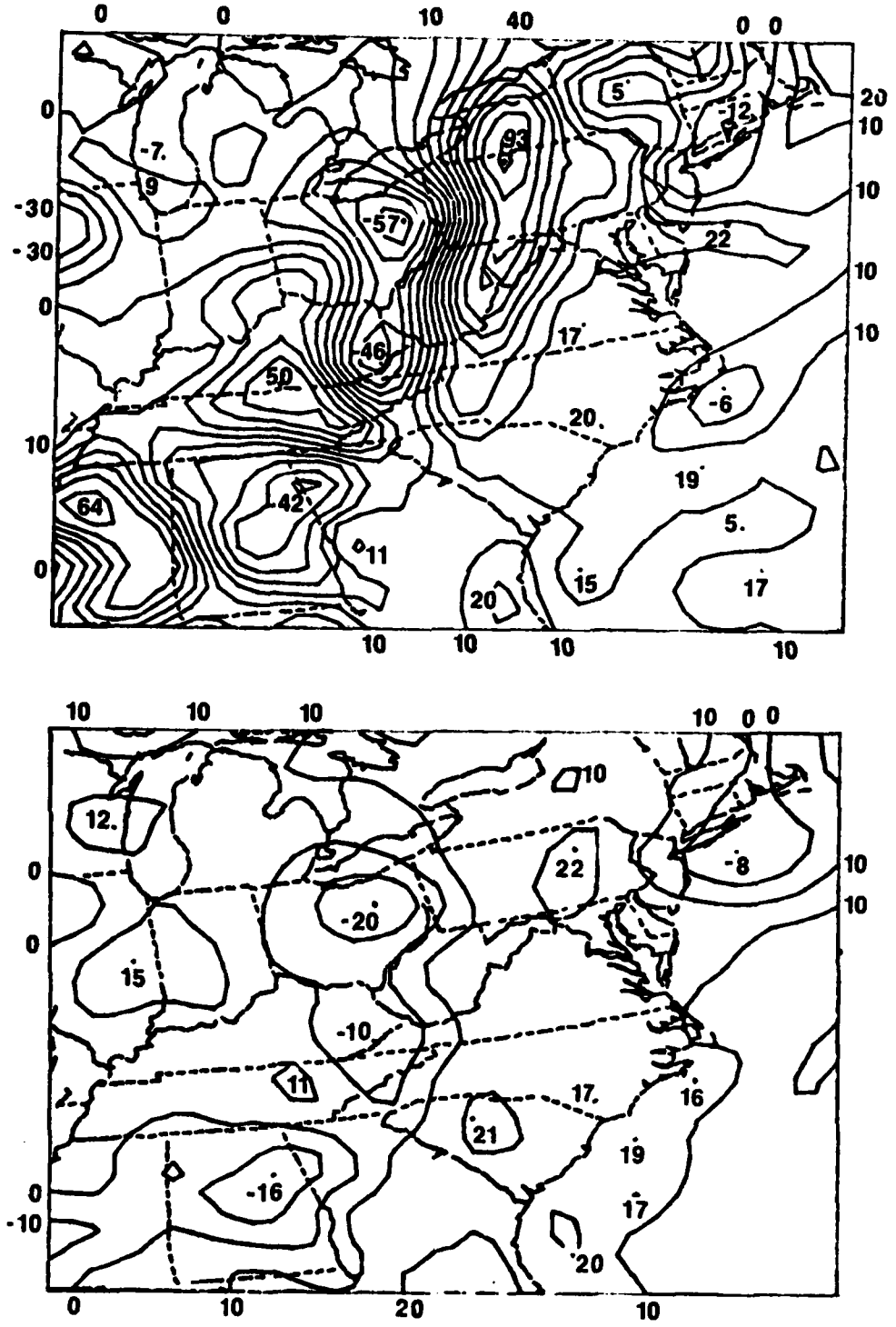

Figure A4.9. Observed (a) and predicted (b) visible count changes between 1500 and 2100 GMT on 17 June 1983.

The warm and cold thickness stratification was performed as an attempt to isolate convective- and synoptic-scale regimes, as suggested by Forbes et al. (1983). A case-by-case inspection of the 30 predictions using eq. (3.1.1) indicates that the biggest problems occur in association with convective developments. Unfortunately, the warm and cold thickness stratification did not solve the problem; results were nearly the same in each sample. A stratification based upon some static stability variable may be necessary. In any event, a number of alternate schemes for handling convective developments have been presented in sections 3.2, 3.3, and 5.1-5.3.

A4.2 Fall and Winter Nighttime

Regression equations and percentage contributions to the reduction of variance by the various predictors have been presented in section 4.1. Table A4.3 presents the individual correlation coefficients between the various predictors and the six-hour change of infrared count value, for the 18-case sample. It can be seen that none of the individual predictors are highly correlated to the predictand, except for initial count value.

Figure A4.10 shows the 0000 GMT and 0600 GMT averaged count values for an example case, that of 28 December 1983. The 80 isopleth traces out the shape of a synoptic-scale comma cloud from Kansas to Minnesota to Illinois to Mississippi. This moves eastward by 0600 GMT. Elsewhere there is a dry tongue surging northeastward out of Texas and another extending northward along the east slopes of the Appalachians.

Figure A4.11 shows the observed and predicted count-change charts for this case. The observed change field is rather noisy, but the main pattern consists of decreases from MS to WS and increases from Lake Superior to near Pittsburgh, PA, and southward into AL and GA, in association with the dry slot and comma cloud. Another area of decreases occurs in KS, behind the comma

Table A4.3

Rank of Predictors and Individual Correlations to Infrared Count Change Between 0000 and 0600 GMT During Winter 1982-83

Predictor	Entire Domain	Low Clouds	Middle Clouds	High Clouds	Large Count Change
0000 GMT Count Value	1 -0.45	6 -0.06	1 -0.34	1 -0.36	1 -0.79
LFM forecast 12-18 h P Change	2 -0.01	7 -0.12	3 -0.09	7 -0.01	2 -0.05
LFM Forecast 12-18 h Mean RH Change	3 0.05	1 0.22	2 0.13	x -0.002	x 0.20
0000 GMT Boundary Layer Forcing	4 -0.14	5 -0.14	4 -0.12	x -0.02	3 -0.29
LFM Forecast 12-18 h 1000-500 Lifted Index Change	5 -0.03	4 -0.06	5 -0.05	5 -0.05	5 -0.17
LFM Forecast 12-18 h 1000-500 Thickness Change	x +0.13	x +0.04	x 0.13	2 0.28	4 0.36
0000 GMT 850 mb U Component	x +0.05	3 -0.09	x 0.06	6 -0.10	x 0.11
0000 GMT 500 mb Wind Speed	x -0.03	2 0.06	x 0.003	x -0.14	x -0.14
0000 GMT 850 mb V Component	x -0.07	x +0.10	x 0.004	3 -0.23	x -0.16
0000 GMT 200 mb V Component	x -0.15	x -0.01	x -0.09	4 -0.30	x -0.32
0000 GMT Weighted Vertical Velocity	x +0.06	x -0.003	x 0.01	x -0.01	x 0.12
LFM Forecast Transition Vertical Velocity	x +0.001	x 0.00	x 0.00	x 0.00	x 0.003

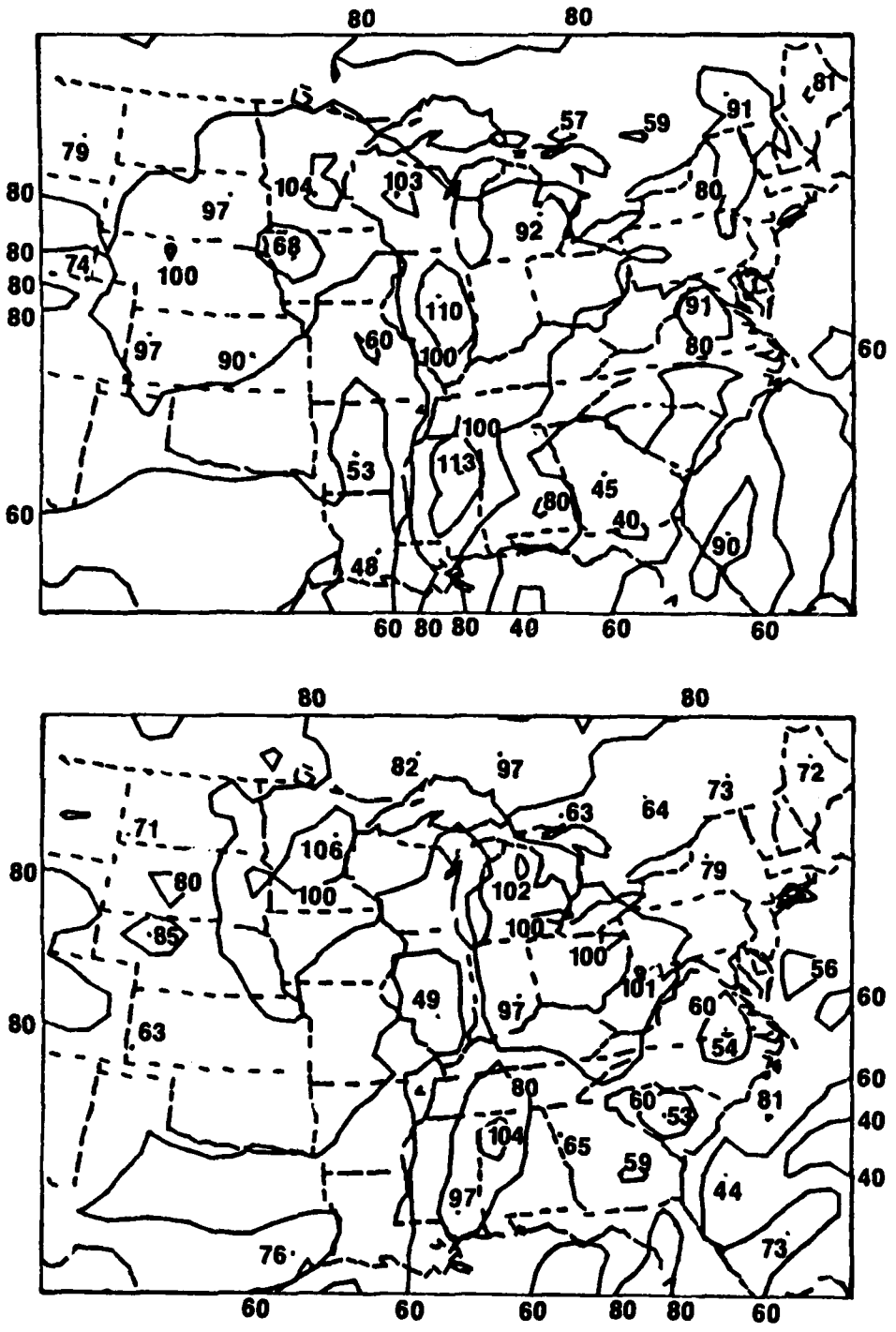

Figure A4.10. Averaged infrared count values at 0000 GMT (A) and 0600 GMT (b) on 28 December 1983.

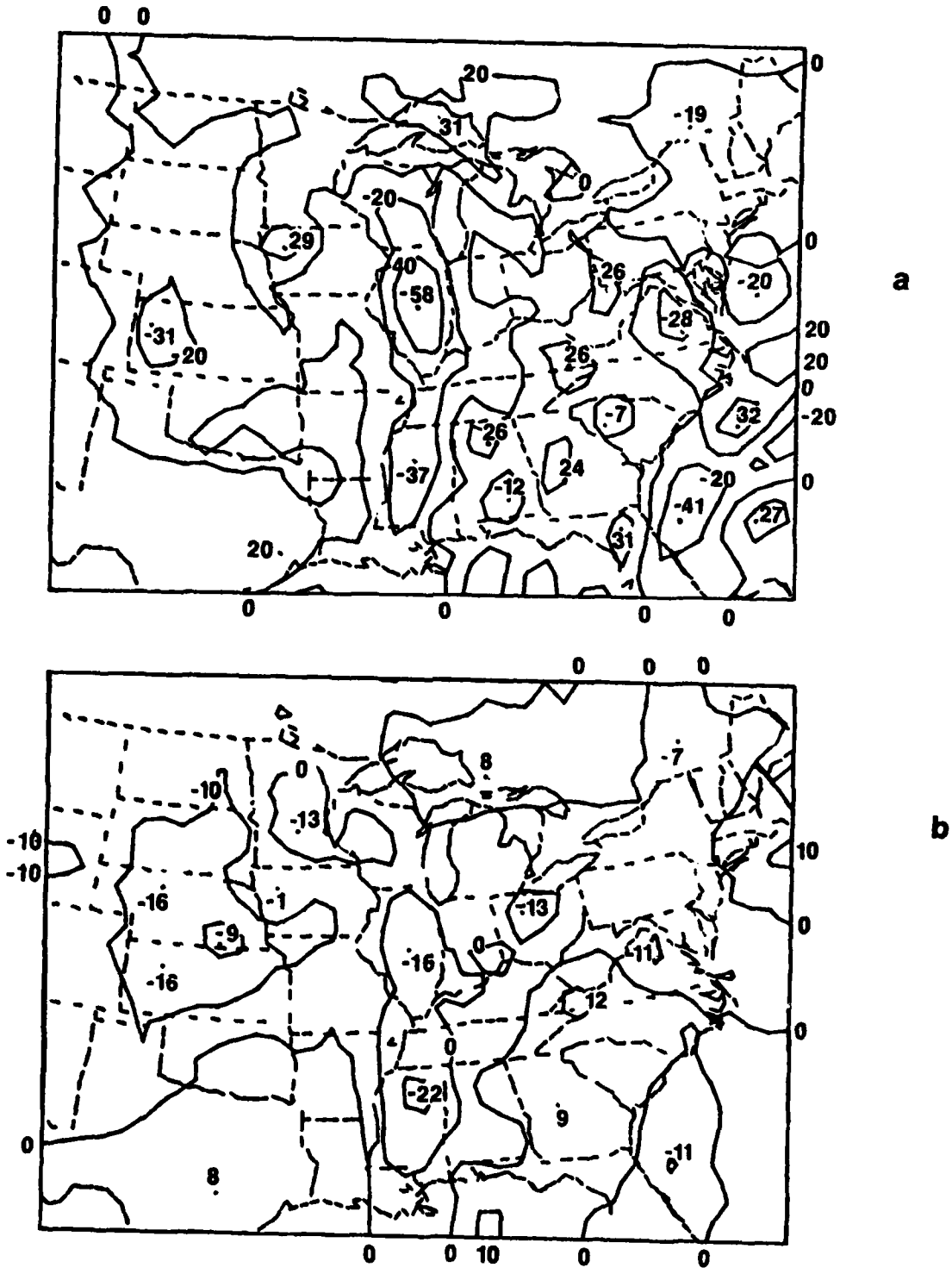

Figure A4.11. Observed (a) and predicted (b) 6-hour changes of infrared count value ending at 0600 GMT on 28 December 1983.

head. An area of increases occurs in TX. An inspection of Fig. A4.11b shows that most of these features were captured in the prediction, but with reduced magnitude. The patterns are better for count decreases than for count increases.

These experiments have shown that patterns of cloudiness change can be forecasted with modest skill. Much work remains, however, before the details of the change patterns can be specified exactly.

Appendix 5

New Evidence on the Cause of Nocturnal Thunderstorms

A5.1 Introduction

Recent investigations of flash flood-producing thunderstorms and mesoscale convective complexes (MCCs) by Maddox et al. (1979), Maddox (1980) and others, have brought renewed attention to the fact that convection is not solely a daytime phenomenon. This fact, of course, has been known for decades, as Kincer (1916), Means (1944, 1952), and Wallace (1975) have shown that thunderstorms and precipitation over the central United States have nocturnal maxima. Furthermore, Goldie (1936), Dexter (1944), and Means (1952) reported that warm frontal precipitation also reaches a maximum during the nighttime.

Because the nocturnal thunderstorm cannot develop in contemporaneous response to destabilization caused by insolation, the mechanisms for the nighttime thunderstorm have not been immediately apparent. Wallace (1975) and Gray and Jacobson (1977) have given thorough reviews of a number of mechanism theories proposed in the literature. These are relatively well known and include: (1) cloud-top radiative cooling and destabilization; (2) the formation of a nocturnal low-level jet--in association with horizontally-differential cooling over sloping terrain or by changes in frictional drag due to diurnal changes in static stability--which enhances warm advection and lifting over frontal surfaces; (3) front-like circulations induced by differential cooling between sizeable areas of cloud and surrounding area; (4) orographically-induced circulations. Additionally, Hoxit et al. (1978) suggest that mesoscale outflow boundaries, resulting from afternoon convection, can initiate subsequent nocturnal convection.

Over a period of years a number of researchers at Penn State (Otten et al., 1984) have examined cases of nighttime thunderstorms, leading to the conclusion that the scenario for their development is more complex than proposed by any of the theories above. This scenario is shown schematically in Figure 1. More than 30 cases have been examined.

These studies indicate that nocturnal convection is commonly associated with an anabatic flow of air of large wet-bulb potential temperature which overruns a sloping frontal surface. The frontal surface is generally of synoptic-scale origin, though meso-alpha-scale outflow boundaries may also suffice. The front or boundary is associated with horizontal gradients of wet-bulb potential temperature (θ_w) and potential temperature (θ), as shown in Fig. A5.1 in top and side views. Adjacent to the front in the warm sector is a tongue or pocket of air of maximum latent instability, manifested by large values of θ_w. The values are typically largest in mid- or late afternoon when the warm-sector boundary layer has been heated to its maximum temperature by insolation.

In the situation described by Otten et al. (1984), proximity soundings have shown that the nocturnal convection is elevated. That is, the planetary boundary layer (PBL) beneath the frontal surface at the site of the convection is latently stable, being colder and drier at the onset of convection than the anabatic flow above. Thus, the diurnal evolution of convection is not related to the conditions in the stable boundary layer at the convection site, but is related to the evolution of the boundary layer in the adjacent warm sector (i.e. upwind of the site).

Otten et al. (1984) have shown that the occurrence and location of nocturnal thunderstorms can be forecasted accurately in these situations by considering the regions where the flow near the top of the warm sector PBL at

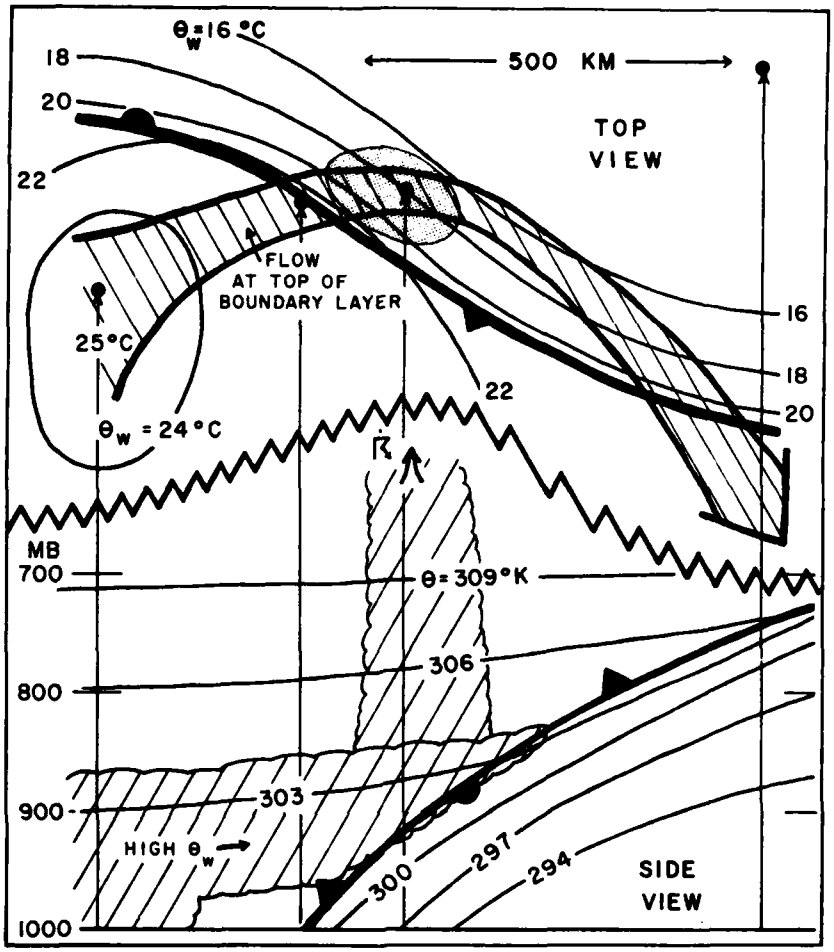

Figure A5.1. Schematic diagram showing the meteorological situation conducive to nocturnal anafront convection. At top is a top view and at bottom is a cross-section through the points indicated in the top diagram. From Forbes et al. (1984a).

2100-0000 GMT is directed toward, and is ascending over, the frontal surface. This has been referred to as the "FLUX technique" (see section 5.2), wherein convection is expected when there is large positive advection of surface θ_w by the 850-700 mb mean wind. An example of this advection field is shown in Figure A5.2.

A5.2 Hypothesis Regarding the Nocturnal Nature of Anafront Convection

Based upon the results of Otten et al. (1984), Forbes et al. (1984a) have formed some hypotheses regarding the nocturnal nature of the anafront convection. The hypotheses are based upon the observation that the latently-unstable air in the warm sector in these situations was inhibited from generating afternoon thunderstorms there by the presence of a capping inversion or lid (Carlson et al., 1983) at the top of the PBL. An example is shown in Figure A5.3. The layer of air above the inversion, however, was observed to be dry and potentially unstable. Therefore, it was possible for the lid to be removed in these cases if the inversion layer attained sufficient lifting during its ascent of the frontal surface, thereby releasing the potential instability. With the lid removed, the latent instability of the air ascending from the PBL would be released and thunderstorms would occur.

Because of this required lift, there is a finite "transit time" required for the air leaving the warm-sector PBL to travel far enough over the frontal surface to attain sufficient lift for its latent instability to be realized. By considering this transit time and the diurnal cycle in the warm-sector PBL, we form these hypotheses: (1) Nocturnal thunderstorms form and intensify in delayed response to the diurnal heating cycle in the PBL of the warm sector upwind of a front experiencing anabatic flow. Typical transit time is about 6 hours, such that the morning warm-sector air having maximum stability ascends

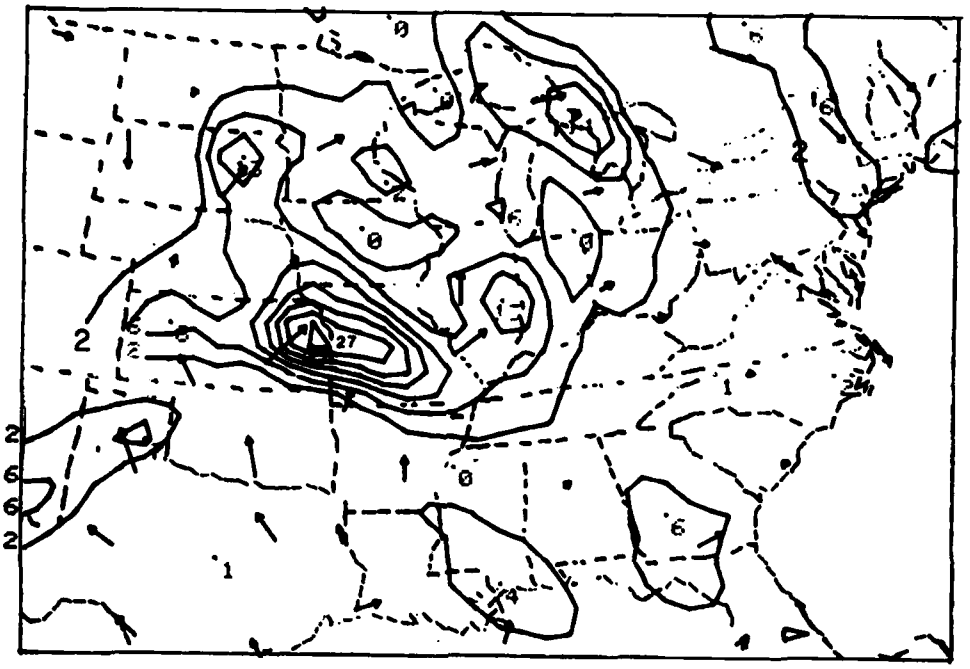

Figure A5.2. The advection of surface wet-bulb potential temperature by the mean wind in the 850-700 mb layer at 0000 GMT on 12 June 1981, in units of 10^{-5} °K s^{-1}. The pocket of large advection with the maximum value of 27 is referred to as the FLUX maximum. From Forbes et al. (1984a).

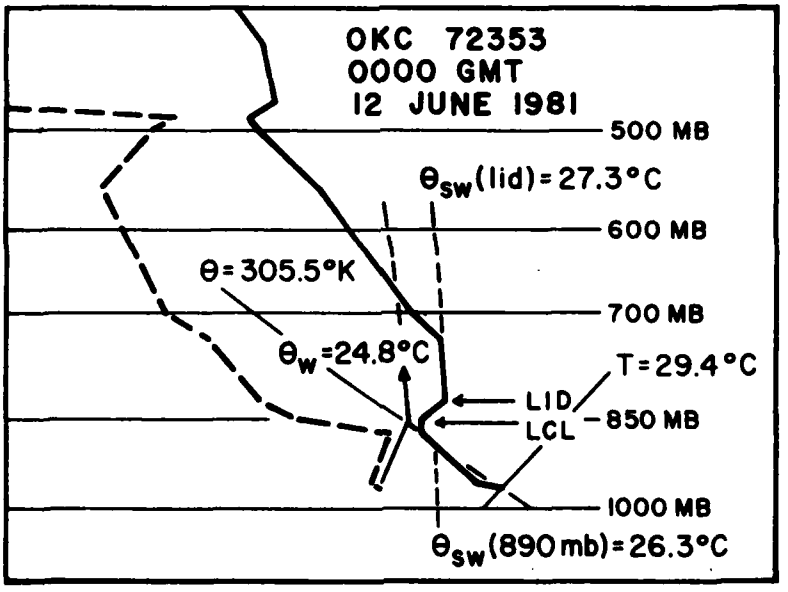

Figure A5.3. Sounding in the warm sector at Oklahoma City, OK (72353) at 0000 GMT on 12 June 1981. From Forbes et al. (1984a).

the front during midday, suppressing daytime frontal convection. Conversely, the air of maximum latent instability from the afternoon PBL ascends the front after sunset, releasing its latent instability and triggering nocturnal thunderstorms. (2) The observed collapse of nocturnal convection around the time of sunrise is a delayed response to the stabilization of the upstream PBL. As the nocturnal inversion layer progressively extends further upward, the well-mixed PBL of the previous afternoon becomes more shallow until the latently-unstable plume ascending the front is eliminated. The persistence of the convection, however, may also depend upon mesoscale feedbacks driven by the nocturnal convective systems.

These hypotheses are not meant to imply that the low-level jet, cloud-top cooling, and horizontally-differential cooling mechanisms listed above do not influence the nocturnal thunderstorms development or persistence. A developing nocturnal jet will reduce the transit time to the site of the thunderstorm system and increase the anabatic vertical velocities. However, we argue that it is the magnitude of the lift (i.e., net vertical displacement) that is crucial for the release of potential instability, rather than the rate of ascent. The diurnal heating cycle, though, does have the potential to alter the net vertical displacement. Daytime heating in the warm sector causes the adiabats to descend, whereas those above the frontal inversion are less likely to do so (since they are decoupled from the PBL by the intervening frontal inversion). This implies a potential for greater lift of the afternoon air during its subsequent transit over the steepened front. The converse may occur at night.

Additionally, anabatic flow is often observed both before the nocturnal convection develops and after it ceases. This observational evidence supports the hypothesis that diurnal variations in the latent and potential instability of the overrunning air are crucial.

AD-A148 011 A SCHEME FOR SHORT-TERM PREDICTION OF HYDROMETEORS USING ADVECTION AND PH.. (U) PENNSYLVANIA STATE UNIV UNIVERSITY PARK DEPT OF METEOROLOGY G S FORBES ET AL.

2/2

UNCLASSIFIED JUL 84 AFGL-TR-84-0199 F19628-82-K-0023 F/G 4/2 NL

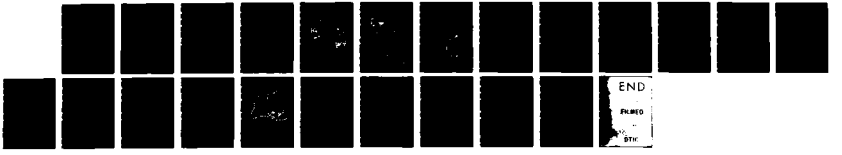

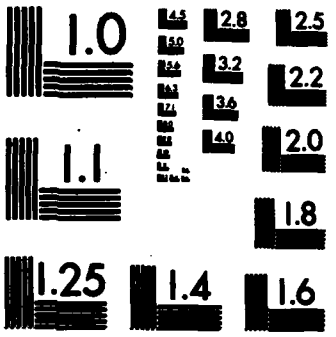

MICROCOPY RESOLUTION TEST CHART
NATIONAL BUREAU OF STANDARDS-1963-A

The diurnal variations which occur in the PBL are well known. Afternoon heating and associated turbulent mixing establish an adiabatic layer of varying depth, with a shallow superadiabatic layer in contact with the surface. As night sets in a surface-based inversion develops and deepens through the night. The nocturnal jet, if it develops, is located at the top of this inversion layer.

The diurnal cycle in PBL mixing ratio is also well known, but has previously been virtually overlooked in the deliberations on the causes of nocturnal convection. With the moisture sources at the surface, daytime turbulent mixing yields a net moistening in the upper portion of the PBL, while some drying takes place near the surface. The daytime moistening at 90 and 444 m is shown in Figure A5.4, from Schaefer (1975). As a result of this

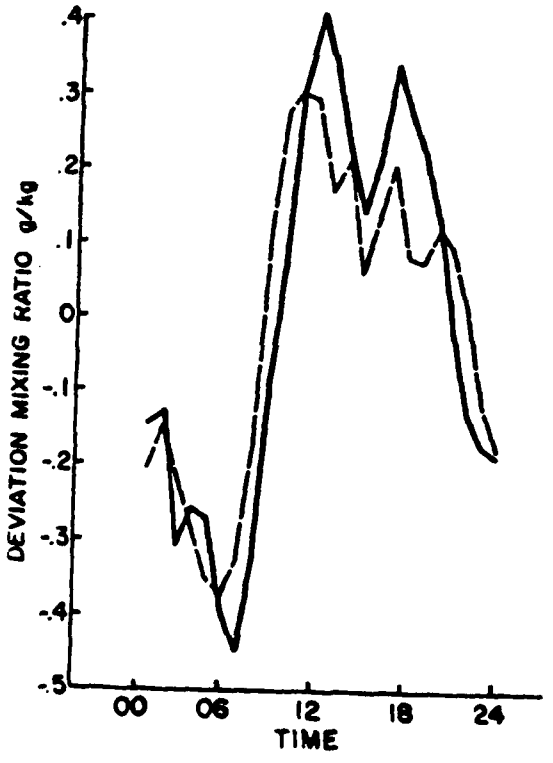

Figure A5.4. Mean diurnal deviation of mixing ratio from daily average (dashed, 90 m; solid, 440 m). From Schaefer (1975).

moistening, in conjunction with increasing potential temperatures, the wet-bulb potential temperature at the top of the PBL reaches a maximum from mid-day to late afternoon. Figure A5.5, from Mahrt (1975), shows that the diurnal cycle of the mixing ratio in eastern Colorado is a maximum (range of about 1 g/kg) at elevations of about 1-2 km above the ground. Over the Midwest this corresponds to pressure levels from about 900 to 700 mb. Probably not fortuitously, these are the levels that Otten et al. (1984) found possessed anabatic flow prior to nocturnal convective development. Thus, there is reason, a priori, to suspect a reaction to this diurnal cycle. We argue that this convective reaction is delayed in many situations because a finite amount of time is required to lift this air enough to release its potential instability.

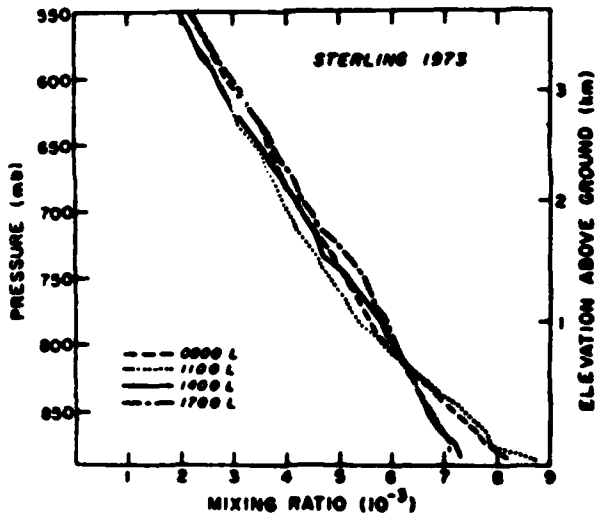

Figure A5.5. Average daytime evolution of mixing ratio profiles at Sterling, CO, in summer 1973. From Mahrt (1975).

Subsequent to the formulation of the above hypotheses, a search of the literature revealed that Dexter (1944) had formulated similar hypotheses. Apparently his hypotheses were never tested; we have tested them recently in 7 cases using the objective ACTIVEX system described in section 5.3 (Forbes et al., 1984a), and subjectively on about 30 cases. In summary, there are no indications that the theory is wrong. In most cases, however, the time and space resolution of the upper-air network is inadequate to allow conclusions to be reached beyond a shadow of a doubt. The STORM Program (Zipser, 1984) should help tremendously here. Fortunately, however, we have found several cases where the evidence seems irrefutable. One of these cases, 11-12 June 1981, is presented below.

A5.3 The Kansas-Missouri-Illinois Convection of 11-12 June 1981

Convection developed dramatically after 0200 GMT on 12 June 1981 in northeastern Kansas, as shown in Figure A5.6. The 0235 GMT radar composite chart shows a lot of convection which remains from the previous afternoon. A single cell in north-central Kansas marks the onset of the nocturnal convection. By 0535 GMT radar indicates a 65,000' top northwest of Topeka, and other convection spreading eastward. By 1135 GMT the convection has nearly reached Peoria, Illinois, while activity continues westward to north of Topeka.

The Peoria, Illinois, "1200 GMT" sounding, launched just prior to Fig. A5.6c, is an excellent proximity sounding, and is shown in Figure A5.7. The lowest layer is cold, and does not experience any positive buoyancy if lifted. On the other hand, the air near 900 mb does become buoyant if lifted a bit further, and has wet-bulb potential temperature of about 22°C. This elevated plume was not generated locally, as the surface θ_w was never that high there

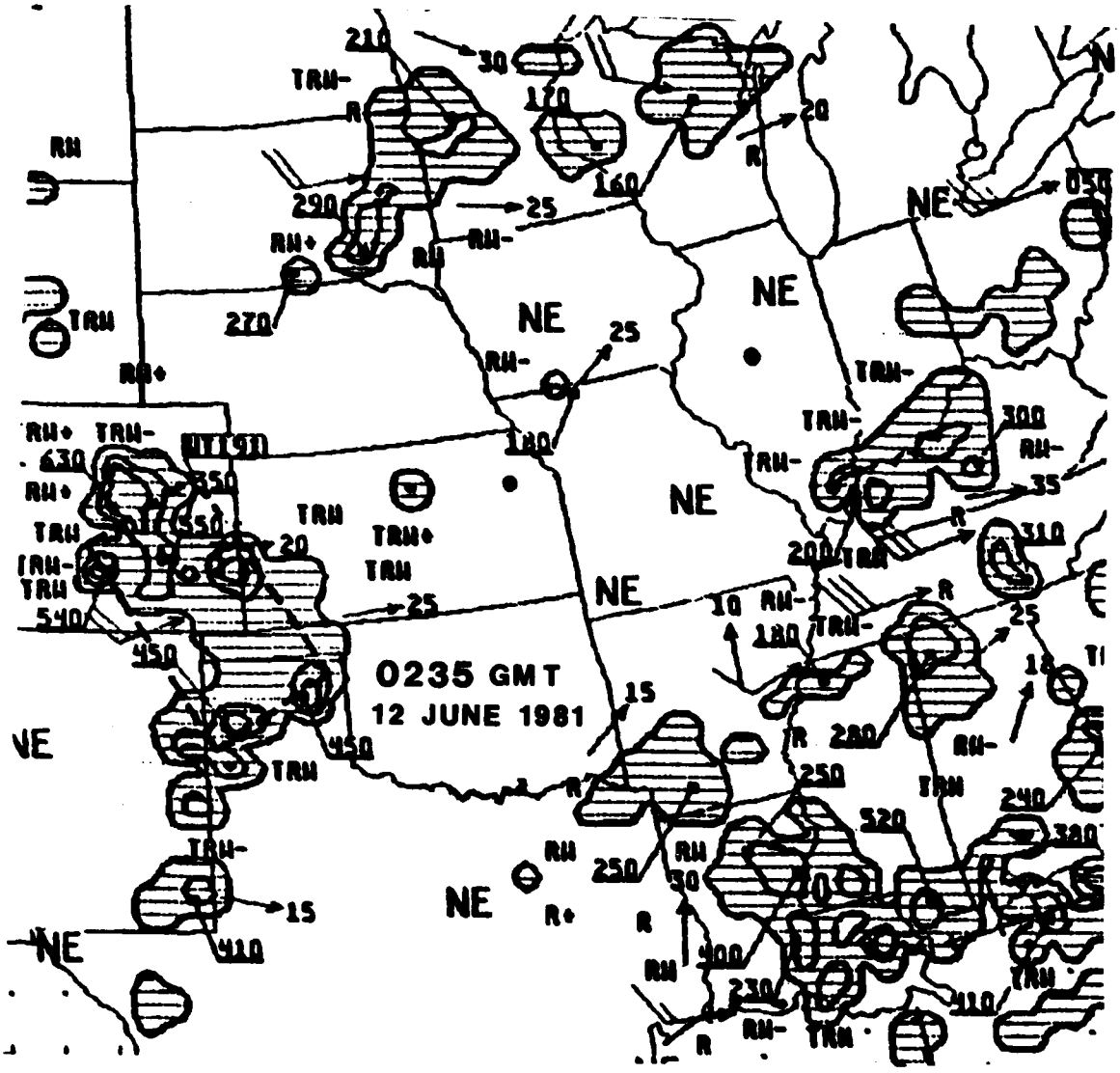

Figure A5.6. Radar composite charts on 12 June 1981. a. 0235 GMT. b. 0535 GMT. c. 1135 GMT.

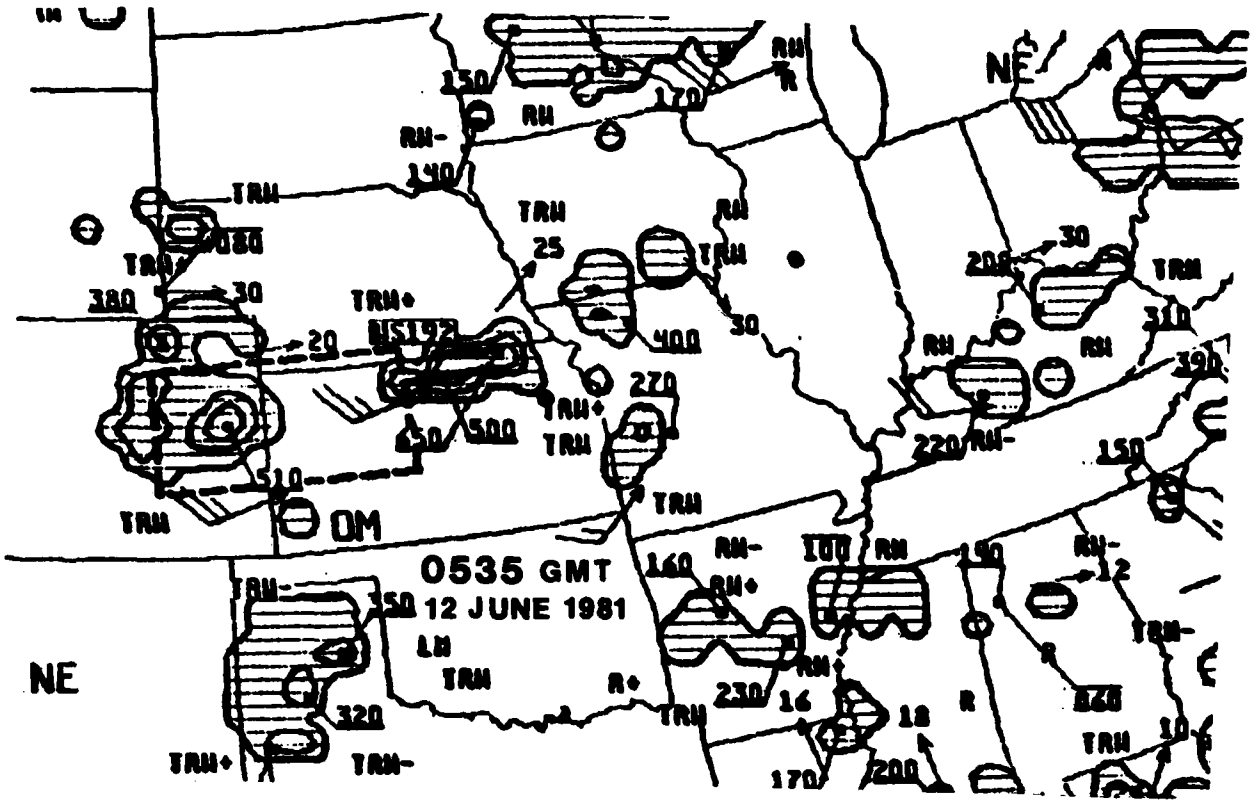

Fig. A5.6 b

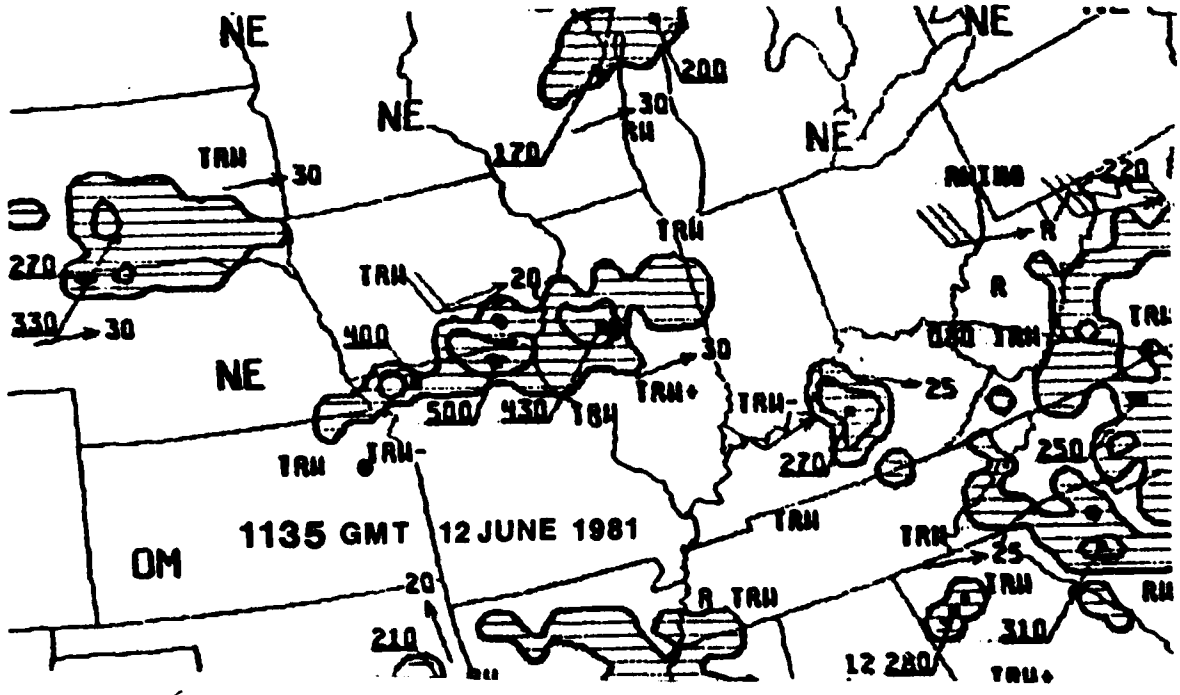

Fig. A5.6 c

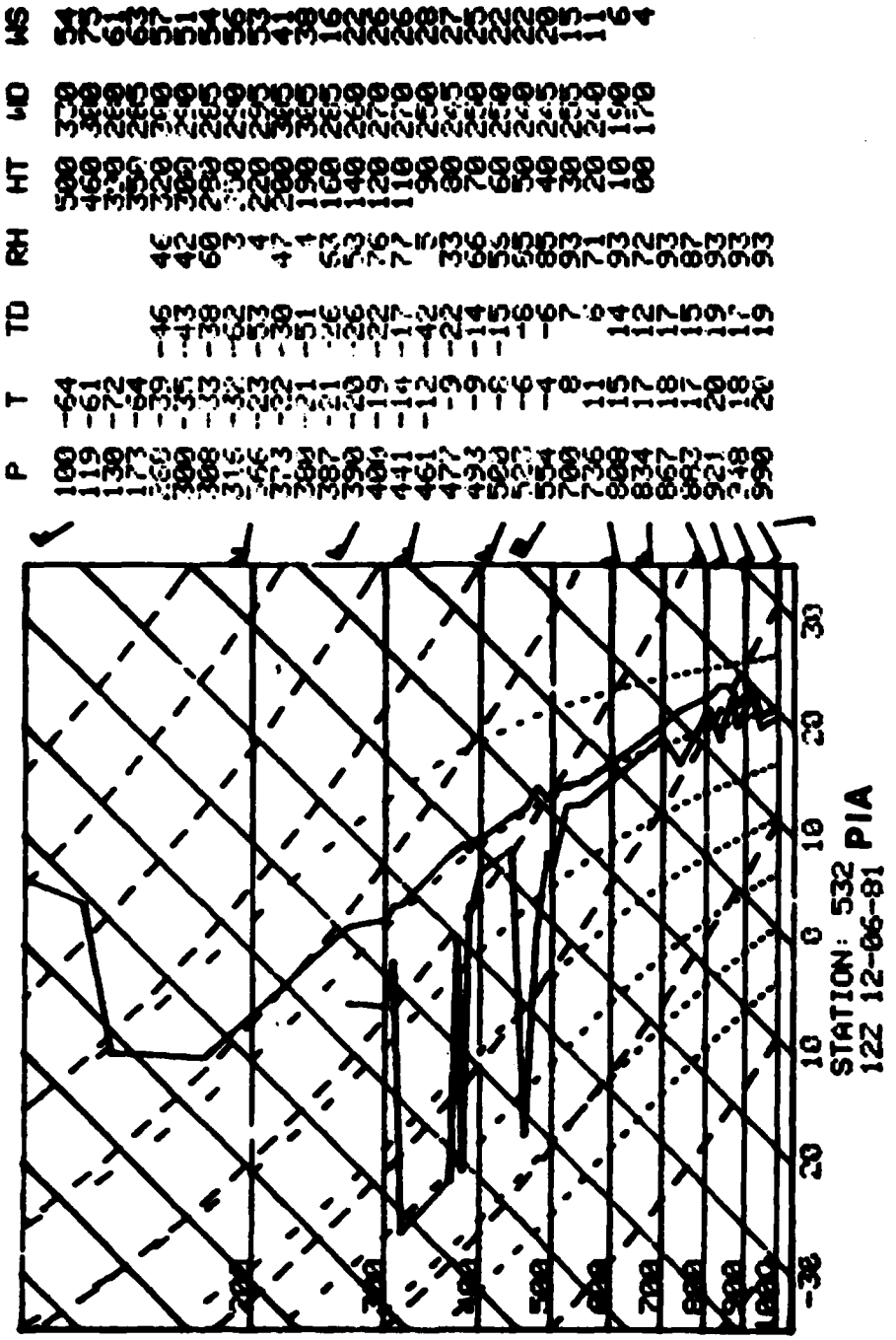

Figure A5.7. Sounding at Peoria, IL (72532) launched about 1115 GMT on 12 June 1981.

during the previous day. Its source was upwind, and at 1200 GMT was arriving at Peoria from the WSW.

Relative isentropic backward trajectories (e.g. Carlson and Ludlam, 1968) were used to deduce the origin of the elevated plume; Figure A5.8 shows the location of the plume at various times. At 0600 GMT the plume was still elevated; surface θ_w was only 19°C near Columbia, MO, whereas the plume θ_w was about 22°C. By 0000 GMT the location was above a region of surface θ_w of about 23°C. Allowing for a 1-2°C decrease of θ_w with height in the afternoon PBL--moisture is not always well-mixed (e.g. Mahrt, 1975)--suggests that this may have been a reasonable origin. The locations at 2100 and 1800 on the 11th are also possible sources, but the values of surface θ_w prior to 1500 GMT were colder than required. Thus, there was a limited domain in northeastern Oklahoma and southwestern Missouri between about 1500 GMT on the 11th and 0000 GMT on the 12th which provided the elevated plume heading into Illinois.

Figure A5.8 also shows backward trajectories for the air arriving at Topeka at 0000 GMT, a few hours prior to convective onset. The 0000 GMT sounding, Figure A5.9, shows that the convection was again elevated and most likely developed from air between about 900 and 750 mb having θ_w of 23-24°C. This came from central and northern Oklahoma and southern Kansas from about 1500 until 2100 GMT on the 11th. Trajectories to the locations of the tallest convection at 0500 GMT and 1200 GMT came from the heart of the area of latent instability at 2100 GMT on the 11th, as shown by Figure A5.10. There was a moisture convergence maximum there at this time, shown in Figure A5.11, which may have bolstered the anabatic flow locally. Afternoon convection was inhibited in this region by the presence of a lid, as shown in Fig. A5.3. The zone of anabatic flow removing this lid was diagnosed well by the FLUX scheme, as shown in Fig. A5.2.

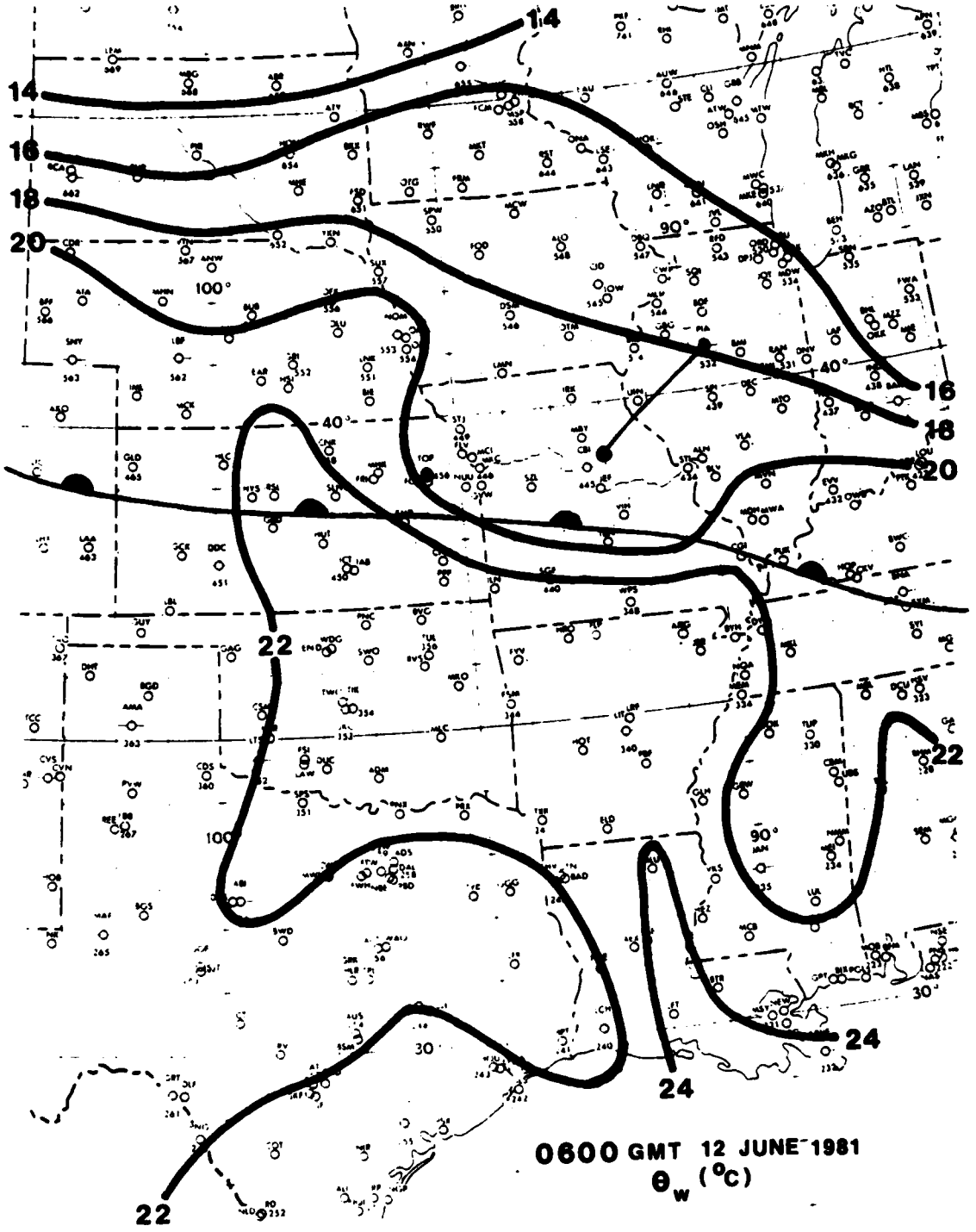

Figure A5.8. Mappings of surface wet-bulb potential temperature, surface front location, and backward trajectories on 11-12 June 1981. a. 0600 GMT June 12. b. 0000 GMT June 12. c. 2100 GMT June 11. d. 1800 GMT June 11.

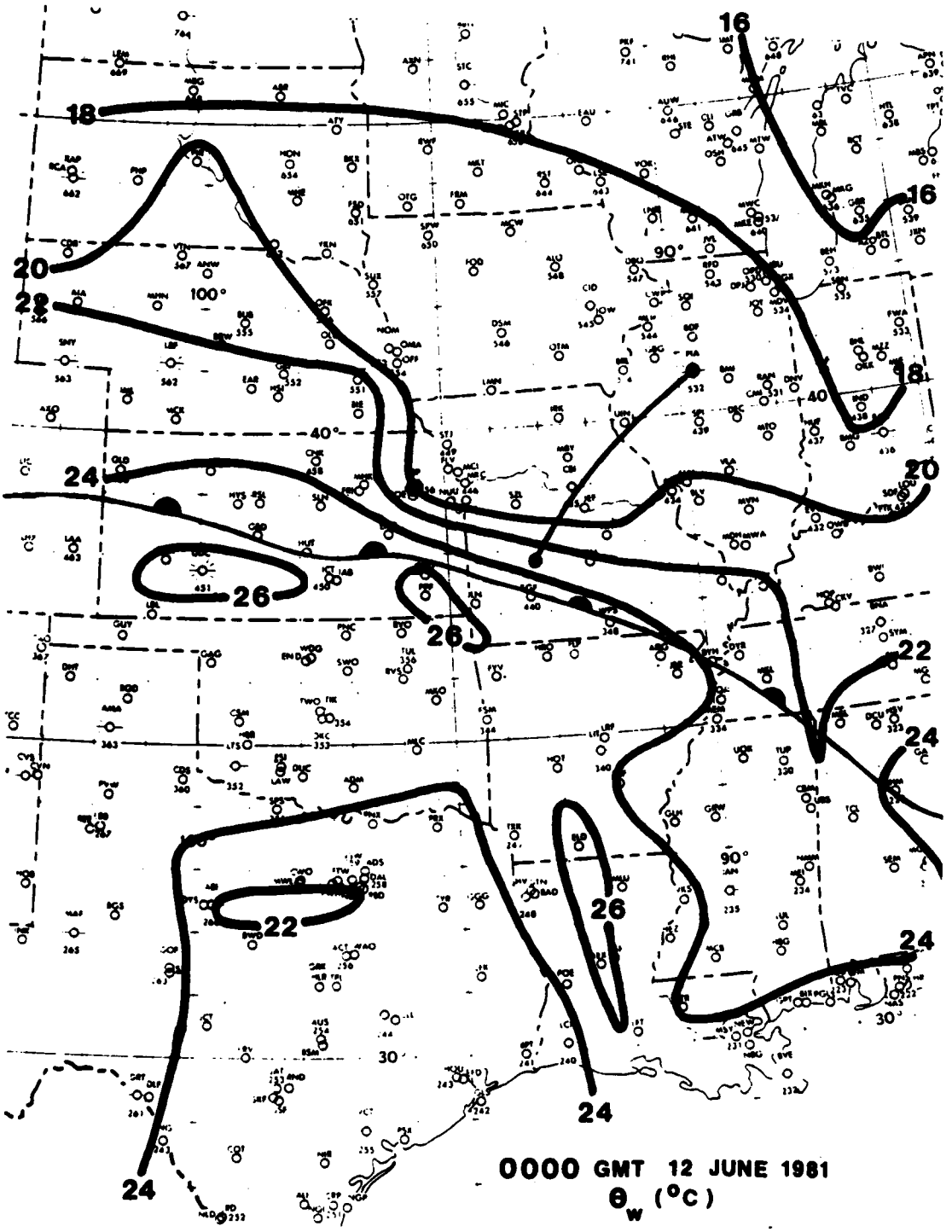
16
18
16
20
22
100°
90°
18
40
40°
24
20
26
26
22
24
90°
22
26
24
30°
30
24
24
0000 GMT 12 JUNE 1981
θw (°C)

Fig. A5.8 b

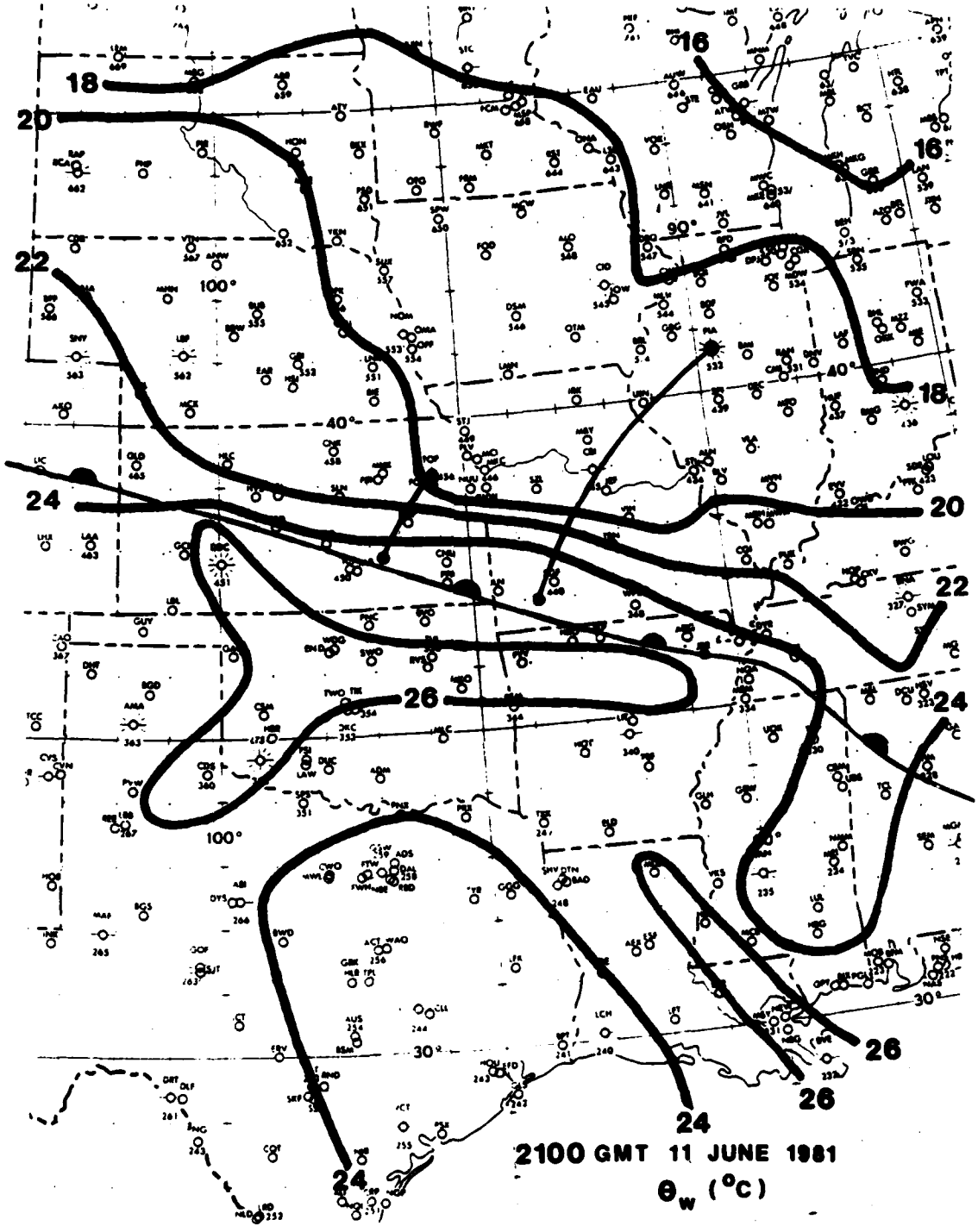
16
18
20
16
22
100°
90°
40°
18
24
20
22
26
24
100°
30°
26
26
24
24
2100 GMT 11 JUNE 1981
θw (°C)

Fig. A5.8 c

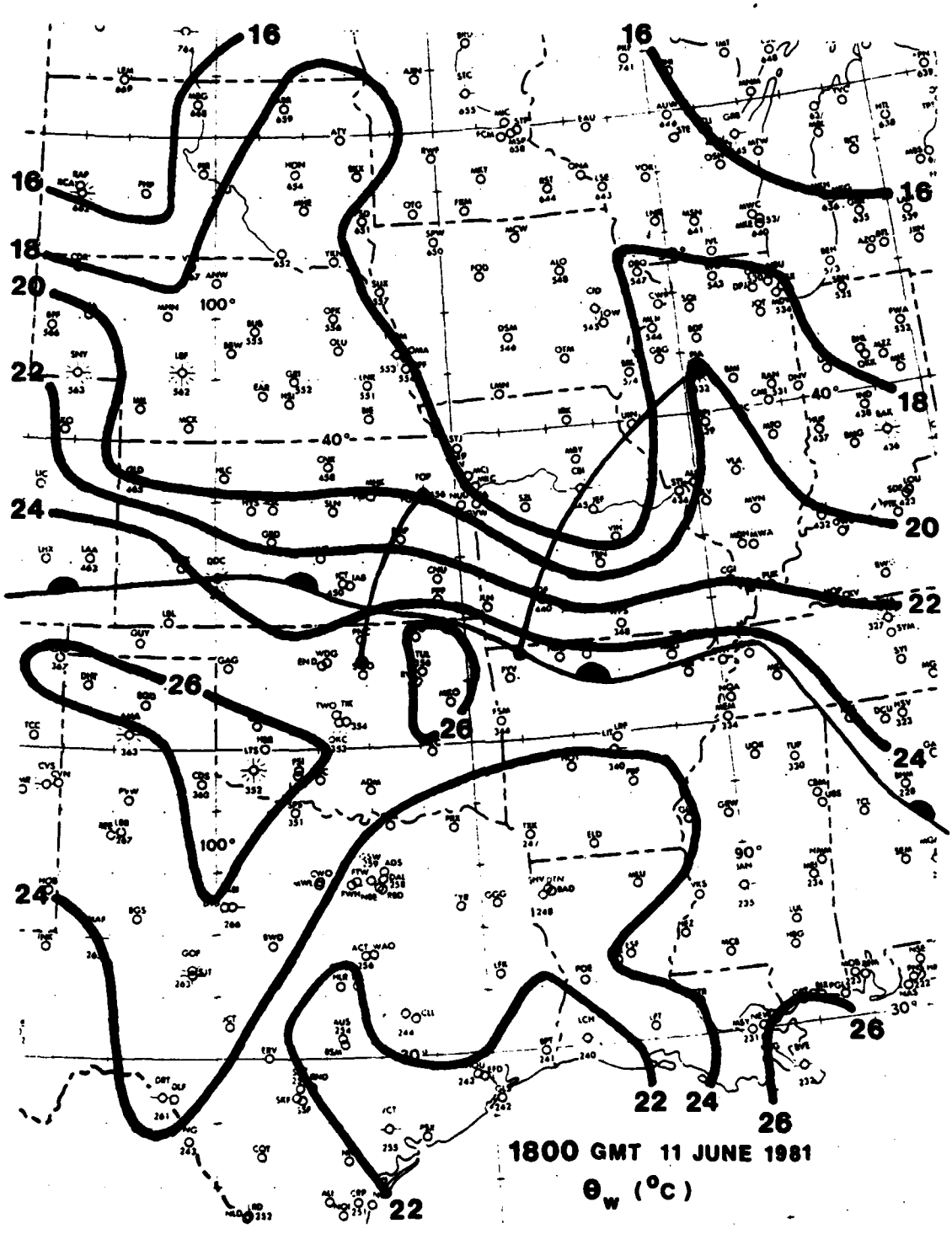
16
16
16
16
18
18
20
20
22
22
24
24
26
26
26
26
24
24
22
22
24
26
100°
100°
40°
40°
90°
30°
1800 GMT 11 JUNE 1981
θw (°C)

Fig. A5.8 d

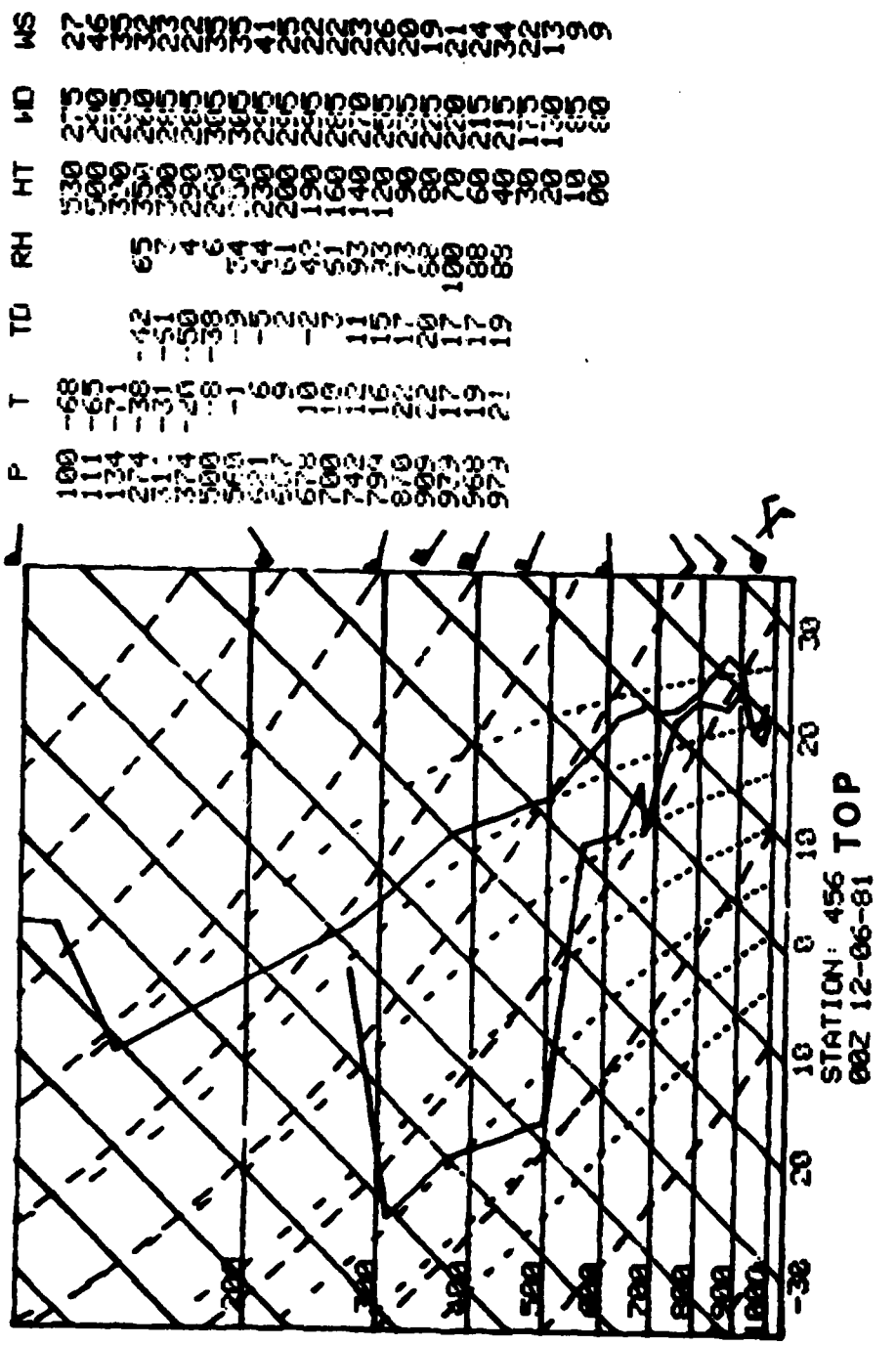

Figure A5.9. Sounding at Topeka, KS (72456) at 0000 GMT on 12 June 1981.

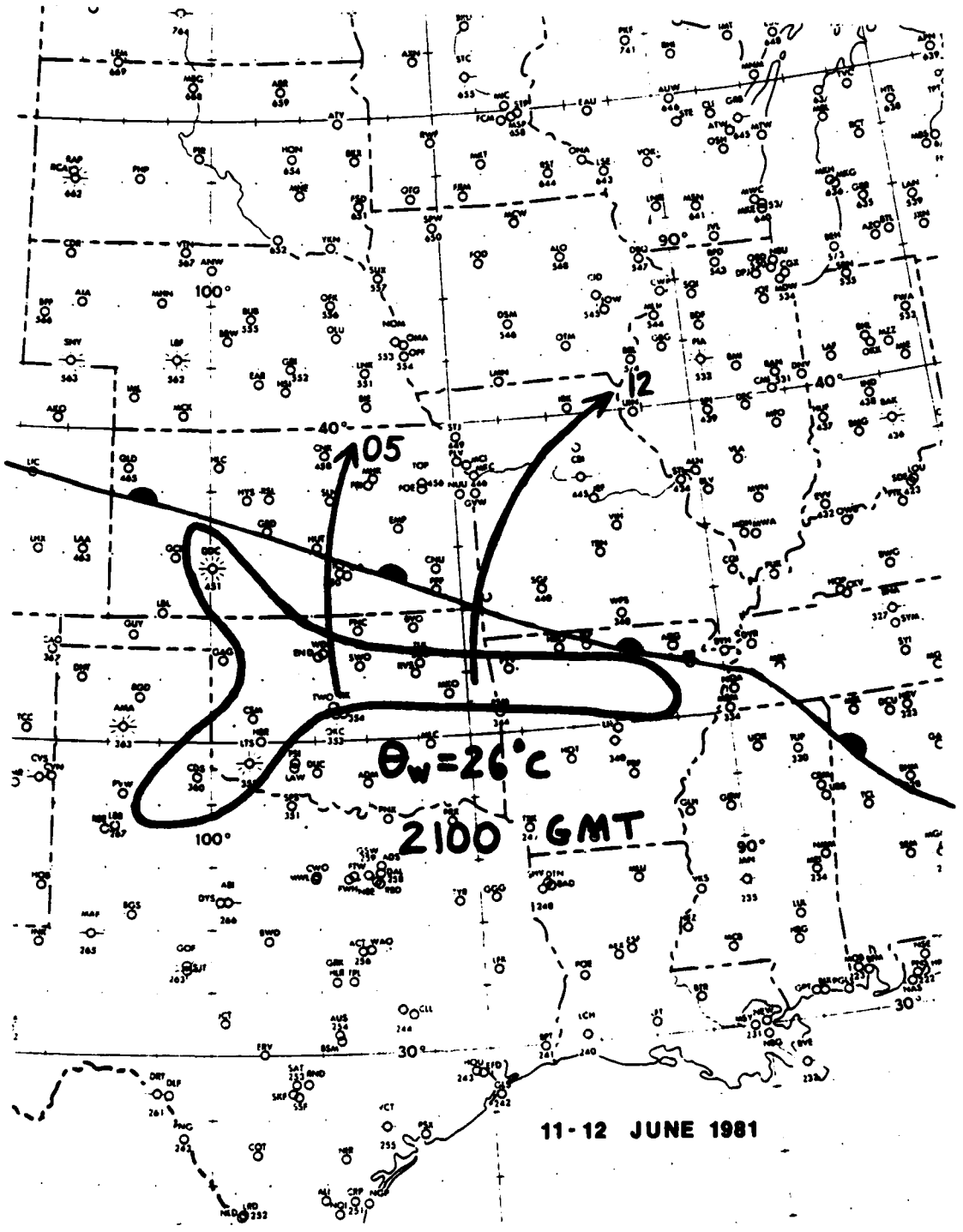

Figure A5.10. Mapping of pocket of maximum surface wet bulb potential temperature at 2100 GMT and backward trajectories from regions of highest radar tops at times indicated.

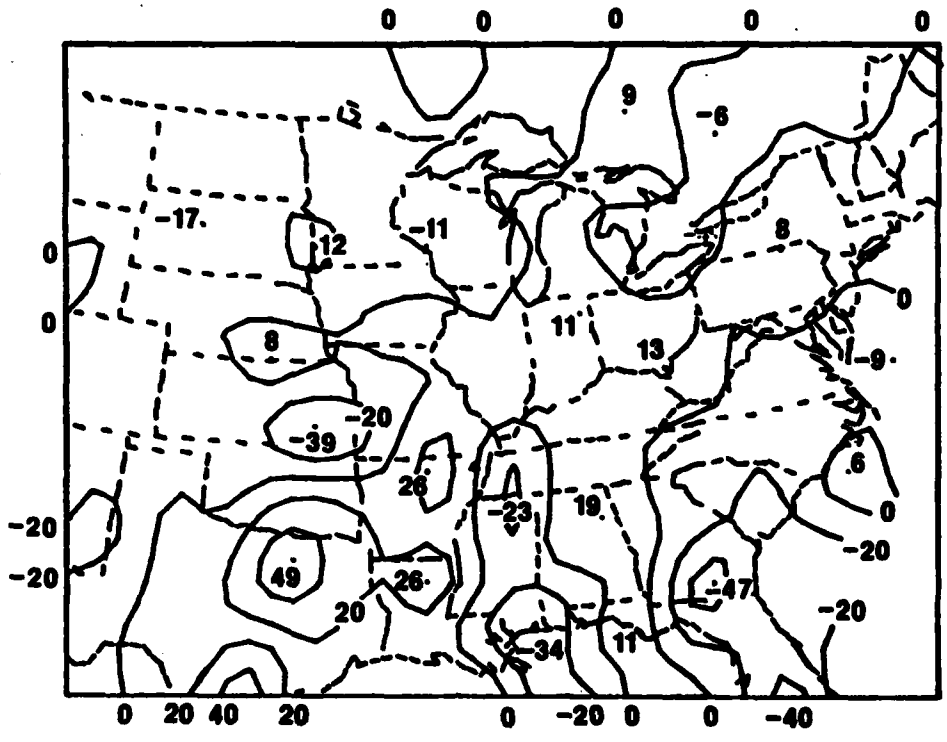

Figure A5.11. Surface moisture divergence (in units of 10^{-5} g kg^{-1} s^{-1}) at 2100 GMT on 11 June 1981.

A5.4 Discussion

The need for afternoon heating is pointed out schematically in Figure A5.12. The Gulf of Mexico is ultimately the origin of the background moisture for almost all nocturnal convection. Air flowing off the Gulf is rich in moisture, but has relatively cool temperature. Its potential temperature of about 27°C is typically about 5-6°C colder than the potential temperature of the elevated plume seen on proximity soundings. Thus, afternoon heating and mixing are crucial. Local evapotranspiration from vegetation and from ground wet from previous rains (and from local water bodies) contribute to the occurrence of mesoscale regions of maximized latent instability.

The studies with the ACTIVEX scheme (section 5.3) and other cases indicate that, whereas the nocturnal jet may not be the controlling factor, the occurrence of the nocturnal jet does affect the timing and location of nocturnal convection. Trajectories calculated using 0000 GMT winds generally go in the proper direction, but do not go far enough to reach the convective region at the time of onset. A nocturnal speed increase of about 20% seems to yield better spatial and temporal results, empirically.

There are cases, owing to poor upper-air sampling and a long fetch between the Gulf of Mexico and the site of the convection, when it becomes difficult to ascertain on which day the elevated plume was generated. That is, it took more than one day for the air from the Gulf of Mexico to reach the anabatic zone. However, elevated convection often occurs on successive nights in these situations. It appears that the convection on the first night may reinforce the front for the second night's activity, just as the afternoon activity on the 11th (Figure A5.13) may have enhanced the cold dome in the case discussed above. This aspect needs to be addressed further. Nevertheless, it is clear that many (probably most) cases of nocturnal convection are

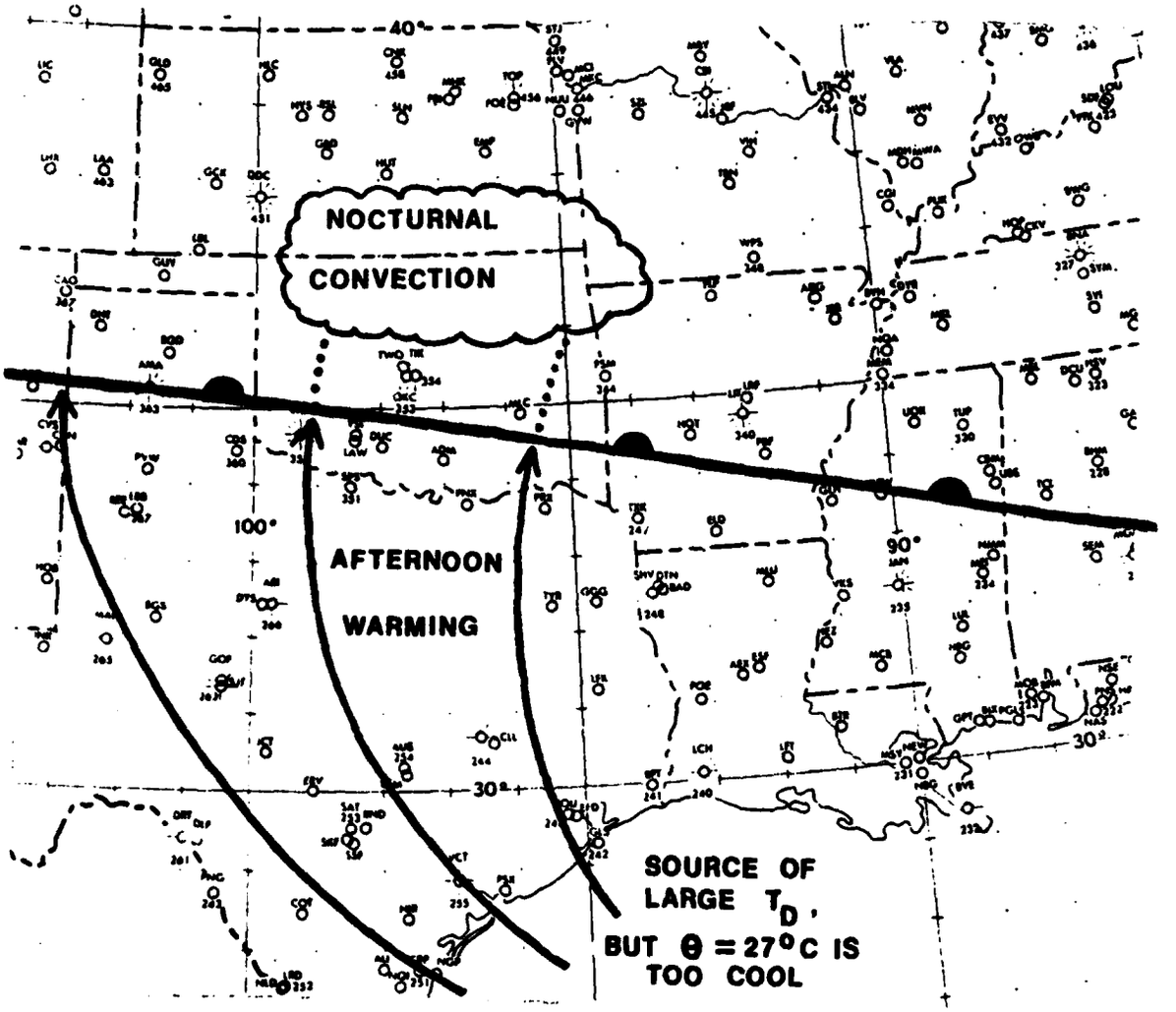

Figure A5.12. Schematic diagrams of three-step approach to obtain nocturnal anafront convection.

a delayed response to warm-sector afternoon heating and mixing and an anabatic flow over the adjacent frontal zone.

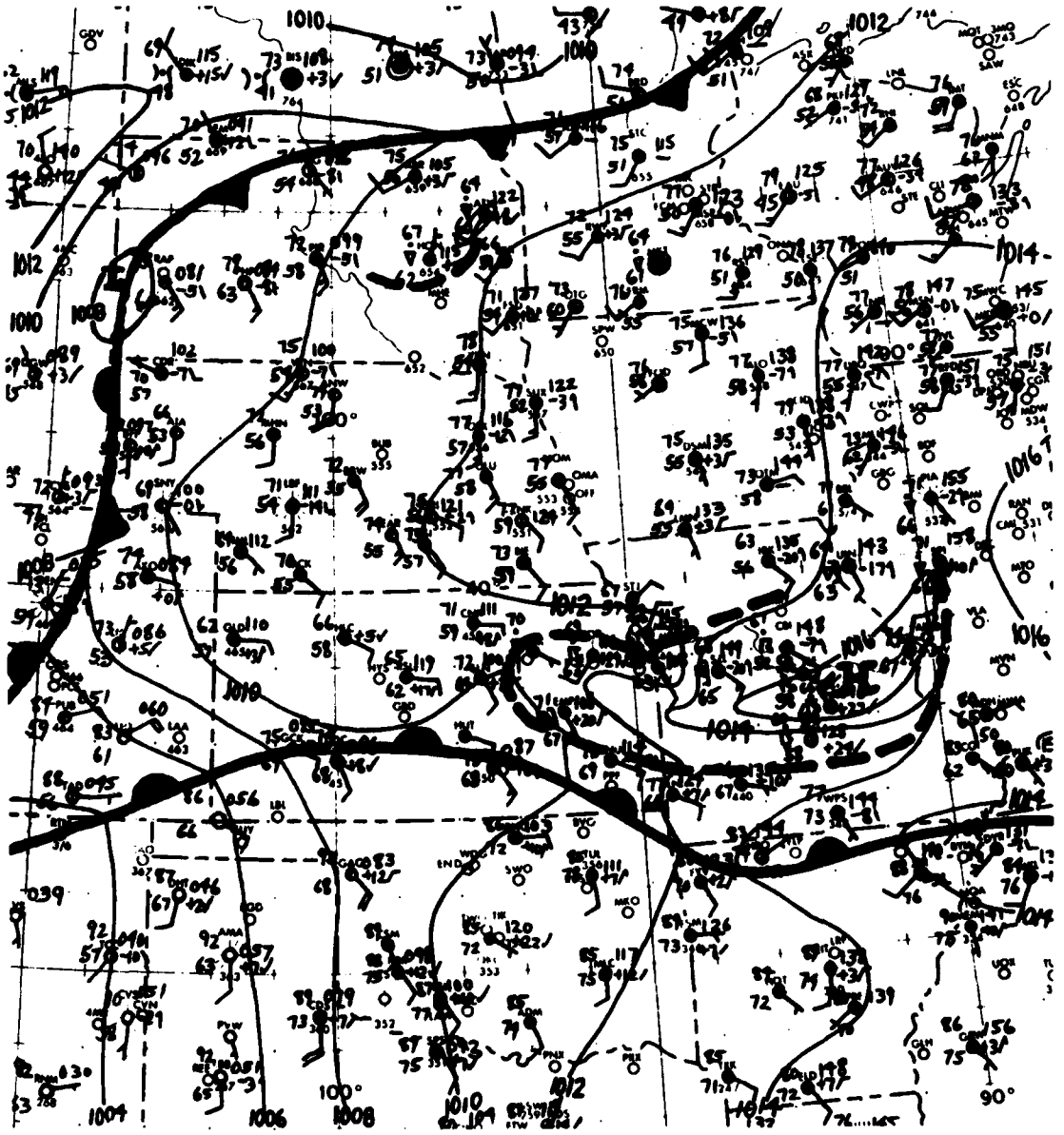

Figure A5.13. Surface analysis at 1800 GMT on 11 June 1981. Heavy dashed lines represent outflow boundaries. From Forbes et al. (1984a).

References

Austin, G.L. and A. Bellon, 1982: Very-short range forecasting of precipitation by the objective extrapolation of radar and satellite data. Nowcasting, K.A. Browning, ed., Academic Press, New York, 177-190.

Bocchieri, J.R. and G.J. Maglaras, 1983: An improved operational system for forecasting precipitation type. Mon. Wea. Rev., 111, 405-419.

Browning, K.A., 1982: Nowcasting. Academic Press, London, 256 pp.

Browning, K.A. and C.G. Collier, 1982: An integrated radar-satellite nowcasting system in the UK. Nowcasting, K.A. Browning, ed., Academic Press, New York, 47-61.

Cahir, J.J., 1980: Analysis of frontal weather by forecaster interaction. Report on Contract T-35406, 1978-1980, The Pennsylvania State University, 88 pp.

Cahir, J.J., J.M. Norman, W.D. Lottes, J.A. Toth, 1976: New tools for forecasters: Real-time cross sections produced in the field. Bull. Amer. Meteor. Soc., 57, 1426-1433.

Cahir, J.J., J.M. Norman and D.A. Lowry, 1978: Use of a real-time computer graphics system for diagnosis and forecasting. Preprints, Conf. on Wea. Forecasting and Analysis and Aviation Meteor., Silver Spring, MD, Amer. Meteor. Soc., 194-196.

Cahir, J.J., J.M. Norman and D.A. Lowry, 1981: Use of a real-time computer graphics system in analysis and forecasting. Mon. Wea. Rev., 109, 485-500.

Cahir, J.J. and W.D. Lottes, 1982: An objective diagnostic aid in locating meteorologically significant boundaries. Preprints, 9th Conf. Wea. Forecasting and Analysis, Seattle, WA, Amer. Meteor. Soc., 296-299.

Carlson, T.N., 1982: A simple model illustrating baroclinic development. Bull. Amer. Meteor. Soc., 63, 1302-1308.

Carlson, T.N. and F.H. Ludlam, 1968: Conditions for the occurrence of severe local storms. Tellus, 20, 203-226.

Carlson, T.N., R.A. Anthes, M. Schwartz, S.G. Benjamin and D.G. Baldwin, 1980: Analysis and prediction of severe storms environment. Bull. Amer. Meteor. Soc., 61, 1018-1032.

Carlson, T.N., S.G. Benjamin, G.S. Forbes, and Y.-F. Li, 1983: Elevated mixed layers in the regional severe storm environment. Mon. Wea. Rev., 111, 1453-1473.

Chapman, K., 1983: Interactive use of combined minicomputer and satellite technology capabilities in assessing short-term changes in cloud patterns. M.S. Thesis, The Pennsylvania State University, 66 pp.

Charba, J.P., 1979: Two-six hour severe local storm probabilities: An operational forecast system. Mon. Wea. Rev., 107, 268-282.

Charba, J.P., 1979: Recent performance of the operational two-six hour objective forecasts of severe local storms on outbreak days. Preprints, 11th Conf. Severe Local Storms, Kansas City, MO, Amer. Meteor. Soc., 600-607.

Chisolm, D.A. and A.J. Jackson, 1984: Short-range terminal forecasting using interactive computer display systems. Preprints, 10th Conf. Wea. Forecasting and Analysis, Clearwater Beach, FL, Amer. Meteor. Soc., 226-233.

Clark, J.D., 1983: The GOES users guide. Dept. of Commerce, National Environmental Satellite, Data and Information Service, Washington, D.C.

Darkow, G.L. and S.F. Tansey, 1982: Subsynoptic fields of boundary layer heat and moisture estimated from hourly surface data. Preprints, 12th Conf. Severe Local Storms, Tulsa, OK, Amer. Meteor. Soc., 79-83.

Dexter, R.V., 1944: The diurnal variation of warm frontal precipitation and thunderstorms. Quart. J. Roy. Meteor. Soc., 70, 129-137.

Dorian, P.A., 1983: Interactive use of minicomputer capabilities in assessing short-term humidity forecasts by the LFM-II model. M.S. Thesis, The Pennsylvania State University, 84 pp.

Dorian, P.A., G.S. Forbes and J.J. Cahir, 1984: Evaluation of humidity forecasts of an operational model. Submitted to Mon. Wea. Rev..

European Space Agency, 1981: Nowcasting: Mesoscale observations and short-range prediction. ESA SP-165, European Space Agency, Paris, 415 pp.

Forbes, G.S., 1983: A simple, interactive scheme for forecasting the short-term movement of cyclones. Memorandum 83-7, Royal Netherlands Meteorological Institute, DeBilt, 13 pp.

Forbes, G.S. and W.D. Lottes, 1982: Characteristics and evolution of mesoscale cloud vortices occurring in polar airstreams. Preprints, Conf. on Cloud Physics, Chicago, IL, Amer. Meteor. Soc., 310-313.

Forbes, G.S., T.A. Paone and J.J. Cahir, 1983: A minicomputer objective scheme for short-range forecasting of mesoscale convection patterns. Preprints, 12th Conf. Severe Local Storms, San Antonio, TX, Amer. Meteor. Soc., 84-87.

Forbes, G.S., J.J. Cahir, P. Dorian, W.D. Lottes and K. Chapman, 1983: Development of a technique for short-term prediction of hydrometeors using advection and physical forcing. Sci. Rept. No. 1, AFGL Contract F19628-82-K-0023 and AFGL Tech. Rept. 83-0082, 72 pp (ADA 132259).

Forbes, G.S. and P.O.G. Heppner, 1984: New evidence on the cause of nocturnal thunderstorms. Submitted to J. Atmos. Sci.

Forbes, G.S., P.O.G. Heppner, J.J. Cahir and W.D. Lottes, 1984(a): Prediction of delayed-onset nocturnal convection based on air trajectories. Preprints, 10th Conf. Wea. Forecasting and Analysis, Clearwater Beach, FL, Amer. Meteor. Soc., 474-479.

Forbes, G.S. and J.H. Merritt, 1984: Mesoscale vortices over the Great Lakes in wintertime. Mon. Wea. Rev., 112, 377-381.

Forbes, G.S., R.L. Scheinhartz, E. Araujo, W.D. Lottes and J.J. Cahir, 1984(b): Short-term forecasting using a REMOS approach. Proc., Second Int'l. Symp. Nowcasting, Norrkoping, Sweden, 379-384.

Forbes, G.S. and W.D. Lottes, 1984: Classification of mesoscale vortices in polar airstreams and the influence of the large-scale environment on their evolutions. Accepted by Tellus.

Fye, F.K., 1978: The AFGWC automated cloud analysis model. AFGWC Tech. Mem. 78-002, 31-43.

George, J.J., 1960: Weather Forecasting for Aeronautics. Academic Press, New York, 410-415.

Glahn, H.R. and D.A. Lowry, 1972: The use of model output statistics (MOS) in objective weather forecasting. J. Appl. Meteor., 11, 1203-1211.

Goldie, A.H.R., 1936: Rainfalls at fronts of depressions. Geophys. Mem., No. 69, Gr. Brit. Meteor. Off., 18 pp.

Gray, W.M. and R.W. Jacobson, Jr., 1977: Diurnal variations of deep cumulus convection. Mon. Wea. Rev., 105, 1171-1188.

Heppner, P.O.G., 1984: Application of an air trajectory model to test a theory concerning nocturnal thunderstorm development. M.S. Thesis, The Pennsylvania State University, in progress.

Hill, F.F., 1981: Mean fields of orographic rainfall enhancement over England and Wales for different wind directions and their application to short-period forecasting. Meteor. Off. Radar Res. Lab. Rept. 26, Malvern, England, 44 pp.

Hill, F.F., K.A. Browning and M.J. Bader, 1981: Radar and raingauge observations of orographic rain over south Wales. Quart. J. Roy. Meteor. Soc., 107, 643-670.

Hoxit, L.R., R.A. Maddox and C.F. Chappell, 1978: On the nocturnal maximum of flash floods in the central and eastern U.S. Preprints, Conf. on Wea. Fcstg. and Analysis and Aviation Meteor., Silver Spring, MD, Amer. Meteor. Soc., 52-57.

Hudson, H.R., 1971: On the relationship between horizontal moisture convergence and convective cloud formation. J. Appl. Meteor., 10, 755-762.

Kincer, J.B., 1916: Daytime and nighttime precipitation and their economic significance. Mon Wea. Rev., 44, 628-633.

Lilly, D.K. and D.J. Perkey, 1976: Sensitivity of mesoscale predictions to mesoscale initial data. Preprints, 6th Conf. Wea. Forecasting and Analysis, Albany, NY, Amer. Meteor. Soc., 174-179.

Maddox, R.A., 1980: Mesoscale convective complexes. Bull. Amer. Meteor. Soc., 61, 1374-1387.

Maddox, R.A., C.F. Chappell and L.R. Hoxit, 1979: Synoptic and meso-scale aspects of flash flood events. Bull. Amer. Meteor. Soc., 60, 115-123.

Maddox, R.A. and C.A. Doswell, III, 1982: An examination of jet stream configurations, 500 mb vorticity advection and low-level thermal advection patterns during extended periods of intense convection. Mon. Wea. Rev., 110, 184-197.

Mahrt, L., 1975: The influence of low-level vertical gradients of moisture on parcel stability. Preprints, 9th Conf. Severe Local Storms, Norman, OK, Amer. Meteor. Soc., 40-44.

Means, L.L., 1944: The nocturnal maximum occurrence of thunderstorms in the midwestern states. Misc. Rept. No. 16, Cloud Physics Lab., Univ. of Chicago, 38 pp.

Means, L.L., 1952: On thunderstorm forecasting in the central United States. Mon. Wea. Rev., 80, 165-189.

Merritt, J.H. and J.M. Fritsch, 1984: On the movement of the heavy precipitation areas of mid-latitude mesoscale convective complexes. Preprints, 10th Conf. Wea. Forecasting and Analysis, Clearwater Beach, FL, Amer. Meteor. Soc., 529-536.

Miller, R.G., 1981: GEM: A statistical weather forecasting procedure. NOAA-TR-NWS-28, 89 pp.

Mogil, H.M. and W.D. Bonner, 1971: On the use of surface observations in boundary-layer analysis. Preprints, 7th Conf. Severe Local Storms, Kansas City, MO, Amer. Meteor. Soc., 7-12.

Muench, H.S., 1981: Short-range forecasting of cloudiness and precipitation through extrapolation of GOES imagery. AFGL-TR-81-0218 [ADA 108678].

Muench, H.S., 1984: Objective short-range weather forecast experiments using mesoscale analyses and upper-level steering. Preprints, 10th Conf. Wea. Forecasting and Analysis, Clearwater Beach, FL, Amer. Meteor. Soc., 241-248.

Otten, H.A.F.M., J.J. Cahir, G.S. Forbes, P.A. Hubanks and W.D. Lottes, 1984: A technique for short-term forecasting of the development of nocturnal convective complexes. Submitted to Mon. Wea. Rev.

Pearson, A.D., J.G. Galway and R.L. Inman, 1967: Relationship of surface dewpoint and integrated moisture in the planetary boundary layer. Preprints, 5th Conf. Severe Local Storms, St. Louis, MO, Amer. Meteor. Soc., 135-139.

Person, A.A., 1983: A prediction method for 3- to 9- hour probability of substantial precipitation amounts near summertime atmospheric boundaries. M.S. Thesis, The Pennsylvania State University, 98 pp.

Pielke, R.A., 1982: The role of mesoscale numerical models in very-short-range forecasting. In Nowcasting, Academic Press, London, 207-221.

Schaefer, J.T., 1975: Moisture stratification in the "well-mixed" boundary layer. Preprints, 9th Conf. Severe Local Storms, Norman, OK, Amer. Meteor. Soc., 45-50.

Steyaert, L.T. and G.L. Darkow, 1973: Diurnal variations in the ability to infer spatial variability in the thermodynamic properties of the lowest kilometer from surface data. Preprints, 8th Conf. Severe Local Storms, Denver, CO, Amer. Meteor. Soc., 238-243.

Wallace, J.M., 1975: Diurnal variations in precipitation and thunderstorm frequency over the conterminous United States. Mon. Wea. Rev., 103, 406-419.

Weaver, J.F. and F.P. Kelly, 1982: A mesoscale, climatologically-based forecast technique for Colorado. Preprints, 9th Conf. Wea. Forecasting and Analysis, Seattle, WA, Amer. Meteor. Soc., 277-280.

Weiss, C.E. and J.F.W. Purdom, 1974: The effect of early morning cloudiness on squall-line activity. Mon. Wea. Rev., 102, 400-402.

Zipser, E.J., Chair, Interagency Team of STORM-Central, 1984: STORM-Central phase preliminary program design. National Center for Atmospehric Research, Boulder, CO, 147 pp.

Zverev, A.S., 1972: Practical work in synoptic meteorology. Hydrometeorological Publishing House, Leningrad, 186-189.

END

FILME

12-84

DTIC